Lappeenranta
University of Technology

Joshua Emuejevoke Omajene

UNDERWATER REMOTE WELDING TECHNOLOGY FOR OFFSHORE STRUCTURES

Thesis for the degree of Doctor of Science (Technology) to be presented with due permission for public examination and criticism in the Auditorium 1382 at Lappeenranta University of Technology, Lappeenranta, Finland on the 27th of November, 2015, at noon.

Acta Universitatis
Lappeenrantaensis 676

Supervisors Professor Jukka Martikainen
LUT School of Energy Systems
Department of Mechanical Engineering
Laboratory of Welding Technology
Lappeenranta University of Technology
Finland

Associate Professor Paul Kah
LUT School of Energy Systems
Department of Mechanical Engineering
Laboratory of Welding Technology
Lappeenranta University of Technology
Finland

Reviewers Professor Victor A. Karkhin
Department of Welding and Laser Technologies
Peter the Great St. Petersburg Polytechnic University
29 Polytechnicheskaya, St. Petersburg
195251 Russia

Professor Leif Karlsson
Department of Engineering Science
University West
Gustava Melins gata 2, S-46132 Trollhättan
Sweden

Opponent Professor Victor A. Karkhin
Department of Welding and Laser Technologies
Peter the Great St. Petersburg Polytechnic University
29 Polytechnicheskaya, St. Petersburg
195251 Russia

ISBN 978-952-265-888-3
ISBN 978-952-265-889-0 (PDF)
ISSN-L 1456-4491
ISSN 1456-4491

Lappeenrannan teknillinen yliopisto
Yliopistopaino 2015

Abstract

Joshua Emuejevoke Omajene

Underwater Remote Welding Technology for Offshore Structures

Lappeenranta 2015
64 pages
Acta Universitatis Lappeenrantaensis 676
Dissertation. Lappeenranta University of Technology
ISBN 978-952-265-888-3, ISBN 978-952-265-889-0 (PDF), ISSN-L 1456-4491,
ISSN 1456-4491

The construction of offshore structures, equipment and devices requires a high level of mechanical reliability in terms of strength, toughness and ductility. One major site for mechanical failure, the weld joint region, needs particularly careful examination, and weld joint quality has become a major focus of research in recent times. Underwater welding carried out offshore faces specific challenges affecting the mechanical reliability of constructions completed underwater. The focus of this thesis is on improvement of weld quality of underwater welding using control theory.

This research work identifies ways of optimizing the welding process parameters of flux cored arc welding (FCAW) during underwater welding so as to achieve desired weld bead geometry when welding in a water environment. The weld bead geometry has no known linear relationship with the welding process parameters, which makes it difficult to determine a satisfactory weld quality. However, good weld bead geometry is achievable by controlling the welding process parameters.

The doctoral dissertation comprises two sections. The first part introduces the topic of the research, discusses the mechanisms of underwater welding and examines the effect of the water environment on the weld quality of wet welding. The second part comprises four research papers examining different aspects of underwater wet welding and its control and optimization. Issues considered include the effects of welding process parameters on weld bead geometry, optimization of FCAW process parameters, and design of a control system for the purpose of achieving a desired bead geometry that can ensure a high level of mechanical reliability in welded joints of offshore structures. Artificial neural network systems and a fuzzy logic controller, which are incorporated in the control system design, and a hybrid of fuzzy and PID controllers are the major control dynamics used.

This study contributes to knowledge of possible solutions for achieving similar high weld quality in underwater wet welding as found with welding in air. The study shows that carefully selected steels with very low carbon equivalent and proper control of the welding process parameters are essential in achieving good weld quality.

The study provides a platform for further research in underwater welding. It promotes increased awareness of the need to improve the quality of underwater welding for offshore industries and thus minimize the risk of structural defects resulting from poor weld quality.

Keywords: Artificial neural network, Bead geometry, Control systems, Cooling rate, Underwater wet welding, Weld microstructure

Acknowledgements

The constant support and encouragement of my supervisors and colleagues at the Department of Mechanical Engineering of Lappeenranta University of Technology has been invaluable. Without their help and counsel, always generously and unstintingly given, completion of this doctoral work would have been immeasurably more difficult.

I wish to express appreciation with a thankful heart to my supervisor, Professor Jukka Martikainen.

I most sincerely wish to express heartfelt gratitude to Associate Professor Paul Kah, whose supervision knows no bounds. You were always ready and glad to offer scientific and technical expert advice. I want to say I was 'a big bone in your throat' because I could call you at any time of the day and visit your office even without prior notice, and you were still ready to listen. I know you will be glad that the bone is now out your throat but I also hope for further collaboration in the next phase of my professional endeavours.

To Associate Professor Huapeng Wu, who has taken particular interest in my research and whose kind support has again and again been of great value, a special debt of gratitude is due.

I wish to express deep gratitude to all those who reviewed this dissertation and contributed to improving the work, particularly, Professor Victor A. Karkhin from Peter the Great St. Petersburg Polytechnic University and Professor Leif Karlsson from University West, Sweden. Thanks also to Peter Jones of LUT Language Centre for his help with the English language.

Copious thanks go to my family and words cannot express how grateful I am to my dad, Goodluck Omajene, my mum, Rebecca Omajene, my brothers, Godwin Omajene, Kingsley Omajene, Onome Omajene, and my sisters, Joan Ofili, Aghogho Ifie and Agheghe Oghenevwerute. I thank you all for all your support and the sacrifices that were made on my behalf during the course of my doctoral studies. Your fervent prayers for me were the key to my sustenance thus far. I also wish to thank all of my friends who supported me, and especially, Nicolus Rotich, who encouraged me to strive towards my goals.

To my beloved wife, Joy Omajene, my one and only Yori-Yori, I heartily express my unending appreciation for your support and enduring the many sleepless nights throughout this difficult journey. You were always a great support and source of motivation in moments when the going got tough. I want to say I LOVE YOU endlessly. To my lovely daughter, Beulah Omajene, daddy wants to say thank you for giving mummy big reasons to smile when daddy was always away from home. You are a source of inspiration, joy and motivation who made it easier to go along this journey. I wish to hereby dedicate this doctoral dissertation to my darling wife and daughter.

I finally say thank you almighty God for your mercies upon my life and I believe you will open the doors of favour and prosperity unto me. Amen.

November 2015
Lappeenranta, Finland
Joshua Emuejevoke Omajene

Contents

List of publications and the author's contribution

This thesis is based on the following papers. The rights have been granted by the publishers to include the papers in the dissertation.

Publication I
Omajene J. E., Martikainen J., Kah P., Pirinen M., (2014), "Fundamental Difficulties Associated With Underwater Wet Welding", International Journal of Engineering Research and Applications,ISSN: 2248-9622, Vol. 4, Issue 6(Version 4), pp. 26-31

Publication II
Omajene J. E., Martikainen J., Kah P., (2014), "Effect of Welding Parameters on Weld Bead Shape on Welds Done Underwater ", International Journal of Mechanical Engineering and Applications, ISSN: 2330-0248, 2(6), pp. 128-134

Publication III
Omajene J. E., Martikainen J., Huapeng W., Kah P., (2014), "Optimization of Underwater Wet Welding Process Parameters Using Neural Network", International Journal of Mechanical and Materials Engineering, ISSN: 1823-0334, 9(26), pp. 1-8

Publication IV
Omajene J. E., Kah P., Huapeng W.,Martikainen J., Izelu C. O., (2015), "Intelligent Control Mechanism for Underwater Wet Welding ",International Journal of Mechanical Engineering and Applications, ISSN: 2330-0248, 3(4), pp. 50-56

In Publication I, the author identified the difficulties faced when carrying out welding operations underwater. The author was able to ascertain the different reasons associated with poor weld quality in the water environment as compared to air welding. This knowledge forms the basis on which further research work in the dissertation was anchored. The author did all the review research work and wrote the paper.

In Publication II, the author identified and analysed the effect of welding parameters on the welding geometry of welds obtained in underwater welding processes. The paper was independently written by the author.

In Publication III, the author designed and implemented a neural network model for analysis of the optimization of welding process parameters in underwater welding. The author was responsible for gathering data from previous research work by other authors, and used this data for the implementation, analysis and validation of the neural network learning process. The author was responsible for the writing of the paper.

Publication IV deals with control of a flux cored arc welding process so as to achieve a desirable and sound weld by adjusting the welding process parameters in the presence of uncertainties from the water environment. The author designed the control mechanism and implemented the design to analyse the different control processes discussed in this dissertation. The author was responsible for the writing of the paper.

Nomenclature

Variables

A	area	m^2
α	thermal diffusivity	mm^2/s
$C_{p,l}$	specific heat of saturated liquid	J/(kgK)
$C_{p,v}$	specific heat of saturated vapour	J/(kgK)
c_v	specific heat capacity at constant volume	J/(kgK)
$C_{s,f}$	empirical constant	-
dB	decibel	dB
F	frequency	Hz
g	acceleration due to gravity	m/s^2
h	coefficient of heat transfer	$W/(m^2K)$
$h_{f,g}$	latent heat of vaporization	kJ/kg
K	thermal conductivity	$W{\cdot}K^{-1}m^{-1}$
k_a	electric field intensity	NC^{-1}
K_d	derivative gain	-
K_e	constant	-
K_i	integral gain	-
K_m	constant related to the anode voltage drop	-
K_p	proportional gain	-
K_s	average resistance per unit length of wire stickout	Ω/m
K_v	thermal conductivity of vapor	W/(m K)
L	characteristic length	m
L	length	m
L_a	arc length	m
L_s	wire stickout length	m
M_s	power source inductance	H
P	pressure	Pa
P	electric resistivity	Ω·m
P_{H2}	partial pressure of hydrogen	atm
P_{H2O}	partial pressure of water	atm
pr_l	Prandtl number of saturated liquid	-
Q	heat flux	W/m^2
$q''_{boiling}$	boiling heat flux	W/m^2
q''_{source}	arc heat flux	W/m^2
q_0	volumetric energy generation rate	W/m^3
Q	total heat input to the workpiece	W/m
R	radius	m
r_0	radius of heat distribution	m
R_a	arc resistance	Ω
Ra_L	Rayleigh number	-
R_s	equivalent source resistance	Ω
T	temperature	K, °C
t	time	s
$t_{8/5}$	cooling time from 800 to 500	s
q_m	mass flow	kg/s
U_c	constant	V

U_s	wire stickout voltage	V
U_{o1}	equivalent open loop voltage	V
V_m	melting rate	m/s
V_f	wire feed rate	m/min
X_{co}	fraction of CO in the welding arc atmosphere	-
X_{H2}	fraction of hydrogen in the weld arc	-
X_{H2O}	fraction of water in the weld arc	-

Greek alphabet

β	thermal expansion coefficient	1/K
γ	gamma	-
ΔD	change in water depth	m
ΔH	change in CTWD	mm
ΔI	change in current	A
ΔP	change in penetration	mm
ΔR	change in reinforcement	mm
ΔU	change in voltage	V
ΔW	change in width	mm
ε_s	surface emissivity	-
μ_l	viscosity of liquid	kg/(s.m)
μ_v	viscosity of vapour	kg/(s.m)
N	kinematic viscosity	m^2/s
ρ_l	density of saturated liquid	kg/m^3
ρ_v	density of saturated vapour	kg/m^3

Dimensionless elements

C	carbon
CO	carbon monoxide
Cr	chromium
Cu	copper
H_2	hydrogen
H_2O	water
Mn	manganese
Mo	molybdenum
Ni	nickel
P	phosphorus
Si	silicon
V	vanadium

Subscripts

∞	infinite
s	surface
sat	saturation
max	maximum
min	minimum
wall	wall

Acronyms

ANN	Artificial neural network
CE	Carbon equivalent
CFD	Computational fluid dynamics
CTWD	Contact-tip-to-workpiece distance
FCAW	Flux cored arc welding
GMAW	Gas metal arc welding
HAZ	Heat affected zone
MSE	Mean squared error
MIMO	Multiple-input multiple-output
NDT	Non destructive test
PID	Proportional-integral-derivative
SCG	Scaled conjugate gradient
SISO	Single-input single-output
CFD	Computational fluid dynamics
UWW	Underwater wet welding
WPSF	Weld penetration shape factor
WRFF	Weld reinforcement form factor

1. Introduction

This doctoral dissertation presents work that was carried out in the Department of Mechanical Engineering of Lappeenranta University of Technology as part of efforts to advance research on underwater welding technology and control mechanism design for underwater welding processes.

There is undoubtedly an increased need for underwater welding in offshore industries, where underwater welding is used for fabrication welding, repair welding and maintenance welding. Producing quality welded joints in underwater welding encounters some challenges, particularly as regards reduced toughness and ductility, although the use of underwater chamber welding has proven to be a partial way of solving the problem. This process, however, has significant limitations as it can only be used to weld regular shapes such as those found in pipeline welding. The chamber welding process is very expensive and often impracticable for general underwater repairs and fabrication [1, 2].

Over the decades, different approaches have been employed in efforts to achieve reasonable weld quality at different water depths. Laser beam welding, friction stir welding, utilization of an oxyrutile electrode, mini-cap local dry underwater FCAW, hammerhead wet spot welding and tubular shielded electrodes using internal gas protection have all been employed, and quite good results have been produced [3-7].

Currently, most widely recognized underwater welding techniques and approaches follow the AWS D3.6M:2010 code, which establishes three specification classes for underwater welding: A, B and O specifications. These specification types ensure that weldments meet certain qualities, which are formulated when the welding specifications are defined. Verification of the welding quality requirements is performed alongside fabrication. The code requires that Class A quality be similar to air welding in respect of ductility, strength, hardness, toughness and bending. The Class B specification is for weldments that are slightly less critical and quality requirements are less stringent, as are welding procedure, welding qualification and acceptance requirements. Class O meets the demands of other underwater specifications or codes usually satisfied by underwater dry habitat welds [3, 8].

In order to expand underwater welding to permanent repairs and structural fabrication instead of only temporary repairs and salvage work, present methods of underwater welding need modification and innovation. This research work elaborates on new ways of tackling some of the welding challenges affecting the strength and ductility of joints welded underwater.

1.1 Background and motivation

In recent years, underwater welding has been applied for repair welding purposes and maintenance of offshore and sub-sea structures. It is used for repair of structures damaged due to fatigue failure, corrosion or collision with movable offshore structures such as offshore vessels [9, 10]. To maintain structural integrity and service life, it is important to achieve good weld quality. The wet environment in which this welding process is carried out makes it more difficult to reach the weld quality required for offshore structures. The high cooling rate in a wet environment affects the microstructure formed after welding.

Most offshore constructions are in marine environments, which can vary from warm marine to arctic marine environments. Major offshore industrial activities are carried out by companies in the oil and gas industries, shipbuilding and renewable energy. In the renewable energy field, companies construct, operate and maintain offshore wind turbines. Installations such as oil platforms, drilling rigs and jack-up are utilized by oil and gas companies. Offshore construction is dangerous and this makes it reasonable for some of the construction activities to be carried out onshore and fabricated parts to be installed offshore. Such activities include fabrication and welding. Materials for offshore applications face harsh conditions and corrosion is a significant concern. Effective material selection and efficient construction of structures is required to ensure structures meet the mechanical requirements for offshore applications at competitive cost.

The importance of underwater welding cannot be overemphasized because it plays a major role in these sectors. The quality of welds achieved determines the life span and integrity of structures used in marine environments. Weld quality plays a direct role in return on investment as well-made structures can be used for a longer time and can also be repaired when failure occurs. Building of new structures is very expensive and the ability to effectively repair structures can lead to considerable cost savings. Underwater welding is also relevant to environmental concerns because if a ship or other offshore structure is damaged and cannot be repaired and reused, this will, in turn, increase the amount of waste that goes into the environment, which has some health hazard implications.

1.2 Objective and focus

The initial aim of this research was to develop a welding approach that excludes water from the weld region and a welding system that incorporates a preheating system before welding. During the research, it became apparent that there is a need for an automated system and an approach that makes fewer demands on the skills of the welder. The aim of the work then changed to a focus on research and development of control of an underwater welding process, such as FCAW, that can be easily automated. It should be noted that the ideas presented in this thesis can be applied to other welding processes that can be easily automated. The necessary control of the welding heat input, which is part of the control architecture, does mean, however, that the approach discussed in this work is not suitable for manual welding. The control of the welding process for different water depth is a closed loop control system whereby fuzzy logic control is applied and the control process parameters follow a set of trained process parameters using an artificial neural network mechanism. A second control method, which employs a hybrid of a fuzzy controller and PID controller, is also analyzed in the doctoral dissertation.

The doctoral dissertation thus focuses on researching and finding solutions for improving the quality of weld bead geometry obtained in UWW by optimizing the welding process

parameters for different water depth. The objective is discussed in further detail in chapters 3 and 4, where additional and more specific objectives are presented.

1.3 Overview of the work

The UWW process involves a wide range of research areas and a large number of topics, as depicted in Figure 1. The issue under study can be divided into questions such as the fundamentals of the UWW process, the difficulties associated with UWW, solidification of the molten weld in UWW, optimization of the process parameters, and control methods for UWW. Study of the fundamentals of the UWW process is concerned with the nature of welding in a wet environment, which is related particularly to the difficulties associated with the process environment and weld pool solidification. Weld pool solidification is related to the fast cooling rate of UWW, and the cooling rate affects the microstructure formed and the quality of the weld. The discussion of optimization of the process deals with the use of artificial intelligent control processes like neural networks, PID and fuzzy logic control to optimize the welding process parameters. Weld parameter optimization is related to the control methods because the artificial intelligent control is a relevant component of the control architecture. This area of the research involves control of the UWW process to achieve optimized bead geometry so as to ensure sound welds.

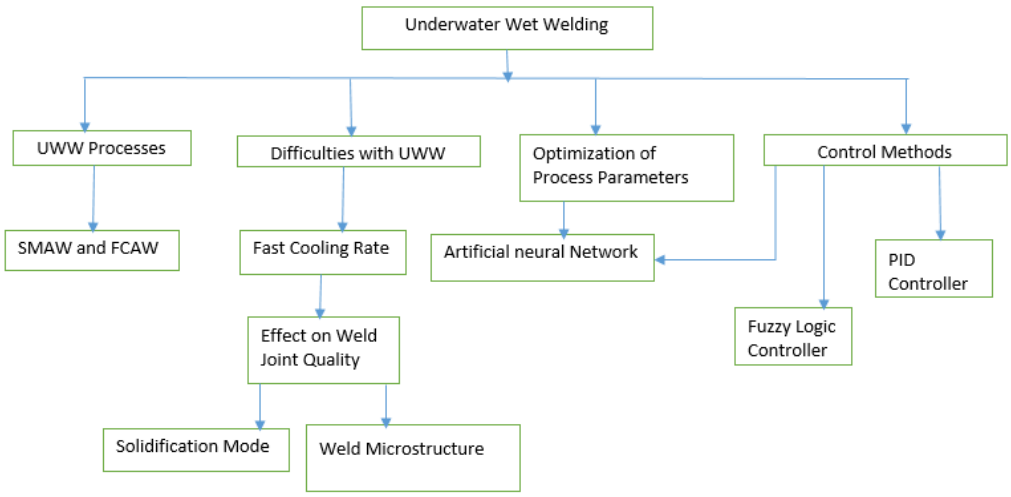

Figure 1 Descriptive overview of the work

1.4 Contribution of the work

The dissertation makes a number of contributions in the area of welding of structural steels and achieving sound welds for offshore applications through improved UWW control. The contributions are summarized below.

Identifying difficulties associated with underwater welding: Key parts of this research were made possible by clear identification of the factors that affect the quality of underwater welding as compared to air welding and the effect of welding process parameters on weld bead shape obtained from underwater welds. It was on the basis of this knowledge that further work was carried out. (Publication I) and (Publication II)

Artificial neural network (ANN) model: ANN is a useful way to control variables that are nonlinear in nature. Welding is a multi-input multi-output process and as such needs an optimization algorithm to achieve optimal variables that are favourable for the welding process. The application of an artificial neural network to optimize the process parameters in underwater welding is proposed in this thesis. (Publication III)

Fuzzy logic control model: Control of underwater welding processes is complex. Fuzzy logic employing the use of a rule based IF current AND voltage THEN bead geometry makes it easy to control the welding process. A fuzzy logic control model is designed in this thesis. (Publication IV)

Process parameter control mechanism: An important aspect of underwater welding is the ability to control arc length and arc stability. It is possible to control the arc length by controlling the welding process parameters. The importance of achieving an optimal weld bead shape makes effective control of the process necessary. The design of the control system is a major breakthrough in this thesis, although future work needs to be carried out to validate the controller for underwater welding experimentally. (Publication IV)

1.5 Impact on society and the environment

The goal of this work is to achieve good mechanical properties in welds done in a wet environment. Meeting such a goal will have impacts on society and the environment. The impact of this work can be looked at in various ways, for example, the effect on industry and job creation, or the effect on the environment.

It is evident that companies that are involved in wet welding operations will benefit from technologies that can guarantee quality welds in underwater welding operations. However, it is not yet clear if the technology will be cheaper than current approaches. However, it is certain that return on investment will be high [11] for underwater welding technology that can guarantee sound welds.

Companies are always searching for ways to do things more effectively. A control system that can control the welding process parameters and optimise the process to achieve quality output will certainly be of interest to engineering companies that carry out welding activities in underwater environments. Whether this technology will create more jobs for skilled workers is uncertain, but the greater use of automation means that less skill is required and therefore fewer skilled workers are needed.

It should be noted that an inability to repair damaged structures underwater, or the failure of structures as a result of poor weld quality will increase the tonnage of waste metals from damaged structures in the offshore environment. This will increase environmental health hazards. The ability to achieve quality welds underwater will increase the life span of offshore structures, as will the ability to repair structures if failure occurs, and thereby reduce the amount of waste metal in offshore environments.

1.6 Thesis outline

The doctoral dissertation contains an introduction of six chapters followed by four original publications in journals of international repute and standing. The six chapters in the first part

of the dissertation cover the principles of underwater welding, control methodology of UWW process parameters, UWW control modelling, simulation result analysis, and conclusions and future work.

Chapter 1 is the introductory part of the research work. The background and objective of the research is discussed in this chapter.

Chapter 2 elaborates on the fundamentals of underwater welding. This chapter considers the mechanism underlying cooling of the weld metal as a result of the presence of water around the workpiece. The effect of the cooling on the quality of the weld is illustrated and the chapter describes the effect of the water environment on the welding process, for instance, arc instability, loss of alloying elements, heat transfer during the weld, and solidification microstructure after the weld.

Chapter 3 focuses on the application of artificial intelligent control methods such as neural networks and fuzzy logic control to optimisation of the welding process parameters of FCAW for underwater welding applications.

Chapter 4 deals with the design of intelligent control systems that operate on feedback control theory. The controllers studied employ a PID controller, fuzzy controller, and a hybrid of a fuzzy and PID controller, respectively. The individual controllers were executed on the MATLAB program and the results of the different controllers compared.

Chapters 5 gives suggestions for further research work in the area studied.

Chapter 6 gives the concluding remarks of the study.

The second part of the dissertation presents four original publications published in international journals. The list below summarizes the publications.

Publication I reviews the effect of the high weld cooling rate due to the presence of the water environment on the weld quality achievable during underwater welding. It discusses the effect of water depth on arc stability and makes general comparisons between wet welding and air welding.

Publication II considers welding process parameters like current, voltage, welding speed, Contact Tip to Work Distance (CTWD), as well as water temperature and water depth, and identifies their effect on weld penetration, reinforcement, and weld width in underwater wet welding.

Publication III discusses the design of a neural network model for use in optimization of welding process parameters in underwater welding. A neural network learning algorithm is used to control the welding current, voltage, welding speed and CTWD, so as to achieve optimized weld bead geometry under the influence of the water environment and water depth.

Publication IV discusses the design of a novel control mechanism for the underwater wet welding process. The control mechanism incorporates the use of a fuzzy logic controller and PID controller. This design is a robust design that integrates the advantages of both the fuzzy logic controller and PID controller approaches, and the simulation results show that it is clearly able to achieve the control targets.

1.7 Review of previous study

This chapter examines published literature in the fields studied in this work. Study of previous literature is useful to gain understanding of the subject of underwater welding and the relevant topics involved. Special attention is paid to understanding the effect of the water surrounding the weld metal during welding and the consequences of the cooling effect of the water on the weld bead shape.

Current theories of the effect of water on weld quality were developed in the 1970s and 1980s and even as early as the 1950s. These theories were the work of Brown et.al. (1972) [1]. The work of Ozaki et al. (1977) [12] investigated hydrogen cracking in underwater wet welding of different steel types. The work of Ibarra et.al. (1988) [13]and Ando et.al. (1983) [14] focused on the metallurgical aspect of underwater welding and the metallurgical properties of steel welds done underwater respectively.

Rosenthal et.al. (1946) [15] presented early theory about moving heat sources. In the area of underwater welding, Chon et al. (1979) [16] studied the mechanism of rapid cooling in underwater welding.

State of the art practice in underwater welding can be found from the work of Ibarra et.al. (1994) [17]. This work touches on metallurgy, welding processes and control of the welding process. More recent research has been conducted on underwater welding, and the work of Faisal et al. (2011) [18], which compares the solidification between wet and dry welding, is an example of progress in study of this field. Other researchers such as Ghadimi et al. (2013) [19] have focused their research on simulation of the underwater welding process and investigation of effective parameters.

In attempts to control the welding process parameters so as to mitigate the effect of the water environment, Chon et al. (2010) [20] developed a microprocessor for tracking the welding operation during underwater welding. Isiklar et al. (2011) [21] designed a numerical model for underwater welding.

Based on previous research, this work incorporates ideas in the field of underwater welding and control dynamics to develop a new approach for using control dynamics for control and optimization of welding process parameters in underwater welding.

1.8 Limitations of the study

In the course of this doctoral research work, no experimental laboratory was available to carry out experimental analysis work validating the designed control system.

In this work, the neural network has a limitation of not being valid for parameters outside the range in which the training of the neural network was done. Training was done within the range of 280 – 340 Amperes for welding current, 26 – 32 Volts for welding voltage, 6 – 12 mm/s for welding speed, 18 – 24 mm for CTWD and 0.1 – 60 m for water depth. In cases where parameter values are outside these values, different parameters are required to be used in the controller and therefore retraining of the neural network with those values should be done.

The component of the fuzzy logic controller presented in Figure 18 is not designed in this thesis. It was only highlighted as a part of the control architecture. The work in Publication III focused on optimization of welding process parameters using neural network modelling.

Therefore the entire control architecture of Figure 18 was not simulated and analysed, which made it unnecessary to design the fuzzy logic controller component of the control architecture. An explanation of how the entire controller works is given in chapter three and further information can be found in Publication III.

2. Theoretical considerations

This chapter gives insight on the major theories behind underwater welding. The basic concepts of underwater welding and thermal characteristics of underwater wet welding is explained in this chapter.

2.1 Underwater welding

The processes most widely used in underwater welding are shielded metal arc welding (SMAW) and flux-cored arc welding (FCAW). These underwater welding processes are very similar to those used in surface welding, with an arc formed between the tip of the electrode and the workpiece. During underwater welding, the arc is sustained in high temperature plasma that is surrounded by gas bubbles due to the presence of water. The plasma contains about 90% ionized hydrogen and some amount of hydrogen, oxygen, nitrogen, carbon dioxide, steam and other trace elements. The water environment in underwater welding results in fast cooling, steep temperature gradients during the welding and decreased arc stability as a result of the pressure reaction [1, 22]. The quality problems associated with underwater welding are weld porosity, depletion of alloying elements from the weld, formation of slag in the welds, increased weld oxygen and carbon content, and high crack formation susceptibility [12, 23]. Underwater welding is classified into wet and dry welding techniques [23-25] as illustrated in Figure 2.

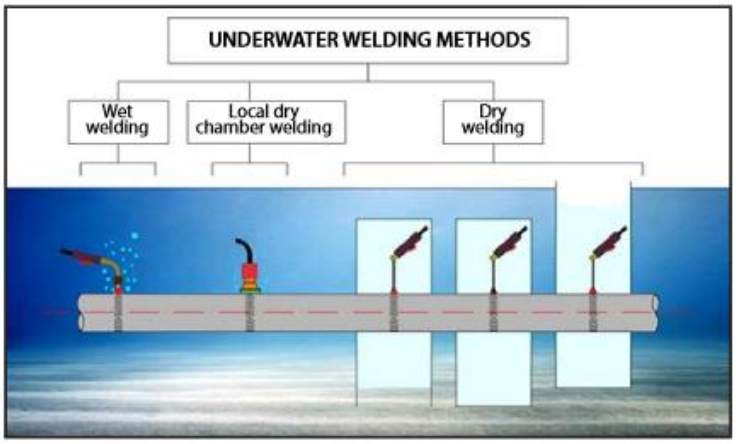

Figure 2 Classification of underwater welding methods [26].

2.2 Wet welding

Wet underwater welding (Figure 3) is performed in direct contact with the wet environment and it is an acceptable repair technique down to 100 meters water depth [27]. There is increased freedom of movement in wet welding compared to dry underwater welding techniques, and this makes it the most effective, efficient and economical underwater welding method for applications such as temporary repairs. However, wet welding suffers the major drawback of the weld metal being rapidly quenched by the water around the weld metal, which makes the quality for permanent repairs a major concern. The rapid quenching leads to increased tensile strength, decreased ductility, increased porosity and hardness, and hydrogen embrittlement

[27-29]. Thus, underwater wet welding is limited to steels of low carbon equivalent (Equation 1.1; CE < 0.4) [30, 31].

$$CE = C + \frac{Mn}{6} + \frac{(Cr+Mo+V)}{5} + \frac{(Ni+Cu)}{15} \quad (1.1)$$

Figure 3 Diver performing underwater wet welding [32].

2.3 Dry welding

Dry underwater welding is usually done in a high pressure underwater environment and the technique is typically used in depths less than 400 meters. The welding is done in a chamber that acts as a dry environment. This underwater welding process results in high quality welds because it is carried out in an enclosure, which allows for pre- and post-weld heating. Dry underwater welding can be achieved in several ways such as dry habitat welding, dry chamber welding, dry welding at one atmosphere, dry spot welding, hyperbaric welding and cofferdam welding. The techniques use different ways to afford the weld region physical protection from the surrounding water. For example, cofferdam welding is done in an enclosed space at one atmosphere inside an open top and a closed bottom. Hyperbaric welding is done in a chamber filled with helium gas that contains 0.5 bar of oxygen gas and the structure is welded in the sealed chamber. Some of the advantages of dry welding, apart from improved quality, are: greater ease of joint preparation, better pipe alignment, and an ability to conduct NDT inspection. However, the high cost of such methods, as earlier mentioned, is a great disadvantage, as is the extremely complex nature of the chamber for each individual task [27, 33].

2.4 Effect of water on the mechanical properties of UWW welded joints

The presence of water around the welding environment has a significant effect on the weld joint, as illustrated in Figure 4. In comparison to air welding, UWW results in the loss of alloying elements from the weld, increased porosity formation, the presence of slags in the welds, increased oxygen and carbon content in the weld, and increased crack tendency, which all contribute to reduced joint quality [23].

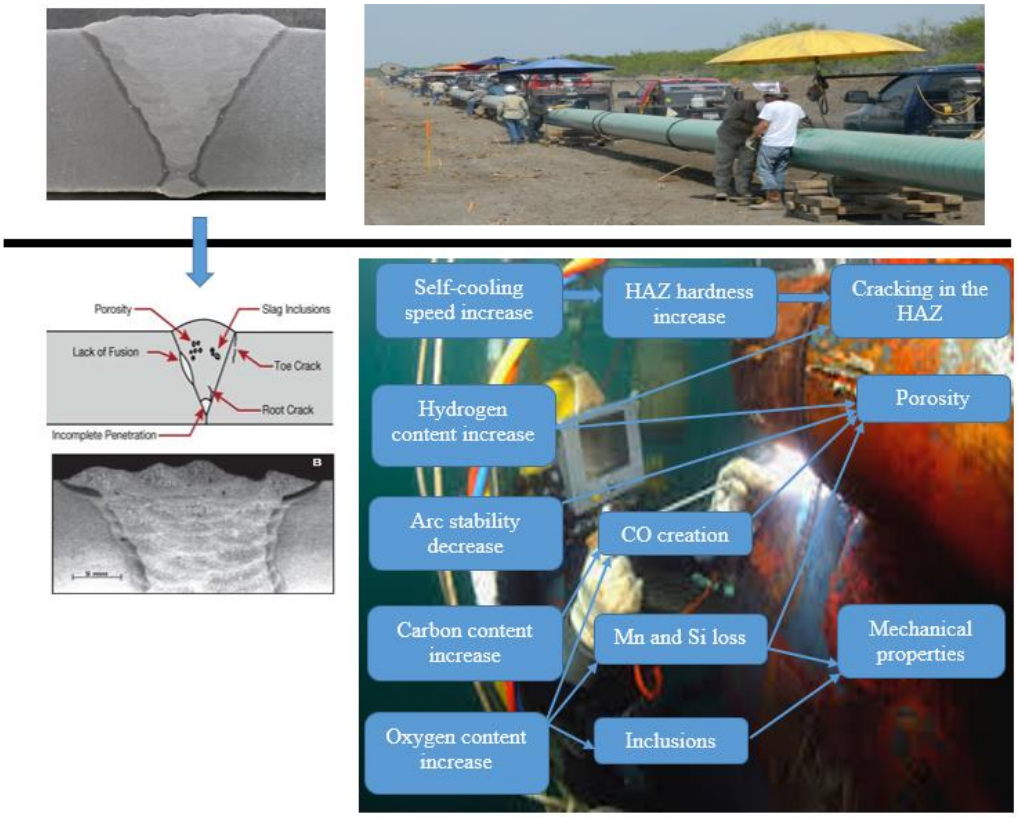

Figure 4 Effect of moving the welding process to an aqueous environment, adapted from [23]

2.5 Chemical reactions in wet welding

Alloying elements in consumables and the base metal have an important role in the quality of welded joints. Manganese helps to increase strength of the base metal without significant loss of toughness. Weld metal containing some amount of silicon acts as deoxidizers. Also some filler metals containing silicon helps in cleaning and deoxidizing when welding on contaminated surface and this results in increased weld metal strength. Carbon increases the strength of the base metal and consequently decreases toughness [34].

Ibarra et al. [13, 17] studied the effect of increased water depth or pressure as it relates to underwater welding. His work on underwater weld metal chemistry and metallurgy indicated that there is a subsequent decrease in weld metal manganese and silicon with increasing pressure or water depth. Thus, there was a substantial decrease of about 0.3 wt % manganese content at 305 m (30 bars), and weld metal silicon decreased by 0.1 wt % at 76 m (8 bars).

During the welding, the decomposition of water in the water environment (Figure 4) produces oxygen and hydrogen as depicted in Equation 1.6, and the resulting presence of oxygen in the weld leads to low toughness characteristics. Research shows that as the water depth increases, the oxygen and carbon content increases for dry hyperbaric SMAW when using a modified E8018-C1 electrode. The increase in oxygen and carbon content as a function of pressure or increased water depth is related to the law of mass action for the carbon monoxide reaction presented in Equation 1.2 [35]:

$$CO(g) = \underline{C} + \underline{O} \tag{1.2}$$

The carbon monoxide reaction equilibrium constant is presented as in Equation 1.3:

$$K = \frac{|c||o|}{P_{co}} \tag{1.3}$$

While by Dalton's law, the partial pressure P_{co} is related to the total pressure.

$$P_{co} = X_{co}P \tag{1.4}$$

The fraction of the welding arc atmosphere is denoted by $X_{co.}$ The product of the weld metal carbon $[C]$ and weld metal oxygen $[O]$ is derived by substituting and rearranging equations 1.3 and 1.4.

$$[C][O] = KX_{co}P = K^{I}P \tag{1.5}$$

Where k^I is a constant.

Wet and dry habitat welding are both subjected to increasing pressure of one bar for every 10 m as the water depth increases. The wet environment in wet welding has a direct influence on the cooling rate when welding, which subsequently has an effect on the phase transformation of the weld metal. The oxygen content down to 50 m is controlled by the carbon monoxide reaction, and the oxidation of manganese and silicon and the subsequent weld metal content are controlled by the oxygen content, as suggested in Figure 5. UWW at 50 m and 100 m water depth leads to moderately constant weld metal carbon, oxygen, manganese and silicon content. This is explained by the weld metal silicon and manganese contents being controlled by the oxygen content present. However, the silicon and manganese contents are not controlled by the carbon monoxide reaction at depth higher than 50 m and the following water decomposition reaction is controlling at depth greater than 50 m [13, 17, 36].

$$H_2O_{(g)} = H_{2(g)} + \underline{O} \tag{1.6}$$

The law illustrating mass action for the water decomposition reaction is represented as:

$$K_2 = \frac{P_{H_2}[O]}{P_{H_2O}} \tag{1.7}$$

Where K_2 is an equilibrium constant for the water decomposition reaction (Equation 1.6).

According to Dalton's law, P_{H2} is the partial pressure of hydrogen and P_{H2O} is the partial pressure of water.

$$P_{H_2O} = X_{H_2O}P \tag{1.8}$$

$$P_{H2} = X_{H2} P \tag{1.9}$$

Where X_{H2O} is the fraction of water and X_{H2} is the fraction of hydrogen in the weld arc.

Equation 1.10 is arrived at by substituting and rearranging the above equations.

$$K = \frac{X_{H2} P[O]}{X_{H2O} P} = \frac{X_{H2}[O]}{X_{H2O}} \tag{1.10}$$

Equation 1.10 suggests that the oxygen content of the weld metal will stay constant if X_{H2} and X_{H2O} are not dependent on water depth or pressure. Decrease in the arc stability as the water depth increases is an indication that hydrogen is more abundant and controls the chemistry of the wet welding. This is because hydrogen has high ionization potential and this leads to difficulty in sustaining the welding arc.

Analyses by Ando and Asahina [14] of the gas contained within the porosity of underwater wet welds shows that the gas composition in the pores is greater than 99 percent hydrogen. Similar work by Suga and Hasui [37] shows that the composition of gas contained in wet weld porosity is 96 percent hydrogen and a small amount of carbon monoxide. It can be concluded that the porosity present in underwater wet welding is induced by the presence of hydrogen.

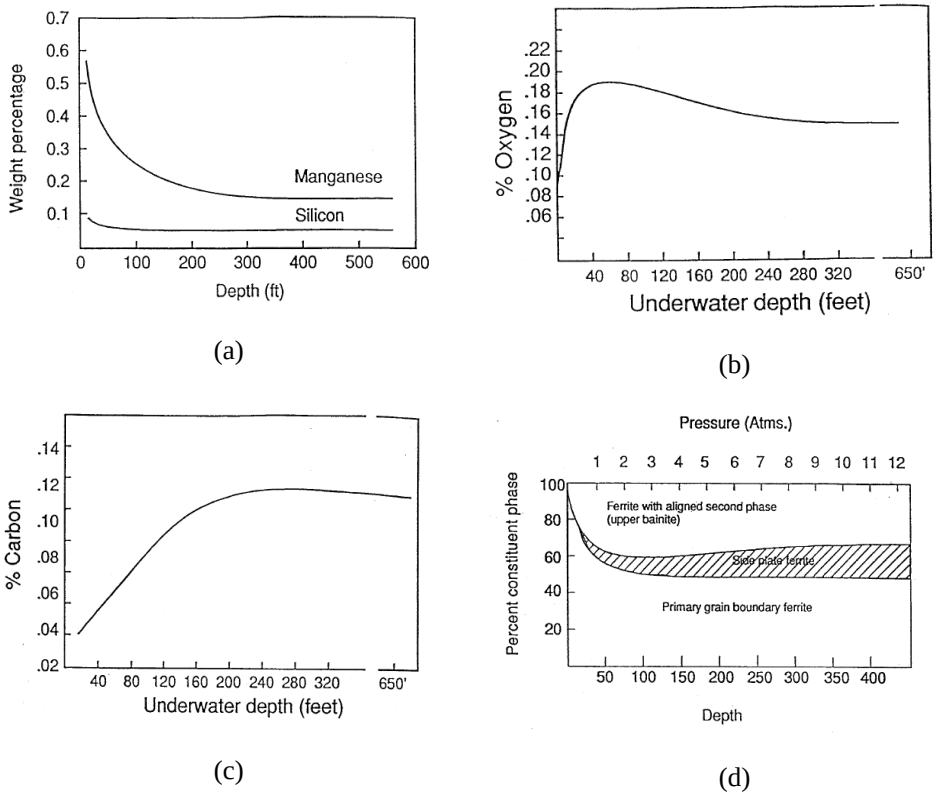

Figure 5 a) Underwater wet weld metal manganese and silicon as a function of water depth. b) Oxygen content of weld metal related to water depth in underwater wet welding. c) Weld metal carbon as a function of water depth in underwater wet welding. d) Constituents percentage of the weld metal microstructure related to water depth in underwater wet welding [17]

2.6 Heat transfer during underwater wet welding

The thermal characteristics of any welding process are very important because they determine the metallurgical structure and residual stress [1]. Due to the direct water contact during underwater wet welding, it is important to understand the heat transfer properties and how they affect weld pool solidification and metallurgical structure [18, 38]. It is necessary to point out that the nature and distribution of heat is a problem that has still not been completely solved. However, researchers have been able to identify the major heat distribution and losses in underwater welding.

The major heat losses in underwater wet welding are from boiling, convection and radiation. The complex nature of boiling heat transfer can be subdivided into different regions, as shown in Figure 6. During underwater welding, the temperature of the plate increases above the saturation temperature and this leads to the formation of bubbles. Bubbles that are formed whirl up the water near the plate surface, which leads to an increase in the heat transfer. In the transition phases, the bubbles come together forming an unstable film, which reduces the heat transfer. At this stage, a final stable film is formed that reduces most of the heat transfer to radiation [1, 19].

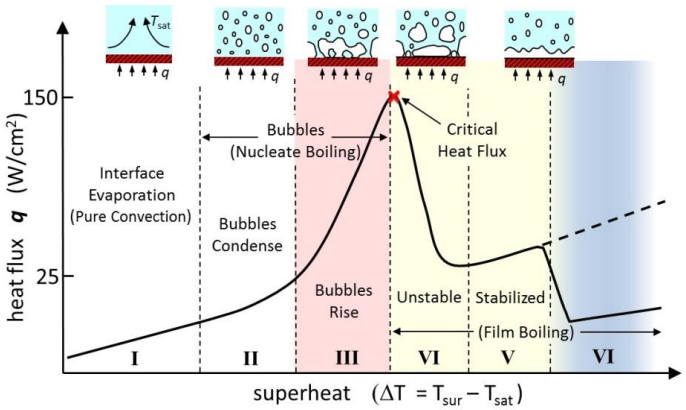

Figure 6 Characteristic boiling curve [39].

The work of Rosenthal [15] in the late 1930s focused on theoretical study of the effect of a moving heat source. In his study, he analysed the fundamentals of heat sources and their effect and derived equations that describe two-dimensional and three-dimensional heat conduction in a solid under the influence of a moving source of heat. The study employed assumptions such as: constant thermal properties, point heat source, melting, zero heat loss from the work piece surface, and an infinitely wide workpiece. A numerical model for transient three-dimensional conduction heat transfer in an underwater welding process on a thick rectangular plate was proposed by Y. V. Isiklar et al. [21]. The numerical scheme of his work is based on a finite volume model that includes convection, radiation and boiling surface thermal boundary conditions.

2.7 Finite volume method

Finite volume method is a CFD technique originally developed for special finite difference methods that have several stages of the numerical algorithm listed as follows [40]:

I. The governing equations of the fluids are integrated on all the finite control volumes of the solution domain.

II. The integral equations are converted into a system of algebraic equations using a discretization method.

III. An iterative approach is used to solve the algebraic equations.

An illustrative example for one-dimensional steady-state heat conduction makes it easier to understand the finite volume method.

The governing equation of one-dimensional steady-state heat conduction is as follow:

$$\frac{\mathrm{d}}{\mathrm{dx}}\left[\mathrm{K}\frac{\mathrm{dT}}{\mathrm{dx}}\right] + \mathrm{S} = 0 \tag{1.11}$$

Where T is temperature, K is thermal conductivity, and S is the rate of heat generation per unit volume.

The domain of the one-dimensional steady-state conduction is divided into small and non-overlapping control volumes as depicted in Figure 7.

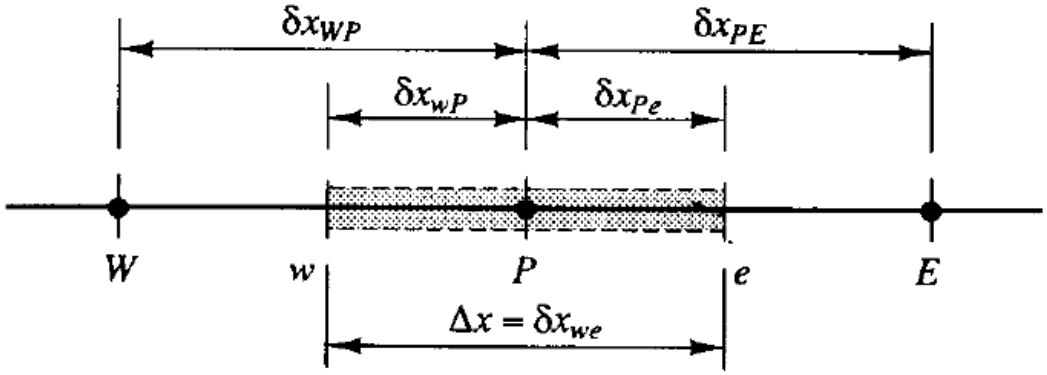

Figure 7 Discretization of one-dimensional steady-state heat conduction geometry [21].

The equation is discretized as:

$$\left[K\frac{dT}{dx}\right]_{\mathrm{e}} - \left[K\frac{dT}{dx}\right]_{\mathrm{w}} + \bar{S}\Delta x = 0 \tag{1.12}$$

$$\mathrm{K_e}\left[\frac{\mathrm{T_E}-\mathrm{T_P}}{\delta_{x\mathrm{PE}}}\right] - \mathrm{K_w}\left[\frac{\mathrm{T_P}-\mathrm{T_W}}{\delta_{x\mathrm{WP}}}\right] + \bar{S}\Delta x = 0 \tag{1.13}$$

$$\mathrm{a_P T_P} = \mathrm{a_E T_W} + \mathrm{a_W T_W} + \mathrm{b} \tag{1.14}$$

Where

$$a_E=\frac{K_E}{\delta_{xPE}}\ ,\ a_W=\frac{K_W}{\delta_{xWP}}\ ,\ a_P=a_E+a_W \text{ and } b=\bar{S}\Delta x$$

2.8 Governing equation and boundary conditions

The governing equation [21] for the numerical model for transient three-dimensional conduction heat transfer (Figure 8) is:
:

$$\rho c\frac{\partial T}{\partial t}=\frac{\partial}{\partial x}\left[K\frac{\partial T}{\partial x}\right]+\frac{\partial}{\partial y}\left[K\frac{\partial T}{\partial y}\right]+\frac{\partial}{\partial z}\left[K\frac{\partial T}{\partial z}\right] \quad (1.15)$$

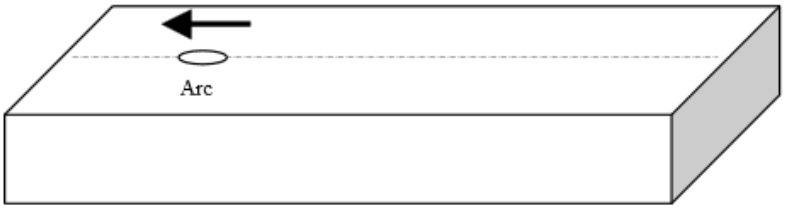

Figure 8 Geometry of transient three-dimensional conduction heat transfer [21].

Top face

The top face has boundary conditions that include convective and radiative heat loss and also heat fluxes:

$$-K\frac{dT}{dx}=h(T_{wall}-T_\infty)+q''+\sigma\varepsilon(T_{wall}^4-T_{surr}^4) \quad (1.16)$$

Where $q''_{top}=q''_{source}+q''_{boiling}$

q''_{source} is the arc heat flux and $q''_{boiling}$ is boiling heat flux.

Other faces

The boundary condition [21] for the other faces of the workpiece are similar to the top face excluding the radiation term, which is presented as:

$$-K\frac{dT}{dx}=h(T_{wall}-T_\infty)+q'' \quad (1.17)$$

Arc simulation

The welding arc is assumed to have a Gaussian distribution at the top face and is represented as:

$$Q=q_0\int_0^\infty e^{-\frac{d}{r_e^2}r^2}\,2\pi r dr \quad (1.18)$$

$$q_0=\frac{Qd}{\pi r_0^2} \quad (1.19)$$

Where Q is total heat input to the workpiece, r_0 is the radius of heat distribution, d is the exponential factor, and q_0 is the volumetric energy generation rate.

Boiling heat transfer

The transient three-dimensional conduction heat transfer analysis employs the boiling mode as follow:

$$\Delta T_e = T_s - T_{sat} \tag{1.20}$$

Where T_s is surface temperature and T_{sat} saturation temperature.

Free convection regime ($\Delta T_e \leq 5℃$)

The natural convection determines the heat transfer mode between the surface temperature and surrounding fluid. Recommendations for top heat surface correlation are [21]:

$$\overline{NU}_L = 0.54 Ra_L^{1/4} \qquad (10^4 \leq Ra_L \leq 10^7) \tag{1.21}$$

$$\overline{NU}_L = 0.15 Ra_L^{1/3} \qquad (10^7 \leq Ra_L \leq 10^{11}) \tag{1.22}$$

Where the Rayleigh number is:

$$Ra_L = \frac{g\beta(T_s - T_\infty)L^3}{\upsilon\alpha} \tag{1.23}$$

Where α is thermal diffusivity, β is the thermal expansion coefficient, g is gravitational acceleration, K is thermal conductivity, υ is kinematic viscosity, and L is characteristic length (surface area/perimeter of plate).

$$\bar{h} = \frac{\overline{NU}_L K}{L} \tag{1.24}$$

$$q'' = \bar{h}(T_s - T_\infty) \tag{1.25}$$

Nucleate boiling regime ($5℃ < \Delta T_e \leq 30℃$)

Equations for the boiling regime are derived by use of the Rohsenow correlation [21].

$$q_s^s = \mu_l h_{fg} \left[\frac{g(\rho_l - \rho_v)}{\sigma}\right]^{1/2} \left[\frac{c_{p,l}\Delta T_e}{c_{s,f} h_{fg} pr_l^n}\right]^3 \tag{1.26}$$

$$\tau = \frac{\pi}{3}\sqrt{2\pi}\left[\frac{\sigma}{g(\rho_l - \rho_v)}\right]^{1/2}\left[\frac{\rho_v^2}{\sigma g(\rho_l - \rho_v)}\right]^{1/4} \tag{1.27}$$

$$q'' = q_s''\left\{1 + \left[\frac{2k_l(T_{sat} - T_{liquid})}{\sqrt{\pi\alpha_l\tau}}\right]\frac{24}{\pi h_{fg}\rho_v}\left[\frac{\rho_v^2}{\sigma g(\rho_l - \rho_v)}\right]^{1/4}\right\} \tag{1.28}$$

where μ_l is viscosity of liquid, h_{fg} is the latent heat of vaporization, ρ_l is density of saturated liquid, $\rho_v$is density of saturated vapor, σ is surface tension of liquid-to-vapor interface, $c_{p,l}$ is specific heat of saturated liquid, $c_{s,f}$ is an empirical constant that is dependent on the kind of

heating surface fluid combination, pr_l is the Prandtl number of the saturated liquid, and n has a value of 1 for water and 1.7 for other fluids.

Transition boiling regime ($30℃ < \Delta T_e \leq 120℃$):

The transition-boiling regime heat flux is between the maximum and minimum heat fluxes [21].

$$q''_{max} = 0.149 h_{fg} p_v \left[\frac{\sigma g(\rho_l - \rho_v)}{p_v^2}\right]^{1/4} \quad (1.29)$$

$$q''_{min} = 0.09 h_{fg} p_v \left[\frac{\sigma g(\rho_l - \rho_v)}{(p_l - p_v)^2}\right]^{1/4} \quad (1.30)$$

The heat flux at a point in the transition regime is given by Equation 1.31, by assuming logarithmic heat flux distribution.

$$\log(q'') = \frac{\log\left(\frac{q''_{max}}{q''_{min}}\right)}{\log\left(\frac{30}{120}\right)} \log\left(\frac{\Delta T_e}{120}\right) + \log(q''_{min}) \quad (1.31)$$

$$q'' = 10^{\log(q'')} \quad (1.32)$$

Film boiling regime ($\Delta T_e > 120℃$):

The correlation for the film boiling regime is presented as Equation 1.33:

$$\bar{h}_c = 0.59 \left\{ \frac{g(\rho_l - \rho_v) p_v k_v^3 [h_{fg} + 0.68 c_{pv} \Delta T_e]}{2\pi \left[\frac{\sigma}{g(\rho_l - \rho_v)}\right]^{1/2} \mu_v \Delta T_e} \right\}^{1/4} \quad (1.33)$$

Where μ_v is the viscosity of vapor, k_v is the thermal conductivity of vapor, and c_{pv} is the specific heat of saturated vapor.

$$\bar{h}_c = \sigma \varepsilon_s \left[\frac{T_s^4 - T_{sat}^4}{T_s - T_{sat}}\right] \quad (1.34)$$

$$\bar{h}_{total} = \bar{h}_c + 0.75 \bar{h}_r \quad (1.35)$$

Where ε_s is surface emissivity, and T_s is absolute surface temperature.

$$q'' = \bar{h}_{total} \Delta T_e \quad (1.36)$$

2.9 Effect of cooling rate on weld metal

The ease of heat transfer from the surface of the workpiece in underwater welding affects the properties of the welded joint. The greatest effects are due to the formation of hardening structures in the HAZ area and residual stresses in the joint, which are favoured by the fast cooling rate of the weld. Heat loss from the welding area is greatly affected by the water environment for plate thickness up to 20 mm. Figure 9 shows that the heat loss in a local dry chamber can be adjusted by controlling the heat input and the plate thickness used. This method makes it possible to attain similar cooling time $t_{8/5}$ for underwater welding as compared to air welding. In order to ensure the weld cooling time, the arc must be stable [41].

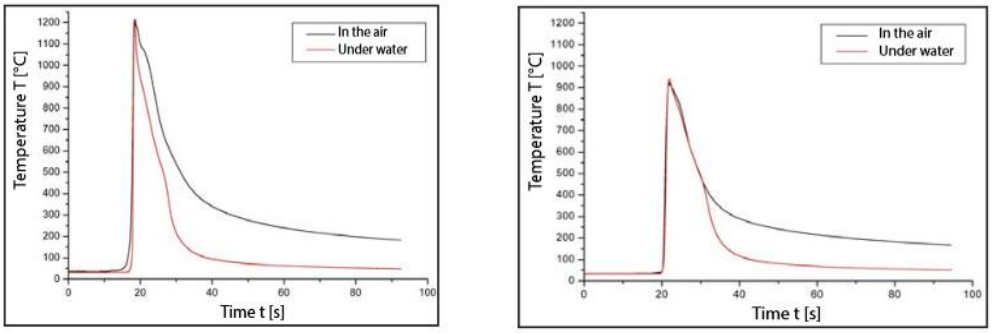

(a) (b)

Figure 9 a) Comparison of thermal cycles for overlay welding of 12 mm thick plate in air and underwater using the local dry chamber method; welding linear energy e_L= 0.9 kJ/mm. b) Comparison of thermal cycles for overlay welding of 16 mm thick plate in the air and underwater using the local dry chamber method; welding linear energy e_L= 1.3 kJ/mm [41].

3. Artificial intelligent control mechanism for underwater welding

Rapid cooling and hydrogen embrittlement are common characteristics of UWW. Chon L. Tsai and Koichi Masubuchi studied the mechanics of rapid cooling and their effects [16]. The final microstructure of the heat affected zone (HAZ) for a given material is determined by the composition, peak temperature and cooling rate. These determining parameters of the HAZ microstructure can possibly be controlled to yield a favourable microstructure. However, controlling the composition of the HAZ of the base metal is difficult. In UWW the formation of martensitic HAZ having high hardness and poor notch toughness are results of the fast cooling effect of the water environment. Water dissociation in UWW results in the formation of hydrogen and this subjects the microstructure of the HAZ to hydrogen cracking [42, 43]. Consequently, it is important to control the cooling rate of the weld metal.

FCAW is a semiautomatic welding process and the operation continues until the weld pass is completed, but in the case of the SMAW process, the electrodes require changing from time to time. FCAW has reduced weld crack sensitivity compared to SMAW because of the interruption of the welding pass in SMAW, especially for steels with CE less than 0.4 %. One major disadvantage of FCAW is the difficulty of tracking the joint precisely in the typically poor visibility conditions underwater. The diver/welder has difficulty hearing the arc sound or seeing the plasma during underwater FCAW, which poses challenges to obtaining information regarding the frequent changes in welding current and voltage [20, 44, 45]. These challenges make it is very important to design a robust control system to control the welding process in the underwater environment.

A constant voltage power source and constant wire feeding rate is usually used in FCAW, as depicted in Figure 10 [20]. The output characteristic of the power supply at the working point is described in Equation 2.1:

$$U = U_{ol} - R_s I \tag{2.1}$$

Where U_{ol} is the equivalent open loop voltage, and R_s is the equivalent source resistance including the cables.

The output voltage is distributed in two parts, which are the arc voltage U_{ol} and the wire stickout voltage U_s.

$$U = U_a + U_s \tag{2.2}$$

FCAW arc voltage-current characteristics can be described as in Equation 2.3:

$$U_a = K_a L_a + R_a I + U_c \tag{2.3}$$

Where K_a is electrical field intensity, which is the voltage drop per unit length of arc column, R_a is the arc resistance, and U_c is a constant that is related to the anode and cathode voltage.

The voltage drop on the wire stickout is described as in Equation 2.4:

$$U_s = \rho \frac{L_s}{A} = K_s L_s I \tag{2.4}$$

Where ρ is the electric resistivity of the wire over the temperature range, A is electrode or wire cross-section area, and K_s is average resistance per unit length of wire stickout.

According to Lesnewich [46] and Halmoy [47], the melting rate can be described as in Equation 2.5:

$$V_m = K_m I + K_e L_s I^2 \quad (2.5)$$

Where V_m is the melting rate, $K_m I$ is the melting rate from the arc heat, and K_m is a constant related to the anode voltage drop. $K_e L_s I^2$ is the stickout wire resistance heat contribution to the melting rate, and K_e is another constant.

$V_m = V_f$ (when in steady state, the melting rate, if represented in wire length per unit time, equals the wire feed rate).

The contact-tip-to-workpiece distance (CTWD) comprises the arc length and stickout length:

$$H = L_s + L_a \quad (2.6)$$

In the welding process, the power source voltage, CTWD, wire feed rate, arc length and current are the controllable parameters.

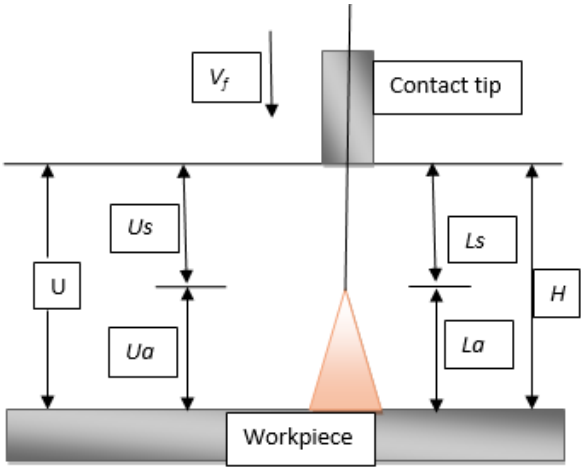

Figure 10 Illustration of arc parameters [20].

3.1 Artificial neural network

A neural network is a modelling tool for data that captures the data and represents them in complex input/output relationships. Figure 11 illustrates the neural network schematic diagram that is analysed in this thesis. The signals from input links are received by the neuron, a new activation level is computed, and an output signal is sent through the output link(s).The synaptic weights of the network are modified by the procedure of the learning algorithm to achieve the desired objective of the design. Long-term memories in artificial neural networks are stored in the weights.

The most commonly used neural network architecture is the multilayer perceptron (MLP) neural network. In MLP neural networks, the inputs go through a weighted sum biasing and are then passed through an activation function to produce the output. Usually, the input data is fedback to the network again and again. After each presentation, the output of the neural network is matched to the output that is desired by the designer, and the difference between them gives an error signal. The weight is adjusted by presenting the error back to the neural network in a manner that will decrease the error for every iteration. This process is aimed at reducing the error value and making the neural network model approach the desired target. The neural network illustrated in Figure 12 uses a back-propagation algorithm in which the weight is changed as the iteration increases, thereby reducing the error and getting closer to the desired target [48, 49].

The artificial neural network (ANN) scheme illustrated in Figure 11 is useful for predicting the weld bead geometry of welds produced during underwater wet welding. This ANN process employs mapping of a set of input data to its output patterns. The process provides a learning pattern of previous examples to estimate how the input parameters relate to the output parameters. The analysis employs a feedforward back-propagation network and the training is applied to a scaled conjugate gradient (SCG) back propagation algorithm. The training pattern fulfilment of the requirement for the accepted ranges of WPSF (penetration shape factor) = *W/P* and WRFF (reinforcement form factor) = *W/R* is employed in verifying the quality of the weld. The accepted range for a weld with good quality is a maximized penetration to width ratio and minimized undercut and reinforcement. Note that too high penetration to width ratio can result in hot cracking [50, 51].

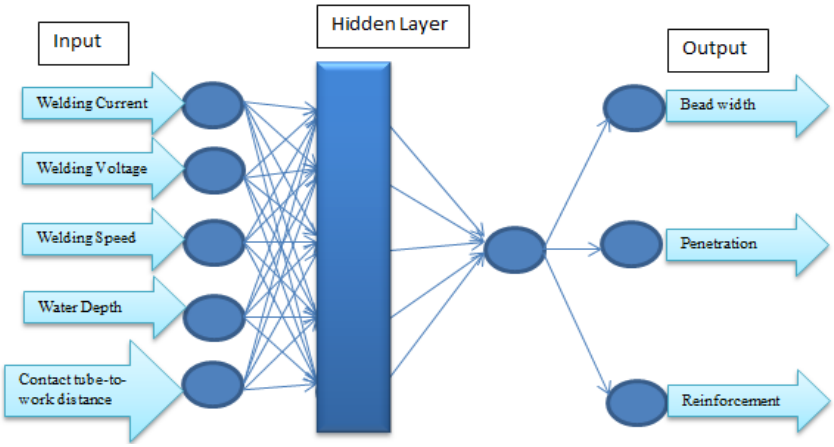

Figure 11Welding input vs output parameters.

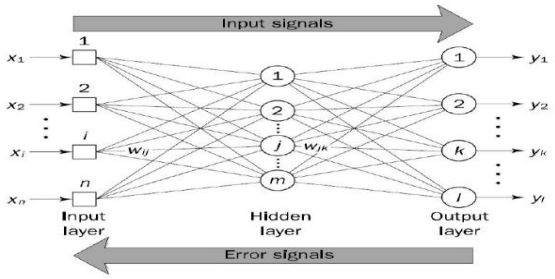

Figure 12 Three-layer backpropagation neural network [52].

The back-propagation training algorithm can be summarized as follows [52]**.**

Step 1: Initialization

$$\left(-\frac{2.4}{F_i},\ +\frac{2.4}{F_i}\right) \tag{2.7}$$

The network weight and threshold levels are set to random numbers that are uniformly distributed in a narrow range. The total number of the inputs in neuron I is represented by F_i in the network.

Step 2: Activation

The inputs to the neural network $x_{1(p)}$, $x_{2(p)},\ldots x_{n(p)}$ and the desiredoutputs$y_{d,1(p)}$, $y_{d,2(p)},\ldots$. $y_{d,n(p)}$ are applied.

The outputs of the neurons are calculated in the hidden layer:

$$y_j(p) = sigmoid[\sum_{i=0}^{n} X_{i(p)} \times W_{ij(p)} - \theta_j] \tag{2.8}$$

The actual outputs of the neurons are calculated in the output layer. The number of inputs m of neuron k in the output layer:

$$y_k(p) = \text{sigmoid}[\sum_{j=0}^{m} y_{j(p)} \times W_{jk(p)} - \theta_k] \tag{2.9}$$

Step 3: Weight training

Adjust the weights in the backpropagation network to propagate backwards the errors of the output neurons.

(a) Obtain the error gradient for the neurons in the output layer:

$$\delta_k(p) = y_{k(p)} \times [1 - y_{k(p)}] \times e_{k(p)} \tag{2.10}$$

Where

$$e_{k(p)} = y_{dk(p)} - y_{k(p)} \tag{2.11}$$

Adjust the weights and calculate the corrections:

$$\Delta w_{jk(p)} = \alpha \times y_{j(p)} \times \delta_{k(p)} \quad (2.12)$$

Adjust the weights at the output neurons:

$$w_{jk(p+1)} = w_{jk(p)} + \Delta w_{jk(p)} \quad (2.13)$$

(b) Obtain the error gradient for the neurons in the hidden layer:

$$\delta_{j(p)} = y_{j(p)} \times [1 - y_{j(p)}] \times \sum_{k=0}^{l} \delta_{k(p)} \times W_{jk(p)} \quad (2.14)$$

The weight corrections are solved.

$$\Delta w_{ij(p)} = \alpha \times x_{i(p)} \times \delta_{j(p)} \quad (2.15)$$

Adjust the weights at the output neurons.

$$W_{ij(p+1)} = w_{ij(p)} + \Delta w_{ij(p)} \quad (2.16)$$

Step 4: Iteration

The iteration p is increased by one and the process goes back to step 2 and the process is repeated. The repetitions will be stopped when the selected error criterion is met.

Validation performance:

A single presentation of each input/output data on the training set, known as the epoch, indicates the iteration at a minimum validation performance [53]. The NN analyses training continued for 1123 more iterations before the training stopped. Figure 13 shows no significant problems with the training, and there is good similarity between the validation and test curve. It is possible that some overfitting might have occurred if there were any significant increase of the training curve before the validation curve increases. The analysis has a small final mean squared error (MSE), which is 9.1499e-4 at zero epochs. The MSE helps in evaluating the performance of the network. The MSE is an average of the squares of all the individual errors between the model and the real measurements. The MSE is important for comparing different models having the same sets of data.

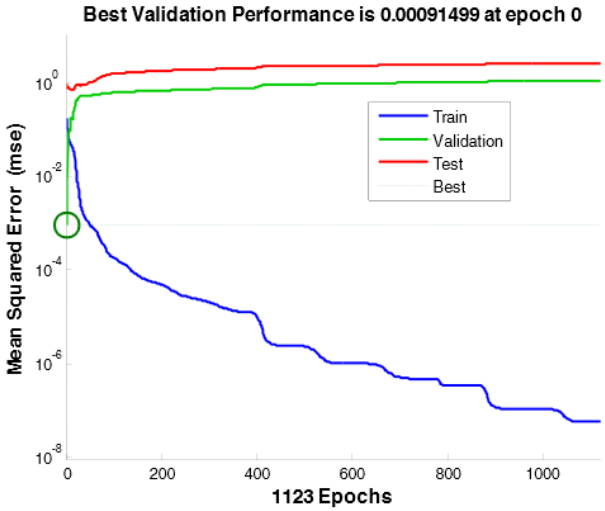

Figure 13 Validation performance curve.

Regression plot:

This plot is useful in validating the network performance. The regression plots in Figure 14 show the targets of the network outputs for training, validation and test sets. The network outputs are equal to the targets for a perfect fit, and the result for this analysis shows a considerably good fit for all sets of data, with the values of R being 0.96637 or above in each case. These results were achieved by retraining of the neural network, which changed the initial weights of the network. In this analysis, 100% of the sets of data were employed in training, validation and testing of the network generalization.

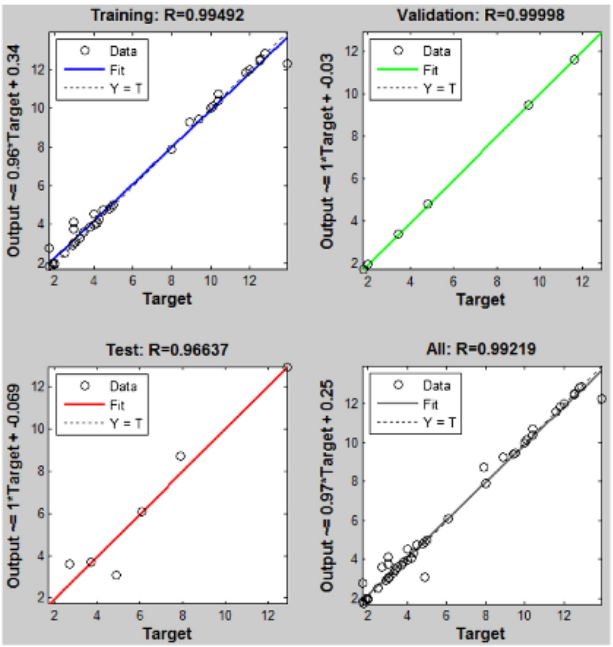

Figure 14 Regression plot.

Design Parameters:
The process parameters values *I*, *U*, *v*, *D* and *H* and bead geometry values *W*, *P* and *R* in Table 1 are the values used for training of the neural network. These values are from experimental data adopted from reference [54]. The modified table includes the error results for each testing. The errors in italics are the errors from the training that are large and not desirable. A smaller error tending to zero is desired or an actual zero, the latter is however not easy to achieve.

Table 1 Experimental data adapted from [54].

Serial number	Process parameters				Water depth	Bead geometry			Error = Output (*W*, *P*, *R*) − Target		
									Target = 0		
	I (A)	*U* (V)	*v* (m/s)	*D* (m)	*H* (m)	*W* (m)	*P* (m)	*R* (m)	Δ*W* (m)	Δ*P* (m)	Δ*R* (m)
1	280	28	10	20	40	10.4	2.5	4.3	0.0061	0.0091	0.0016
2	320	32	6	20	20	12.5	3.8	8	0.0022	−0.0394	0.0998
3	300	32	10	22	60	10.4	3	4	−0.3280	*−1.1397*	*−0.5471*
4	340	28	6	22	0.1	13.9	3.5	3	*1.6136*	−0.1071	*−0.7470*
5	280	30	6	24	60	12.9	3.7	6.1	0.0223	−0.0104	0.0083
6	320	26	10	24	0.1	11.6	1.8	2	0.0093	0.0650	0.0269
7	300	26	6	18	40	12	2.9	5	−0.0177	−0.0126	0.0080
8	340	30	10	18	20	9.4	4.2	4.3	−0.0193	0.1365	0.0038
9	280	26	12	22	20	8.9	1.7	4.5	−0.3662	*−1.0633*	−0.2616
10	320	30	8	22	40	11.8	3.3	4.8	−0.0323	0.0312	0.0007
11	300	30	12	20	0.1	12.8	1.7	1.9	−0.0363	−0.1342	−0.0876
12	340	26	8	20	60	9.5	3.4	4.8	0.0169	−0.0132	0.0008
13	280	32	8	18	0.1	12.5	2	2	0.0089	0.0151	0.0553
14	320	28	12	18	60	7.9	2.7	4.9	*−0.8149*	*−0.9025*	*1.8429*
15	300	28	8	24	20	10.1	3.1	4.9	−0.0211	0.0055	−0.0067
16	340	32	12	24	40	10	3	4	0.0011	−0.0140	0.0213

3.2 Fuzzy logic control

Fuzzy logic:

SMAW and FCAW are widely used in underwater welding. The two techniques depend on process parameters that usually vary over a large range. Fuzzy logic (Figure 15) is able to learn the dependency of interaction between the process variables of the welding input variables and welding output variables. The theory of fuzzy sets is valuable in experimental data modelling involving uncertainties that arise between the relationships of the process variables of the welding inputs and the subsequent bead geometry output. The fuzzy model is useful in studying the suitability of the relationships that exist in the fuzzy logic for predicting the profile characteristics of the weld bead geometry. The structure of the membership function of two inputs (error and error change) and subsequent output for the fuzzy controller and the three outputs (proportional gain K_p, integral gain K_i and derivative gain K_d) for the hybrid fuzzy-PID controller designed for this research is shown in Figure 16. The linguistic variables defined are sentences in normal English language such as *negative big*, *negative small*, *zero*, *positive small* and *positive big*, and these are expressed by fuzzy sets. The fuzzy sets are described by membership functions, fuzzy rules, fuzzification, inference system and defuzzification. Fuzzy set outputs are obtained in crisp form [55, 56]. Figure 15 summarizes the operations that are carried out in the fuzzy logic controller. In this research, the output from the defuzzifier, which is two inputs (error and error change) and the subsequent output for the fuzzy controller and three outputs (proportional gain K_p, integral gain K_i and derivative gain K_d) for the hybrid fuzzy-PID, is fed into the input signal of the welding machine. These variables are subtracted from the desired input signal, thus giving the actual input signal to the welding machine.

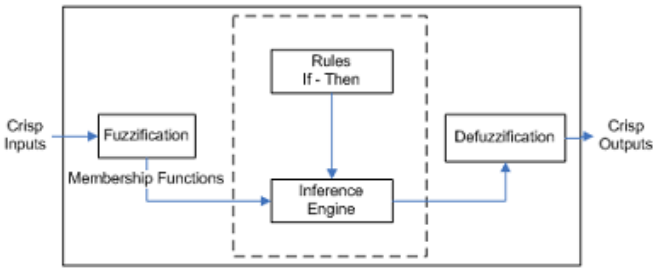

Figure 15 Fuzzy logic controller block diagram [57].

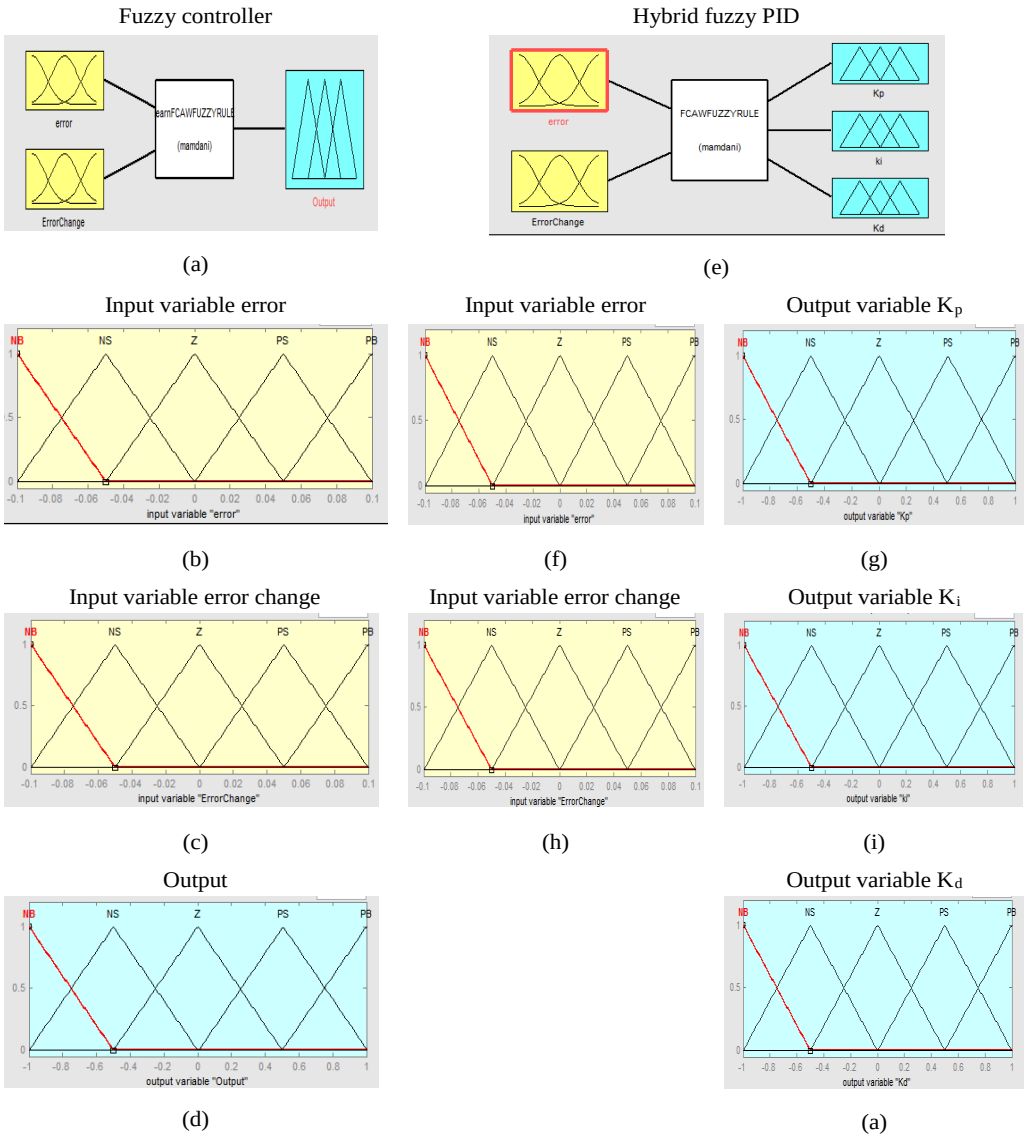

Figure 16 Membership function diagram.

Rules:

The fuzzy control rule is a collection of fuzzy IF-THEN rules in which the preconditions are the error and error change variable and the consequences are the output from the fuzzy logic variables that involve linguistic variables. The fuzzy control rule for the fuzzy controller and hybrid fuzzy PID controller have preconditions as the error and error change variable and consequences as output and gain parameters respectively.

Defuzzification process:

The defuzzification process converts the fuzzy output into a crisp output using a defuzzification technique that combines membership functions with fuzzy rules [58, 59]. This work uses the centroid defuzzification technique. Based on the assumption made for the membership function and fuzzy rules, the defuzzification process is as shown in Figure 17. From the figure, it can be seen that as each individual set of input parameters is changed, there is a subsequent change in the output.

Rules for fuzzy controller

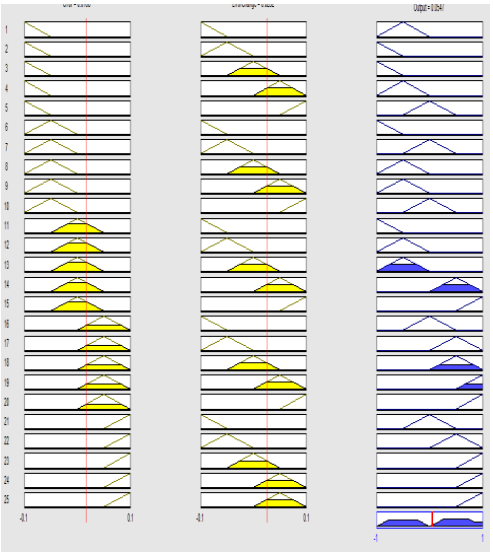

Rules for hybrid fuzzy PID

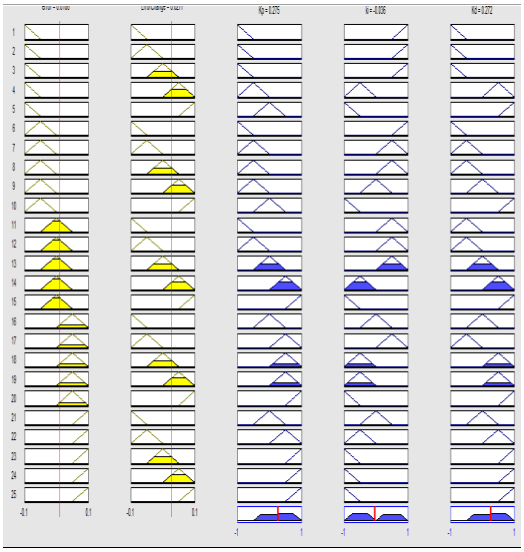

(a) (b)

Figure 17 Centroid defuzzification technique.

3.3 Underwater welding hybrid fuzzy-neural controller

The proposed schematic diagram shown in Figure 18 is a possible controller for an underwater wet welding process in which NN optimization of the welding process parameters is used. The neural network model analysed in this dissertation can be an essential part of the control architecture of the proposed controller with the target of designing a robust control system for UWW. The major objective of this controller is aimed at controlling the welding process parameters for different measured water depth *H*. It should be noted that the water depth is not a control parameter but a parameter that is measured as the welding operation occurs. Thus, the water depth parameter for the welding process is measured as the depth at which the welding activity takes place. As the water depth varies, the change in the measured water depth consequently changes the welding process parameters and this also affects the bead geometry *W, R* and *P*. The fuzzy controller acts as a compensator for this change and re-adjusts the welding process parameters *I, u, V* and *D*.

The inverse NN has a fixed parameter value that represents the desired bead geometry parameter as inputs to the inverse NN and the best parameter of the welding process as output from the inverse NN. The training gave rise to errors in experiment 1 from Table 1, which are the best set of parameters because the errors for *W, R* and *P* are closer to zero compared to the values for the other experiments. The fixed output parameters *I0, U0, v0, D0*, and *H0*are for water depth at zero position. These output parameters from the inverse NN are added up with the difference from the change in the output parameters $\Delta I, \Delta U, \Delta V, \Delta D$ of the fuzzy controller. The change in the output parameters $\Delta I, \Delta U, \Delta V, \Delta D$ of the fuzzy controller compensates for the change in the welding process parameters and inputs the adjusted welding process parameters to the welding machine. For every measured change in the water depth H, a change in the bead geometry $\Delta W, \Delta P$ and ΔR that is the input to the fuzzy controller occurs and gives an output of $\Delta I, \Delta U, \Delta V, \Delta D$. The welding process parameter from the welding machine is equal to the NN forward model and as such any change in the NN forward model is a subsequent change in the welding process itself. This control mechanism has the advantage of eliminating the need for online measurement of the weld bead geometry, which in most cases is difficult to achieve.

This system is a possible robust system that requires further investigation. The simultaneous control of the welding process parameters is essential in achieving a stable welding arc and optimal heat input that is capable of producing desired weld bead width, penetration and reinforcement.

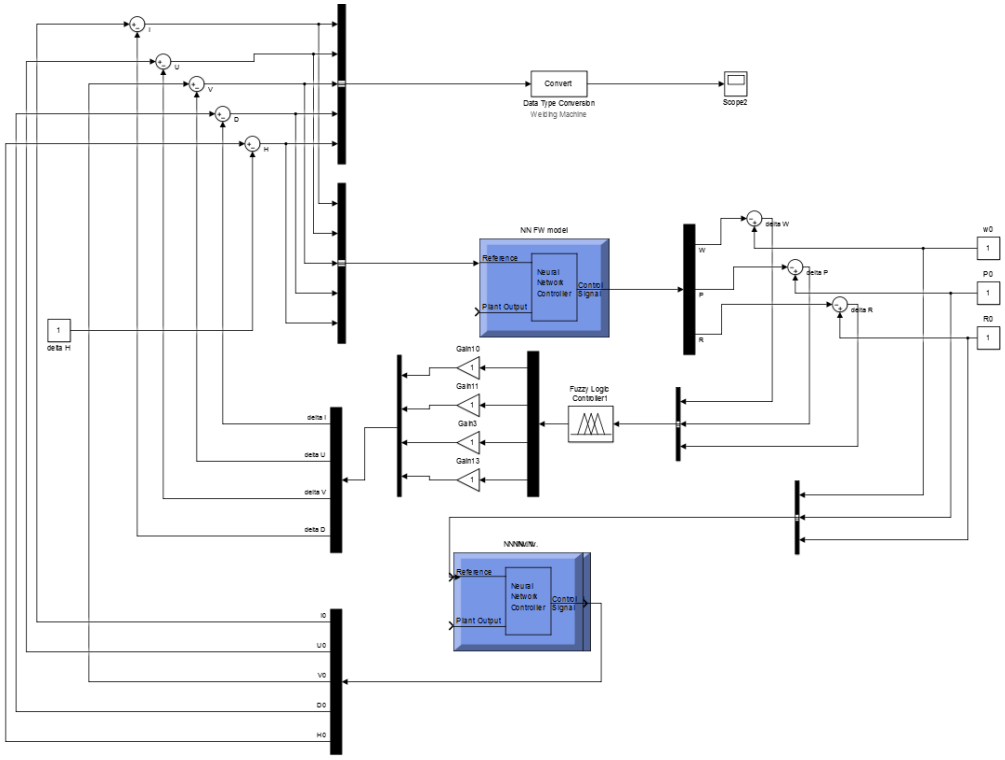

Figure 18 MIMO controller design schematic diagram.

4. Intelligent control systems theory

A classical SISO (single-input-single-output) control system (Figure 19) is designed in this section. MIMO (multiple-input-multiple-output) control systems such as the one shown in Figure 18are usually more complicated [60]. The input of the control system is the desired value and the output is the actual value. A supposedly perfect system should have the actual value equal to the desired value. However, this is usually not the case, which makes control system design very important. When the actual value is different from the desired value, a controller is designed to give a zero error between the actual value and the desired value. In a closed loop system, the controller takes action when the error is not zero. This error is fedback to the system to correct the differences as a result of any disturbances or uncertainties. The error signal is the output of the compensator and input to the controller.

Various types of controllers exist, such as PID controllers and fuzzy logic controllers [61]. This section deals with utilizing the advantages of a PID controller and fuzzy logic controller to control the FCAW process for underwater welding activities.

Figure 19 SISO control system.

The vital issue when designing control logic is to make sure that the dynamics of the closed loop system is stable. This means that bounded disturbances give bounded errors that are sufficiently efficient enough to reject any unforeseen disturbances and that have fast response to changes during operation [62]. A number of techniques are employed in this work to determine the stability of the closed loop system, namely root locus , Routh-Hurwitz criterion, Nyquist plot and Bode plot [63, 64].

4.1 PID controller

The PID (proportional, integral, derivative) controller is the most widely used industrial controller. The name describes the three different actions that the controller executes in responding to a non-zero error input to the controller. These three actions occur at the same time, operating parallel to each other, and the output is summed up as shown in Figure 20. The error input signal in the first path is directly multiplied by the proportional gain K_p, and the output is proportional to the error. In the first path, no action is taken on the input signal. In the second path, the error input signal is first integrated, thereby producing an output integral of the error. This means that the error is integrated and multiplied by K_i. The third path is the derivative action, where the error is first differentiated and multiplied with K_d [61]. The control logic of the PID controller is implemented by finding suitable gain parameters K_p, K_i, and K_d. The PID controller's transfer function is obtained by adding three terms which are the proportional, integral and derivative controls (Equation 3.1). One major drawback with a PID controller is that it is not suitable for controlling a system having a big lag and many uncertainties and parameter variations. To address this deficiency, a fuzzy-PID hybrid control system can be used [65].

$$PID(s) = K_p + K_i/s + sK_d \tag{3.1}$$

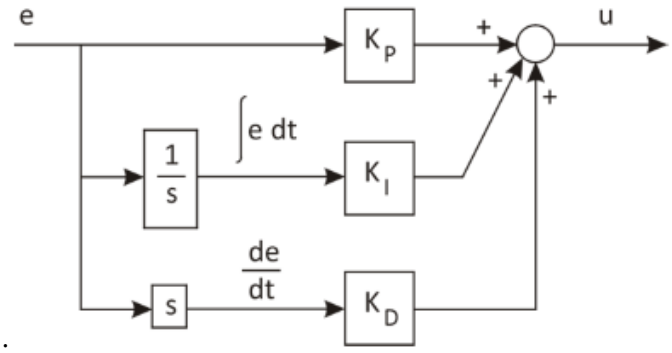

Figure 20 PID controller structure [61].

4.2 Hybrid fuzzy PID controller

The control system (Figure 21) is a typical fuzzy-PID hybrid control system. The hybrid control system utilizes the advantages of a fuzzy controller and a PID controller. The controller is able to overcome nonlinearities and uncertainties in a system. Fuzzy logic is useful in tuning different parameters of PID controllers. The aim of the fuzzy rule design is to tune the parameter K_p, K_i, and K_d according to the actuating error signal function. The proportional term is responsible for the control process that is proportional to the error. The integral term with the help of an integrator assists in reducing the steady state errors by the use of low frequency compensation. The derivative term is responsible for improving transient response through high frequency compensation [65].The design and implementation of the control system uses efficient techniques that can meet performance requirements in the presence of disturbances and uncertainty [66].

The basic process model of FCAW for underwater welding control has been derived by Chon L. Tsai et al. [20]. In the welding process, the power source voltage, CTWD, wire feed rate, arc length and current are controllable parameters. In welding practice, it is observed that an

increase in the length of CTWD will at the same time increase the arc length and later shorten when a steady state is reached, that is, the arc is stable at the state of fixed CTWD, wire feed rate, and power source setting.

The dynamic model of welding arc power describes the transient characteristics in the change of one or more parameters. The dynamic model is based on the equations in the static model deviation from the arc parameter derivation in chapter 3 [20].

The dynamic equation of the power source is:

$$U = U_{ol} - R_s I - M_s \frac{di}{dt} \tag{3.2}$$

Its frequency domain expression (Fourier Transform) is:

$$\Delta U(s) = - R_s(T_p S + 1)\Delta I(s) \tag{3.3}$$

Where M_s is power source inductance.

The final dynamic model after setting a reasonable range of GMAW is given by the transfer function as presented in Equation 3.4. Note that the GMAW process is similar to FCAW, the difference being that in FCAW the wire electrode is flux cored rather than solid as in GMAW.

$$\frac{I(S)}{H(S)} = -3.46 \frac{0.0168S^2+0.457S+1}{1.28e-005S^2+0.01576S^2+0.1776S+1} \tag{3.4}$$

The transfer function presented in Equation 3.4 is used as the plant model of the control system in Figure 22. The transfer function represents the relationship between the arc current and the CTWD. The system transfer function is unstable but can be made stable by adjusting the position of the poles by the addition of a real zero. Implementation of the algorithm shown in Table 2 is used to adjust the poles and zeros of the transfer function. The MATLAB SISOTOOL adjusts the position of the poles or zero in the root locus. The Bode plot (Figure 21) shows the relationship between the output signal *I(S)* and the input signal *H(S)* that describes the linear system. The stability of the system was also determined using the Bode plot and it indicates that the system is unstable. The closed loop Bode plot has a gain margin of -10.8 dB at 0 rad/sec and phase margin of 74.7 degrees at 4390 rad/sec. This indicates that for stability to be achieved, the gain needs to be decreased by 10.8 dB. Adding a real zero at s = -943 will make the transfer function of this system stable. The closed loop Bode plot (Figure 21D) of this system has a peak response of 2.96 dB at a frequency of 3.71e-008 rad/sec. The step response (Figure 21E) of the system has input amplitude of 1.4. The output response follows closely the input response without an overshoot.

Table 2 MATLAB implementation

```
NUM=-3.46*[0.01685 0.4575 1]
DEN=[1.28e-5 1.576e-2 1.776e-1 1]
sys=tf(NUM,DEN)
sisotool(sys)
```

Root locus and Bode plot showing the unstable system

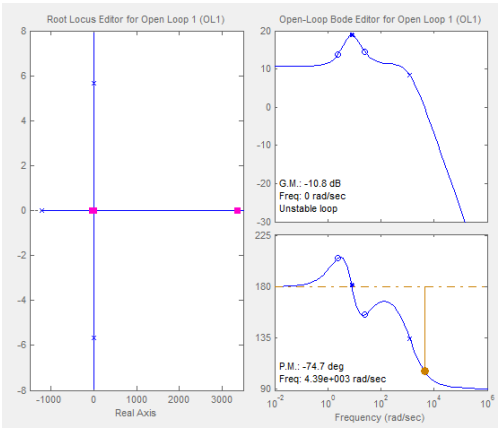

(a)

Root locus and Bode plot showing the stable system by adding a real zero

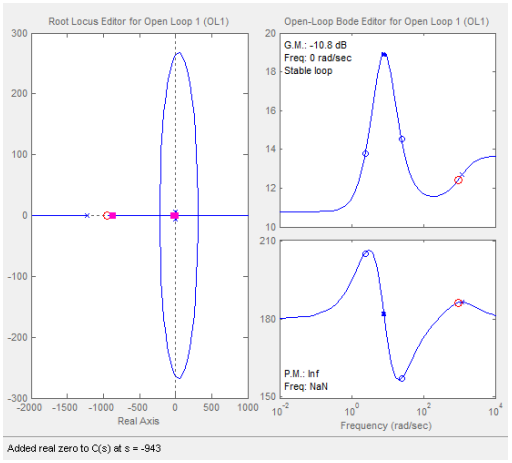

(b)

Closed loop Bode plot for the unstable system

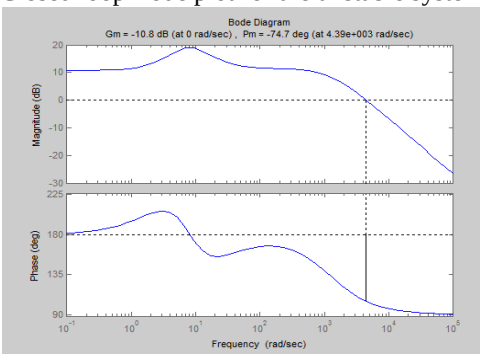

(c)

Closed loop Bode plot for the stable system

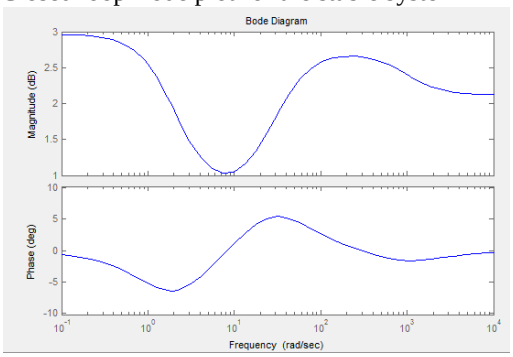

(d)

Step response for the stable system

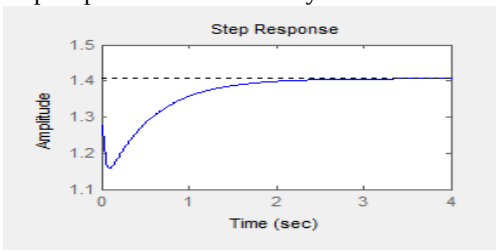

(e)

Figure 21 Results from MATLAB implementation of Table 2.

The PID, fuzzy and hybrid fuzzy PID control algorithm is a part of the plant model shown in Figure 22. The performances for the different control systems are compared in the simulation results in Figure 23. The system response was tested by using a step input signal. The dynamic response of the various control systems shows that the fuzzy controller gives a better result than the PID controller. The fuzzy controller was faster that the PID controller. Furthermore, the PID controller gave rise to overshoot. The hybrid fuzzy PID controller gave a more satisfactory result for overshoot, rise time and steady state error. The proposed hybrid fuzzy PID controller demonstrates the advantages of integrating fuzzy and PID controllers. The hybrid fuzzy PID controller is suitable for the FCAW process used in underwater welding since the input current and output CTWD can be predicted and controlled.

In FCAW for underwater welding, control of the welding arc current relative to CTWD is an effective way of ensuring the desired heat input and arc length during welding. The application of a hybrid fuzzy PID controller has the potential of mitigating the effect of uncertainties and disturbances during underwater welding. A properly controlled underwater welding process will result in bead geometry that is favourable for sound and reliable welds in welding of offshore structures underwater. A sound and reliable weld implies a maximized penetration to width ratio and minimized undercut and reinforcement.

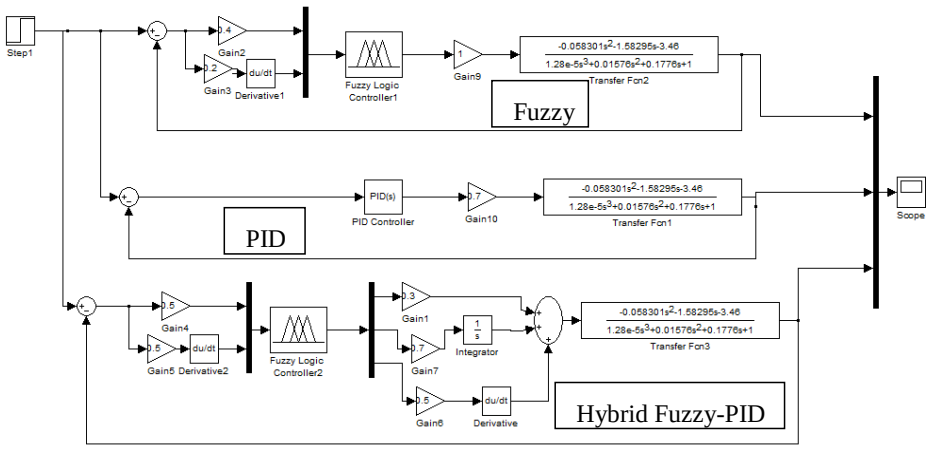

Figure 22 Control system for underwater FCAW.

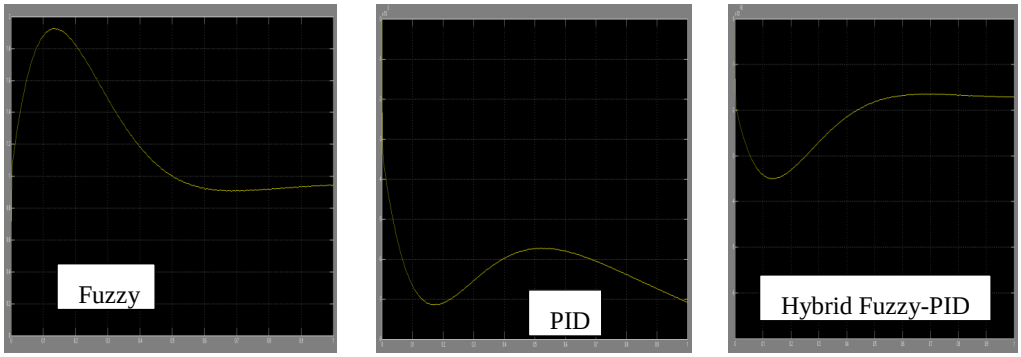

(a) (b) (c)

Figure 23 Matlab simulation results of PID, Fuzzy and hybrid fuzzy PID control.

5. Suggestions for further study

Use of an intelligent control mechanism in underwater welding processes obviously has great potential. However, considerable further study is necessary in this regard. Laboratory investigation of intelligent control will make it possible to understand clearly how to improve the control dynamics of the welding process during underwater welding.

The first points of interest are to clearly verify how control of the arc current and CTWD during underwater welding affects the heat input and cooling rate and how to minimize heat losses from the plate surface.

One relevant point that is worthy of further investigation is the proposed controller in this thesis. Practical welding operation with this controller and analysis of the weld bead geometry to verify the quality of weld joints produced will go a long way to validating the controller for industrial use.

Within the area of underwater welding as a whole, much interesting work has been done and many interesting ideas presented. Researchers have proposed ways of improving the underwater weld quality such as the development of special electrodes for underwater welding, the building of barriers against water to shield the weld metal, and the use of induction heating methods to optimize the heat input to the weld metal thereby reducing the cooling effect and temper bead welding. It is important to study these processes further and work on finding a means to integrate the advantages of these various approaches to arrive at a simple and effective method of ensuring good weld quality in underwater wet welding.

Other issues that could be worthwhile addressing include the possible development of fully automated hybrid arc-laser welding for underwater welding and the use of remote welding operations in underwater welding. The use of hybrid arc-laser welding will hopefully lead to improvements in the weld penetration and reduce the cooling effect of the water environment. Additionally, it could be interesting to investigate the role of a shielding process that has the ability to disperse the water from the plate surface, as well as methods for underwater preheating before welding is done.

6. Conclusion

There is no shortage of exciting research topics in the area of underwater welding and underwater welding research is wide open to innovative research. About 80% of underwater welding activities are in the form of dry underwater welding. Wet underwater welding accounts for about 20% of welding activities. In the light of the complicated nature and high costs of dry underwater welding, the potential gain from improved knowledge of wet underwater welding is obvious – there is a lot of research to do in the area of wet underwater welding.

This thesis covered several aspects of underwater wet welding. A thorough literature review investigated the fundamental difficulties associated with underwater wet welding and compared them with air welding. The metallurgical characteristics of underwater wet welding and the various welding processes commonly used in underwater welding were investigated. The research work identified a number of ways of improving the weld qualities of welded joints done underwater.

The weldability of structural steels in the offshore environment was reviewed, and based on current knowledge of grades of steels suitable for offshore applications, it became evident that the alloying elements of the steels and their chemical composition play avital role in the weld quality achieved. The harsh conditions of the offshore environment impose particular demands. It is clear that steels with carbon equivalent greater that 0.45 % by weight are not suitable as there is a high tendency of cracking and martensitic microstructure after welding. Thermo-mechanically rolled steels have shown greater potential for offshore applications because these steels have high strength with reduced carbon content and have high toughness in the HAZ.

Underwater welding is important in the oil and gas industries, ship building industry and renewable energy industry. It was observed that the fast cooling rate of the weld metal during underwater welding is a major concern. Weld joints done underwater suffer a major setback on the basis of the structural integrity of the welded joints as it affects the HAZ toughness because of the cooling effect of water around the weld. The loss of alloying elements and instability of the welding arc are other factors that reduce the quality of underwater wet welding welds as compared to air welding.

Direct current electrode negative (DCEN) polarity power source is suitable for underwater wet welding. The control of the welding process parameters to achieve a stable arc will yield higher penetration because of the reduction of arc wander and efficient heat transfer.

This thesis has been able to identify the effects of various welding parameters in underwater welding applications and the effect of the water environment. Based on this knowledge, an intelligent control mechanism for underwater FCAW process is proposed. The control mechanism utilizes the advantages of fuzzy control, PID control and neural network control. The Fuzzy-Neural control method and Fuzzy-PID control method are

possible solutions for controlling underwater welding processes. Most importantly, the hybrid of fuzzy and PID control proposed in this paper is capable of successfully controlling the welding input and achieving a desired welding output. In this case, current is the input and CTWD is the output. The use of the proposed controller will allow for arc stability and appropriate heat input, thereby mitigating the cooling effect of the water environment during underwater welding.

The MATLAB simulation results for control of FCAW welding using a hybrid of a fuzzy and PID controller clearly show that a properly designed hybrid of fuzzy and PID control gives satisfactory rise time and overshoot of the system. Thus, the control system is evidently capable of adapting the control to uncertainties and disturbances that may arise from the environment.

An increase in the water depth will lead to decrease of weld bead width, however it will result in increased penetration and reinforcement. Increasing voltage results in increased weld bead width, penetration and reinforcement. However, increasing voltage beyond the optimal value will lead to loss of alloying elements from the weld. The effect of welding current is greater on penetration than on bead width and reinforcement. An effective way of minimizing porosity in underwater welds is the use of direct current electrode positive (DCEP) with low current output or the use of direct current electrode negative (DCEN) with high current output.

References

[1] Alan J. Brown, James A. Staub and Koichi Masubuchi, "Fundametal study of underwater welding," in *Offshore Technology Conference*, USA, 1972.

[2] Akhil Chhaniyara, "Underwater Welding," *International Journal of Mechanical and Production Engineering Research and Development,* vol. 4, no. 1, pp. 63-72, 2014.

[3] Santos V. R., Monteiro M. J., Rizzo F. C., Bracarense A. Q., Pessoa E. C. P., Marinho R. R. and Vieira. L. A., "Development of an Oxyrutile Electrode for Wet Welding," *Welding Journal,* vol. 91, pp. 319-328, 2012.

[4] Keats David J., "Underwater wet welding made simple: benefits of hammerhead wet-spot welding process," *International Journal of the Society for Underwater Technology,* vol. 28, no. 3, pp. 115-129, 2009.

[5] Shi Y., Wang G. and Liu C., "Study on Mini-cap Local Dry Underwater Flux-Cored Arc Welding and Online Control of Weld Penetration," in *The Twentieth International Offshore and Polar Engineering Conference*, China, 2010.

[6] Zhang X, Chen W., Ashida E. and Matsuda F., "Metallurgical and Mechanical Properties of Underwater Laser Welds of Stainless Steel," *Journal of Materials Science and Technology,* vol. 19, no. 5, pp. 479-483, 2003.

[7] Szelagowski P., Schafstall H.G., Rothe R. and Sepold G., "Wet Underwater Welding with High Power CO2 Lasers," in *Proceedings, International Conference of Beam Technology,* UK, 1987.

[8] AWS, "underwater welding code," USA, 2010.

[9] Liu S., "Fundamentals of underwater welding," in *Underwater wet welding seminar*, Mexico, 1999.

[10] Rodriguez-Sanchez J.E., Rodriguez-Castel-lanos A., Perez-Guerrero F., Carbajal-Rome-ro M.F. and Liu S., "Offshore fatigue crack repair by grinding and wet welding," *Fatigue and Fracture of Engineering Materials and Structure,* vol. 34, no. 7, pp. 487-497, 2011.

[11] Pignanelli A. and Csillag J. M., "The impact of quality management on profitability: An emperical study," *Journal of Operations and Supply Chain Management,* vol. 1, no. 1, pp. 66-77, 2008.

[12] Ozaki H., Naiman J. and Masubuchi K., "A study of hydrogen cracking in underwater steel welds," *Welding Research Supplement,* pp. 231-237, 1977.

[13] Ibarra S., Grubbs E. C. and Olson D. L., "Metallurgical Aspect of Underwater Welding," *Journal of Metals,* vol. 40, no. 12, pp. 8-10, 1988.

[14] Ando S. and Asahani T., "A Study on The Metallurgical Properties of Steels Welds with Underwater Gravity Welding," in *Underwater Welding:Proceedings of The International Conference held at Trondhein*, Norway, 1983.

[15] Rosenthal D., "The Theory of Moving Sources of Heat and Its Application to Metal Treatments," *Transactions of the ASME,* vol. 68, pp. 849-866, 1946.

[16] Chon-Liang Tsai and Koichi Masubuchi, "Mechanisms of rapid cooling in underwater welding," *Applied Ocean Research,* vol. 1, no. 2, p. 99–110, 1979.

[17] Ibarra S., Grubbs C. E. and Liu S., "State of the art and practice of underwater wet welding of steel," International workshop on underwater welding of marine structures, USA, 1994.

[18] Faisal M. Al-Abbas, Tariq A. Al-Ghamdi and S. Liu, "Comparison of Solidification Behavior Between Underwater Wet Welding and Dry Welding," in *ASME 2011 30th International Conference on Ocean, Offshore and Arctic Engineering*, Netherland, 2011.

[19] Ghadimi P., Ghassemi H., Ghassabzadeh M. and Kiaei Z., "Three-Dimensional Simulation of Underwater Welding and Investigation of Effective Parameters," *Welding Research,* vol. 92, pp. 239-249, 2013.

[20] Chon L.Tsai, Baojian Liao, David A. Clukey and Joseph S. Breeding, "Development of a Microprocessor based Tracking and Operation Guidance System for Underwater Welding," Ohio State University, USA, 2010.

[21] Isiklar Y. V. and Girgin I, "Numerical modelling of underwater welding," *Journal of Naval Science and Engineering,* vol. 7, no. 2, pp. 11-29, 2011.

[22] Rowe M. and Liu S., "Recent developments in underwater wet welding," *Science and Technology of Welding and Joining*, vol. 6, no. 6, pp. 387-396, 2001.

[23] Labanowski Jerzy, "Development of underwater welding techniques," *Welding International,* vol. 25, no. 12, pp. 933-937, 2011.

[24] Szelagowski P. and Pachniuk I., "State of the art and practice of underwater hyperbaric dry welding," in *International Workshop on Underwater Welding of Marine Structures*, USA, 1994.

[25] Cotton H. C., "Welding under water and in the splash zone," in *A review. Proceedings of the International Conference „Underwater Welding*, Norway, 1983.

[26] Ibarra S. and Olson D.L., "Underwater welding of steel," *Key Engineering Materials*, pp. 69-70, 1992.

[27] Verma K and Garg H. K., "Underwater welding recent trends and future scope," *International Journal of Emerging Technologies,* vol. 3, no. 2, pp. 115-120, 2012.

[28] Pessoa E. C. P., Bracarense A. Q., Zica E. M., Liu S. and Faustino P.-G., "Porosity variation along multipass underwater wet welds and its influence on mechanical properties," *Journal of Materials Processing Technology*, vol. 179, no. 1-3, pp. 239-243, 2006.

[29] Pérez-Guerrero F. and Liu S., "Explaining Porosity Formation in Underwater Wet Welds," in *ASME 2007 26th International Conference on Offshore Mechanics and Arctic Engineering* , 2007.

[30] Chaveriat P. F., Kim G. S., ShahS. and Indacochea J. E., "Low carbon steel weld metal microstructures: The role of oxygen and manganese," *Journal of Materials Engineering*, vol. 9, no. 3, pp. 253-267, 1987.

[31] Masumoto I., Matsuda K. and Hasegawa M., "Study on the crack sensitivity of mild steel welded joint by underwater welding," in *Proceedings of the International Conference „Joining of Metals – 2*, Denmark, 1984.

[32] Wikimedia. [Online]. Available: http://commons.wikimedia.org/wiki/File:Working_Diver_01.jpg. [Accessed 1 March 2015].

[33] Akselsen O. M., Aune R, Fostervoll H. and Hårsvcer A. S., "Dry hyperbaric welding of subsea pipelines," *Welding Journal,* pp. 52-55, 2006.

[34] Shuji A, “High tensile strength steel having superior fatigue strength and weldability at weld and methods for manufacturing the same”. Japan Patent Patent EP0666332A1, 1995.

[35] Weslley Carlos Dias da Silva, Leandro Fonseca Ribeiro, Thales Lucas Diniz de Avila and Alexandre Queiroz Bracarense, “Diffusible hydrogen on underwater wet welds produced with tubular shielded electrodes using internal gas protection,” in *Proceedings of COBEM*, Brazil, 2011.

[36] Rowe M. D., Liu S. and Reynolds T. J., “The Effect of Ferro-Alloy Additions and Depth on the Quality of Underwater Wet Welds,” *Welding Research,* pp. 156-166, 2002.

[37] Suga Y. and Hasui A., “On Formationof Porosity in Underwater Wet Metal,” *Transaction of The Japan Welding Society,* vol. 17, no. 1, pp. 58-64, 1986.

[38] Lindhorst L. and Mahrenholtz O., “On the influence of wet underwater welding on CTOD-δ5,” *nternational Journal of Fracture,* vol. 97, no. 1-4, pp. 263-277, 1999.

[39] P. Group, “http://www.putnamlabs.com,” [Online]. Available: http://www.putnamlabs.com/Videos/VideosPage.html. [Accessed 21 February 2015].

[40] Versteeg H.K. and Malalasekera W., An Introduction to Computational Fluid Dynamics The Finite Volume Method, Longman Group Ltd, 1995.

[41] Dariusz Fydrych, Grzegorz Rogalski and J. Łabanowski, “Problems of Underwater Welding of Higher-Strength Low Alloy Steels,” *Biuletyn Instytutu Spawalnictwa* , vol. 5, pp. 187-195, 2014.

[42] Tsai C. L., Liao B. J., Joseph D. A. C. and Breeding S. “Control Algorithm for Underwater Wet Flex Cored Arc Welding Process,” Ohio State University, USA, 1998.

[43] Nakpradit T and Poopat B., “Investigation of Diffusible Hydrogen Content and Microstructure E|xamination of Underwater Welding,” *Asian International Journal of Science and Technology Production and Manufacturing Engineering,* vol. 3, no. 3, pp. 45-51, 2010.

[44] Khanna O.P., A Textbook of Welding Technology, India: Dhanpat Rai Publications (P) Ltd, 2004.

[45] ZHAO Bo, WU Chuansong, JIA Chuanbao and Y. Xin, "Numerical analysis of the weld bead profiles in underwater wet flux-cored arc welding," *Acta Metallurgica Sinica*, vol. 49, no. 7, pp. 797-803, 2013.

[46] Lesnewich A, "Control of melting rate and metal transfer in gas-shielded metal-arc welding," *Welding Research Journal Supplement,* vol. 37, no. 8, pp. 343s-353s, 1958.

[47] Halmoy E, "Wire melting rate, droplet temperature, and effective anode melting potential," in *Proceedings of International Conference on Arc Physics and Weld Pool Behavior*, Cambridge, 1979.

[48] Juang S. C., Tarng Y. S. and Lii H. R., "A comparison between the backpropagation and counterpropagation networks in the modeling of TIG welding process," *Journal of Material Processing Technology,* vol. 75, pp. 54-62, 1998.

[49] Al-Faruk et.al., "Prediction of weld bead geometry and penetration in electric arc welding using artificial neural networks," *International Journal of Mechanical & Mechatronics Engineering,* vol. 10, no. 4, pp. 19-24, 2010.

[50] Hari Om and Sunil Pandey, "Effect of process parameters on weld penetration shape factor in ASAW based surfacing," *International Journal of Innovative Research in Science, Engineering and Technology,* vol. 3, no. 6, pp. 1-7, 2014.

[51] Brown R. T. and Masubuchi K., "Effects of Water Environment on Metallurgical Structures of Welds," *Welding Research Supplement,* pp. 178-188, 1975.

[52] Negnevetsky M., Artificial Intelligence, UK: Addison Wesley, 2005.

[53] Fahlman, S. An empirical study of learning speed in backpropagation, USA: Carnegie Mellon University, 1998.

[54] Yong-hua SHI, Z.-p. ZHENG and J. HUANG, "Sensitivity model for prediction of bead geometry in underwater wet flux cored arc welding," *Transaction of nonferrous metals society of China,* pp. 1977-1984, 2013.

[55] Naaz S., Alam A. and Biswas R., "Effect of different defuzzification methods in a fuzzy based load balancing application," *International Journal of Computer Science Issues,* vol. 8, no. 5, pp. 261-267, 2011.

[56] Passino K. M. and Yurkovich S., Fuzzy control, USA: Addison Wesley Longman, 1998.

[57] T. Engineering. [Online]. Available: http://www.tribalengineering.com/technology/fuzzy-ictl.aspx. [Accessed 21 February 2015].

[58] Rao D. H. and Saraf S. S., "Study of Defuzzification Methods of Fuzzy Logic Controller for Speed Control of a DC Motor," *IEEE Transactions*, pp. 782-787, 1995.

[59] Mathworks. [Online]. Available: http://se.mathworks.com/help/fuzzy/fuzzy-inference-process.html#a1054218744b1. [Accessed 3 March 2015].

[60] Budiyono A. and Sudiyanto T., "An Algebraic Approach for the MIMO Control of Small Scale Helicopter," in *ICIUS2007-A012*, Indonasia, 2007.

[61] Owen F., "Control systems engineering a practical approach," USA, California Polytechnic State University, 2012, pp. 1-25.

[62] Astrom K. J. and Murray R. M., Feedback Systems, 2007, pp. 1-401.

[63] Ding W., "Analysis Method for Closed-Loop System," in *Self-Excited Vibration*, Berlin Heidelberg, Springer , 2010, pp. 108-139.

[64] Dale E. Seborg, Duncan A. Mellichamp, Thomas F. Edgar and Francis J. Doyle, Process Dynamics and Control, USA: John Wiley & Sons, Inc, 2011.

[65] Pornjit Pratumsuwan, S. Thongchai and S. Tansriwong, "A Hybrid of Fuzzy and Proportional-Integral-Derivative Controller for Electro-Hydraulic Position Servo System," *Energy Research Journal*, vol. 1, no. 2, pp. 62-67, 2010.

[66] Majid Ali, Majid Ali, Saifullah Khan, M. Waleed and Islamuddin, "Application of an Intelligent Self-Tuning Fuzzy PID Controller on DC-DC Buck Converter," *International Journal of Advanced Science and Technology*, vol. 48, pp. 139-148, 2012.

[67] Wachem B. V. and Sasic S., "Derivation, simulation and validation of a cohesive particle flow CFD model," *AIChE Journal*, vol. 54, no. 1, pp. 9-19, 2008.

Errata

Publication	Statement
I	The errata is to make correction in the discussion section of publication I which deals with the Figure 10 explaining the diffusion of hydrogen from the weld metal to the HAZ during welding. Correction: The solubility of hydrogen is high in austenite and low in ferrite. This is why hydrogen diffuses out of the transforming weld metal into the austenitic HAZ.
II	Correction made to Table 1 in paper III. The units for *D, W, P, R, ΔW, ΔP, ΔR* are all in millimeters (mm) and v is measured in $mm.s^{-1}$

Publications

Publication I

Omajene J. E., Martikainen J., Kah P., Pirinen M., (2014)

Fundamental Difficulties Associated With Underwater Wet Welding

The paper has been published in the journal "International Journal of Engineering Research and Applications", Vol. 4, Issue 6(Version 4), pp. 26-31.

Link:(http://www.ijera.com/papers/Vol4_issue6/Version%204/E046042631.pdf)

RESEARCH ARTICLE OPEN ACCESS

Fundamental Difficulties Associated With Underwater Wet Welding

Joshua E. Omajene, Jukka Martikainen, Paul Kah, Markku Pirinen
LUT Mechanical Engineering, Lappeenranta University of Technology, P.O.Box 20, FIN-53851, Lappeenranta, Finland

ABSTRACT
The offshore industries carry out welding activities in the wet environment. It is evident that the wet environments possess difficulties in carrying out underwater welding. Therefore there is the need to improve the quality of weld achieved in underwater welding. This paper investigates the difficulties associated with underwater welding. The objective of this research paper is to identify and analyze the different difficulties in underwater welding so as to make a clear background for further research to identifying the processes of eliminating these difficulties. The major difficulties in underwater welding are the cooling rate of the weld metal and arc stability during underwater wet welding at a higher depth. Methods of decreasing the cooling rate of weld metal and how to achieve arc stability are the major methods of approach. The result of welds achieved in underwater welding will be much improved as compared to air welding if the effects of the difficulties associated with underwater welding are eliminated. This will lead to a more robust welding activities being carried out underwater.

Keywords **–** Arc stability, Cooling rate, Porosity, Underwater welding, Water depth

I. INTRODUCTION

The increasing demand for oil and gas has led the oil and gas companies to explore into the deep marine environment. The desire to repair damaged offshore structures as a result of corrosive defects, material fatigue, accident during assembly, construction errors, excessive operational loads, has brought about underwater welding [1]. The first underwater welding was done by British Admiralty – Dockyard for the repair of leaking ship rivets. Most recently, a lot of underwater activities have been going on, for example, platform installation, pipeline welding, watercraft welding, seashore components and offshore structures welding [1, 2]. Underwater wet welding is one of the most common repair measure because of its relative low cost and and high efficiency.

The desired qualities of a sound underwater weld are flexibility of operation in all positions, minimum electrical hazard, good visibility, good quality and reliable welds. However, the quality of underwater welding is impeded by loss of alloying elements from the weld metal, porosity of the welds, slag in the welds, increase in carbon and oxygen content in the welds, and increased tendency to cracking [1, 2]. The reduction in the mechanical properties in underwater wet welding is because of the water environment in which the welding arc is operating. The ease to remove heat from the welded area and the decomposition of water during the welding process are critical factors responsible for poor weld quality during underwater wet welding.

Underwater welding is classified according to their physical and mechanical requirements that load bearing welds must satisfy. These specifications are according to AWS D3.6M:2010 underwater welding code. The three underwater welding specifications are A, B, and O. Each type fulfils a set of criteria for weldment properties which have to be established during welding qualifications, and also a set of weld soundness requirements that should be verified during construction. Class A is comparable to air water welding in terms of toughness, strength, ductility, hardness, and bending. Class B is for less critical application with limited structural quality, where both the test applied for procedure qualification and acceptance criteria are less strict. While class O is to meet the requirements of another designated code or specification [3].

Nowadays. The commonly used underwater welding processes are shielded metal arc welding (SMAW), and flux cored arc welding (FCAW). Steels with low carbon content (CE < 0.4) are preferable for underwater welding process, this is because the fast quenching medium hardens the heat affected zone (HAZ) and thereby making it susceptible to hydrogen cracking. Most underwater welding are either in vertical or overhead positions, and therefore maintaining joint coverage in a moving water environment is difficult [4, 5]. The Fig. 1 below summarizes the effect of welding process carried out underwater on the welded joint. These effects will be fully examined in the next chapters of this paper.

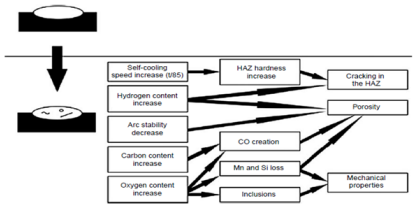

Fig. 1 The effect of moving the welding process to water environment [1].

II. COMPARING AIR WELD AND WATER WELDS

Underwater welding requires a higher current for the same arc voltage as compared to air welding so as to achieve a higher heat input. The weld bead size is quite similar for corresponding underwater and air welding. However, wet welding has a narrower weld bead and a higher reinforcement as compared to air welding. The general shape for air and wet welding does not appear to be significantly different. This means that the critical effect of the water only begins when the weld puddle starts forming and solidifies. The HAZ in underwater welds is reduced by 30 to 50% as compared to air welding, which suggest that heat dissipates rapidly from the weld bead into the base metal. Underwater welds bead shape are more spread out and less penetrating than air welds. The structure tends to change across the HAZ in underwater welding unlike the air welding which is more homogenous. The HAZ widths for air welding are 20 to 50% wider than the corresponding wet welding [6].

III. COOLING RATE AND SOURCES OF HEAT LOSSES IN UNDERWATER WELDING

The effect of rapid cooling for welds made underwater causes a change in the mechanical strength of the weld as a result of the fast cooling rate. The cooling rate is strongly affected by the welding procedure used as it relates to the heat input and weld joint design. Fast cooling can result in the formation of constituents such as martensite and bainite for welding conventional steels. These constituents are both high strength and brittle and are susceptible to hydrogen cracking. Cracking susceptibility is a function of weld metal microstructure, the weld metal microstructure is a function of hardenability and cooling rate. Fig. 2 shows the effect of welding heat input on the cooling time between 800 and 500 ^{0}C. The welding heat input for wet underwater welding is usually between 1.0 to 2.0 kJ/mm, and therefore having a short cooling time between 2 to 4 seconds. Fig. 3 shows that the cooling time decreases with increasing base metal thickness. However, there is a constant cooling time at 2 seconds for plate thickness above 15 mm [7]. Low welding speed is an effective way to reduce cooling rates in HAZ. Shielded metal arc welding (SMAW) for surface welding cools from 800 to 500 ^{0}C in the range of 8 to 16 seconds. Whereas typical wet welding for the same heat input range has a cooling range of 1 to 6 seconds depending on the heat input range of 0.8 to 3.6 kJ/mm and plate thickness [8]. One unique characteristics of cooling rate is that it is independent of the distance from the heat source especially in the HAZ [9]. The Fig. 4 shows the effect of cooling rate and distance to plate surface.

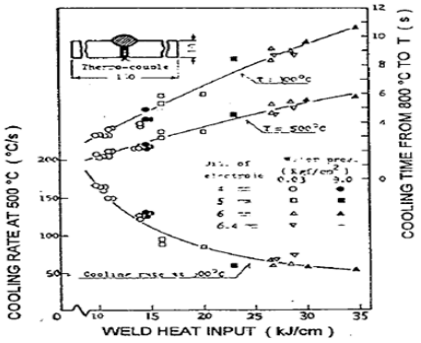

Fig. 2 Cooling rate vs heat input [12].

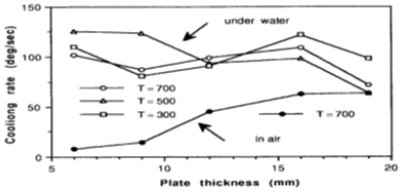

Fig. 3 Cooling rates for wet welding compared with welding in air [7].

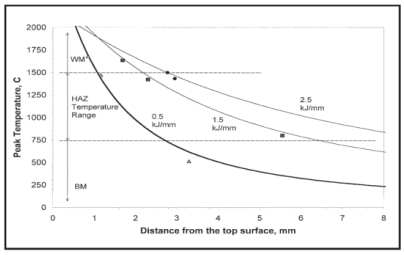

Fig. 4 Peak temperature profiles weighted and fitted for different weld samples; heat input values 0.5, 1.5, 2.5 kJ/mm [9].

Heat losses in air welding are from the molten surface outside the heat input circle which is basically due to radiation. The heat loss from the

surface at some distance from the arc is due to natural convection. However, heat losses in underwater welding are mainly conduction heat losses from the plate surface into the moving water environment, the motion of the moving water is created by the rising bubble column in the arc area [10]. Formation of bubbles stirs up the water around the surface of the plate thereby increasing the heat transfer. The bubbles come together during the transition phase forming unstable film and thereby reducing the heat transfer. A stable film is finally formed which reduces the heat transfer to radiation [11]. Conduction and radiation account for the major heat losses in underwater welding.

The cooling rates of a wet SMAW welds are in inverse proportion to the thickness of the welded plate, up to a limiting thickness. The cooling rate increases at thickness above the limiting plate thickness level. This continues to a second limit above which cooling rates are approximately not affected by any increase in plate thickness as shown in Fig. 5. However, air welding demonstrates direct relationship to a limiting thickness value above which cooling rates are not a function of plate thickness [4]. The cooling rate increase with increase of plate thickness above the first limit because of higher conductive ability of the plate. Increasing the plate thickness beyond the first limit, makes the plate back side convection to decrease. Thermal insulation is a means of slowing the cooling rate in wet weld by slowing the rate of heat loss through convection to the surrounding water [4]. The difference in cooling rate between water welding and air welding is shown in Fig. 6A and 6B [6].

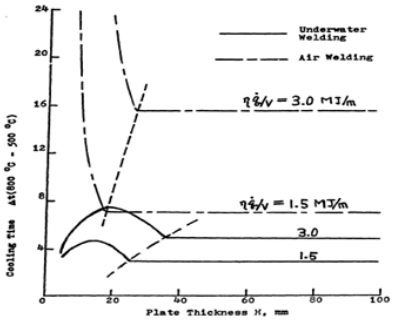

Fig. 5 Cooling time vs. plate thickness in wet and dry welds for two heat input values [4].

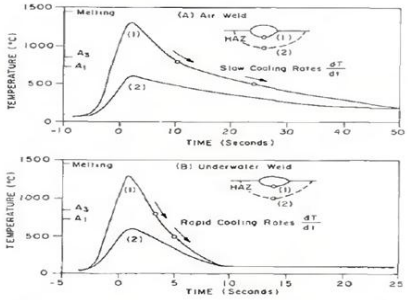

Fig. 6 Temperature histories of air welds compared to those of underwater welds [6].

IV. SOLIDIFICATION AND MICROSTRUCTURAL TRANSFORMATION

The mode and size of the solidification substructure affects the mechanical properties of weld joint. Achieving finer grains result in good weld joint properties and quality. This is achievable by controlling the welding parameters such as voltage, current, welding speed, and the welding environment which include air and water [13]. The molten weld pool in wet welding travels at a constant speed with the electrode. The weld puddle has tear drop geometry. The weld pool geometry is as a result of heat losses in the weld area behind the arc. The weld pool geometry affects the mode of solidification growth. This leads to the formation of coarse columnar grains which meet at the centerline. This grain type is susceptible to segregation and solidification cracking. The fast cooling rate during weld solidification leads to large amount of hydrogen in the weld pool to diffuse into the adjacent base metal and HAZ. Structural steel weld metal with microstructure such as martensite and upper bainite are more susceptible to hydrogen cracking. The formation of these phases in the HAZ is dependent on weld metal and base metal chemical composition, heat input and cooling rate, water temperature, and water pressure. The Fig. 7 shows continuous cooling transformation (CCT) diagram showing a bainite region with superimposed cooling curves. The obtained microstructure and corresponding temperature at which each microstructure will start and finish can be identified on the diagram.

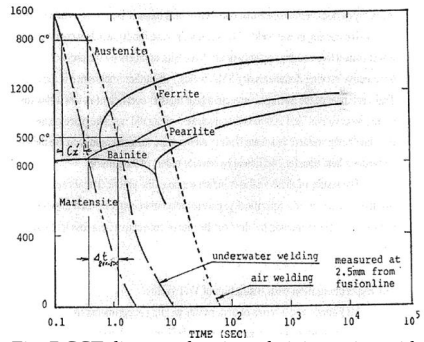

Fig. 7 CCT diagram showing a bainite region with superimposed cooling curves [14].

Acicular ferrite is a microstructural constituent that gives a high resistance to cleavage fracture and the formation of acicular ferrite is desirable in welded joint microstructure for improved toughness. It is possible to achieve acicular ferrite in underwater welds with the addition of alloying elements such as boron and titanium with the proper weld metal oxygen and manganes contents[8]. The Fig. 8 shows weld metal microstructure as a function of depth in underwater welding. The weld metal is basically grain boundary ferrite at shallow depth, with 10 to 20% aligned carbide. As the depth increases, the relative amount of grain boundary ferrite decreases to about 50%, and the amount of aligned carbide and sideplate ferrite increases. A drastic change in microstructure occurs in the first 50 m of depth. As the depth increases further from 50 m, the weld metal composition and microstructure remain fairly constant [8].

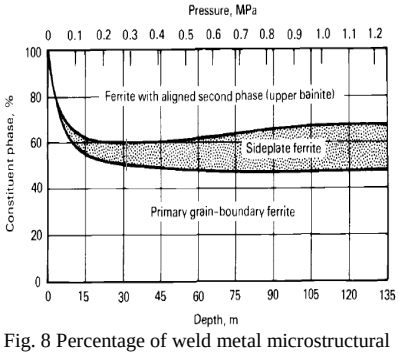

Fig. 8 Percentage of weld metal microstructural constituents for wet underwater welds as a function of water [8].

V. ARC STABILITY

The welding arc is constricted at increased water depth or pressure. However, welding in shallow depths is more critical than higher depth. But this is only to a certain depth of 1.5 to 6 m, where further increase in depth makes the arc unstable again. Unstable arc results in porosity. The electrical conductivity of the arc can be maintained with higher voltage. Although, this increase in voltage results in fluctuations in arc voltage, thereby porosity and slag are entrapped in the molten weld pool. It is evident that electrode diameter plays a role in arc stability with water depth and increase in current density. A smaller electrode diameter can increase the arc stability, an unstable arc affects the soundness of a weld done underwater [12].

VI. PRESSURE –INFLUENCE OF DEPTH IN UNDERWATER WELDING

The water environment affects the weld metal chemical composition. This is because of the decomposition of water which releases oxygen, hydrogen, and loss of alloying elements such as manganese and silicon. Manganese and silicon which are deoxidizers are increasingly lost at increasing depth or pressure as can be seen in Fig. 9. Increase in weld metal carbon content increases with depth due to carbon monoxide reaction when flux containing calcium carbonate is used. Welds carried out at greater water depth have lower densities. This is because of the formation of internal porosity. The shape of the pores changes from almost spherical to a more elongated one at depth between 20 to 30 m. the spherical pore is hydrogen concentration pore, while the elongated pore is bubble type pore [8].

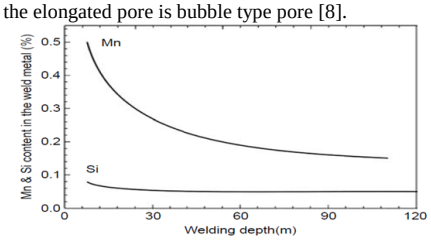

Fig. 9 Influence of depth of underwater welding on the content of elements in the weld deposit [1].

VII. DISCUSSION

The Fig. 10 below shows how hydrogen is diffused from the weld metal to the HAZ during welding. From the figure TF is the transformation of the weld metal from austenite into ferrite and pearlite while TB is the transformation from austenite to martensite. Hydrogen in the TF phase is rejected and moved to the TB phase because austenite cannot absorb hydrogen and hydrogen is soluble in ferrite. The base metal has higher carbon content than the weld metal because the filler metal usually has lower carbon content. And in that case, the HAZ is transformed from austenite into martensite after the weld metal has transformed from austenite into ferrite and pearlite [15]. For hydrogen induced cracking to

occur, low temperature due to the fast cooling rate of the weld metal by the surrounding water helps in the formation of martensite and the presence of hydrogen from the decomposition of water.

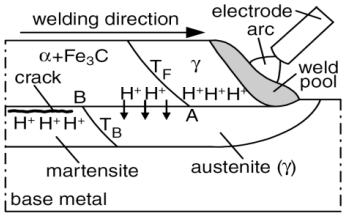

Fig. 10 Diffusion of hydrogen from weld metal to HAZ during welding [15].

Experimental evidence shows that underwater welds have increased strength and decreased ductility. Underwater welds show strength increase from 6.9% to 41%, while ductility decreases about 50% for most weld assemblies. This examination is in terms of the base steel material, weld orientation and corrosion of base steel material [16]. The effect of water environment on strength and ductility is shown in Fig. 11 which compares the strength and ductility for different base material welded underwater and in air. The shape of the base material whether the base plates are flat sheet pile or curved pipe do not have an influence on either the strength and ductility. However, the chemical composition differences have a significant influence on the strength and ductility.

A change in the orientation in the weld affects the mechanical properties of fillet welds. A change in the orientation for welds on SY295 indicates that changing the orientation from transverse to longitudinal direction, will increase the strength and decrease ductility from 24% to 41% and from 28% to 61% respectively. However, longitudinal fillet weld are more sensitive to wet welding environment with increase in strength of 29% and decrease in ductility of 65% on average, while transverse fillet weld with a strength increase of 20% and ductility decrease of 49%.

Underwater welds on corroded SY295 steel exhibit strength increase of 22%, and a huge decrease in ductility of 83%when compared with air welding [16].

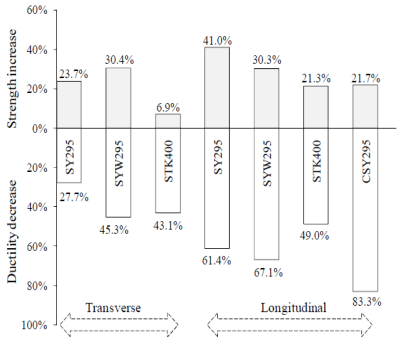

Fig. 11 Relative changes of strength and ductility from air welds to underwater welds [16]

VIII. CONCLUSION

Rapid quenching causes steep thermal gradient and high residual stresses which increases the weld susceptibility to crack initiation when loaded. Fast cooling also increases weld bead convexity reinforcement and thereby making welds more susceptible to toe cracking.

The influence of increased water depth on arc stability and loss of alloying elements, as well as fast cooling rates are important factors when considering an improvement strategy of welds done underwater.

REFERENCES

[1] J. Labanowski, "*Development of underwater welding techniques*," *Welding International*, vol. 25, no. 12, pp. 933 - 937, 2011.

[2] K. Verma and H. Garg, "*Underwater welding - Recent trends and future scope*," *International Journal on Emerging Technologies*, vol. 3, no. 2, pp. 115 - 120, 2012.

[3] AWS, "*Underwater welding code*," AWS, USA, 2010.

[4] P. J. Keenan, "*Thermal insulation of wet shielded metal arc welds*," MIT, USA, 1993.

[5] V. R. Santos, "*Development of an oxyrutile electrode for wet welding*," *Welding Journal*, vol. 91, pp. 318-328, 2012.

[6] R. T. Brown and. K. Masubuchi, "*Effects of water environment on metallurgical structures of welds*," *Welding Research Supplement* , pp. 178-188, 1975.

[7] T. Fukuoka and S. Fukui, "*Analysis for cooling process of underwater welding-comparison with welding in air*," MESJ, Japan, 1994.

[8] S. Liu and D. Olson, "*Underwater welding*," *ASM International*, vol. 6, pp. 1010-1015, 1993.

[9] K Poorhaydari, B. M. Patchett and D. G. Ivey "*Estimation of cooling rate in the welding of plates with intermediate thickness*," *Welding Journal* , pp. 149-155, 2005.

[10] P Ghadimi, H. Ghassemi, M. Ghassabzadeh and Z. Kiaei"*Three dimensional simulation of underwater welding and investigation of effective parameters*," *Welding Journal* , pp. 239-249, 2013.

[11] Alan J. Brown, James A. Staub and K. Masubuchi "*Fundamental study of underwater welding,"* in *Offshore Technology Conference*, USA, 1972.

[12] S Liu, A. M. Pope and R. Daemen "*Welding consumable and weldability*," USA.

[13] M. Faisal, A. Abbas, Tarig, A. Ghamdi and S. Liu "*Comparison of Solidification Behavior Between Underwater Wet Welding and Dry Welding,*" *ASME,* vol. 3, pp. 285-296, 2011.

[14] Chon L Tsai and B. J. Liao, "*Control algorithm for underwater wet flux cored arc welding process*," OSU, pp. 410-417, USA, 1998.

[15] S. Kou, Welding Metallurgy, USA: Wiley Interscience , 2003.

[16] C. Xiao, "*Design method to repair corrosion damaged offshore steel structures underwater*," University of Nagoya, Japan, 2011.

Publication II

Omajene J. E., Martikainen J., Kah P., (2014)

Effect of Welding Parameters on Weld Bead Shape on Welds Done Underwater

The paper has been published in the journal "International Journal of Mechanical Engineering and Applications", 2(6), pp. 128-134.

Link:(http://article.sciencepublishinggroup.com/pdf/10.11648.j.ijmea.20140206.17.pdf)

International Journal of Mechanical Engineering and Applications
2014; 2(6): 128-134
Published online December 31, 2014 (http://www.sciencepublishinggroup.com/j/ijmea)
doi: 10.11648/j.ijmea.20140206.17
ISSN: 2330-023X (Print); ISSN: 2330-0248 (Online)

Effect of welding parameters on weld bead shape for welds done underwater

Joshua Emuejevoke Omajene, Jukka Martikainen, Paul Kah

LUT Mechanical Engineering, Lappeenranta University of Technology, Lappeenranta, Finland

Email address:
Joshua.omajene@yahoo.com (J. E. Omajene)

To cite this article:
Joshua Emuejevoke Omajene, Jukka Martikainen, Paul Kah. Effect of Welding Parameters on Weld Bead Shape for Welds Done Underwater. *International Journal of Mechanical Engineering and Applications.* Vol. 2, No. 6, 2014, pp. 128-134. doi: 10.11648/j.ijmea.20140206.17

Abstract: The desire to model a control system so as to optimize the welding process parameters and the effect of the environment during underwater wet welding makes it necessary to study the effects of these parameters as it affects the weld bead geometry of welds achieved in underwater welding. The objective of this paper is to analyze how welding arc current, voltage, speed, and the effect of the water environment affect the weld bead geometry such as bead width, penetration, and reinforcement height. Comparing the differences of the effects of welding input parameters for air and wet welding as it affects the welding output quality parameter is the method employed in this research paper. The result of this study will give a better understanding of applying control mechanism in predicting the quality of a weld during underwater welding. A clearer insight of the weldability of structural steels for offshore applications as it relates to underwater welding, having a full knowledge of the nonlinear multivariable parameters is indicative of better control methods.

Keywords: Bead Geometry, Process Parameter, Water Depth, Water Temperature, Underwater Welding

1. Introduction

Underwater welding is used for repair welding of ships and other offshore engineering structures. The quality of welds achieved from underwater wet welding faces some quality challenges because of the rapid cooling of the weld by the water surrounding the weld zone. There is reduction in ductility and tensile strength of 50% and 20% respectively of the heat affected zone (HAZ) of welds in underwater welding as compared to air welding [1]. The bead geometry of an underwater weld is important in determining the mechanical properties of a weld joint [2].This paper gives a background for the design of an artificial neural network control of the welding process parameters as it affects the weld bead geometry. The optimization of the welding parameters (Fig. 1) which are nonlinear multivariable inputs will be discussed in the subsequent paper by the author. The water temperature and water depth are not welding process parameters but parameter of the water environment that affects the welding quality of underwater wet welding. The illustration of the weld bead geometry (Fig. 2) parameters, where W is the weld bead width (mm), R is the height of reinforcement (mm), and P is height of penetration (mm). WPSF (penetration shape factor) = W/P, WRFF (reinforcement form factor) = W/R. The strength of a weld is influenced by the composition of the metal, distortion and also the weld bead shape. The desired weld bead shape is dependent on the heat energy which is supplied by the arc to the base metal per unit length of weld, welding speed, joint preparation and the water environment in the case of wet welding [3, 4].

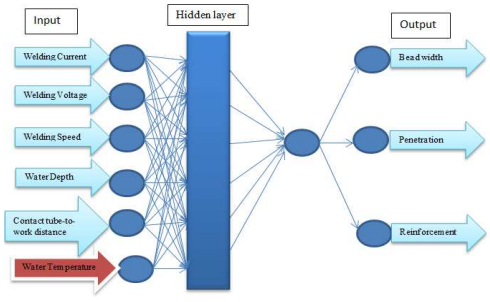

Fig. 1. *Welding input vs output parameters.*

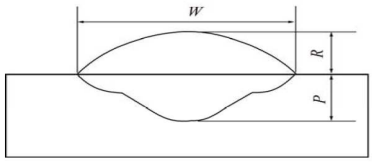

Fig. 2. *Weld bead geometry of underwater wet FCAW [2].*

2. Underwater Welding Processes

2.1. Shielded Metal Arc Welding (SMAW)

Shielded metal arc welding process is one of the most widely used welding processes. The process employs the heat of the arc to melt the base metal and the tip of the consumable covered electrode, and the flux covering the electrode melts during the welding. The melted flux forms gas and slag which act as a shield to the arc and molten weld pool (fig 3). The flux adds deoxidizes, scavengers and alloying elements to the weld metal. The welding current for SMAW can either be alternating current (AC) or direct current (DC) depending on the electrode used. Underwater SMAW uses a DCEN polarity. The use of DC is common in SMAW because of fewer arc outages, less spatter, easier arc starting, less sticking, and better control in out-of-position welds. Underwater welding electrodes are usually water proofed, and the flux creates bubbles during the welding process and displaces water from the welding arc and weld pool area. The welding speed and voltage have to be properly adjusted to create a stable bubble formation by the flux, because the gas bubble makes welding possible underwater. Underwater SMAW process uses two basic techniques known as the self-consuming techniques and the manipulative or weave technique. In the self-consuming technique, the electrode is dragged across the workpiece and pressure is applied by the welder. The manipulative technique, the arc is held as in surface welding and little or no pressure is required on the electrode. The manipulative technique requires more skills than the self-consuming technique [5, 6].

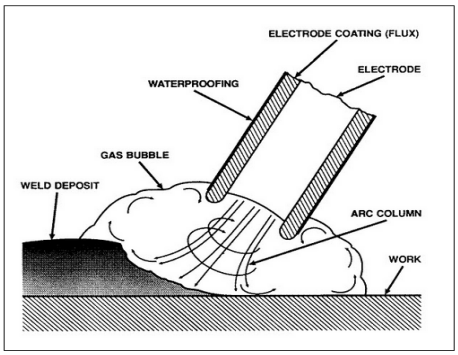

Fig. 3. *Schematic illustration of SMAW process [5].*

2.2. Flux Cored Arc Welding (FCAW)

FCAW uses heat generated by a DC electric arc to join the metal in the joint area. This welding process utilizes a continuously fed consumable welding wire that consists of a metal sheath which is composed of flux and alloying elements (Fig. 4). The flux formed is used to stabilize the welding arc, formation of slag, and produces shielding gas which protects the molten metal transfer and weld puddle as in SMAW process. The shielding in FCAW is achieved either by an additional gas shield supplied from an external source, or by the decomposition of the fluxing agent within the wire also known as self-shielding.The need for automation, out of position welding proficiency, high deposition rate and self-shielding capability has led to the development of underwater FCAW welding process [7]. FCAW technique using rutile type wire has a potential for high deposition rate and can be adapted to automated equipment [8]. The FCAW is suitable for underwater wet welding because of its self-shielding possibilities, ease of automation and out of position welding efficiency.

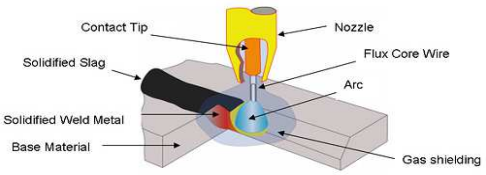

Fig. 4. *Schematic illustration of FCAW process [9].*

3. Welding Inputs

3.1. Welding Current

Welding current is an important parameter which affects the weld bead shape. The current controls deposition rate because it controls the melting rate of the electrode. The amount of melted base metal, the HAZ, depth of penetration is controlled by the welding current. An increase in welding current increases penetration and reinforcement. A low welding current will lead to unstable arc, low penetration and overlapping. Changing the polarity from direct current electrode posistive (DCEP) to direct current electrode negative (DCEN) affects the amount of heat generated at the electrode and workpiece which affects the metal deposition rate, weld bead geometry and mechanical properties of the weld metal. The positive electrode generates two third of the total heat, while the negative electrode generates one third of the total heat. The DCEN polarity produces higher deposition rate and reinforcement than the DCEP polarity in submerged arc welding. The level of hydrogen absorption in underwater wet welding which results in porosity can be minimized by using low current DCEP or a high current DCEN [3, 10, 11].

3.2. Welding Voltage

The length of the arc between the electrode and molten

weld metal determines the variation of the welding voltage. An increase in the arc length increases the voltage. The voltage determines the shape of the weld bead cross section and external appearance. Increasing the voltage at a constant current will result in a flatter, wider, and reduced penetration, which also leads to reduced porosity caused by rust on steels. Increase in arc voltage results to an increase in the size of droplets and thereby reduce the number of droplets. Increase in voltage enhances flux consumption, but a further increase in voltage will increase the possibility of breaking the arc and hinder normal welding process. Increase in arc voltage beyond the optimum value leads to an increase in loss of alloying elements which affects the metallurgical and mechanical properties of the weld metal. Arc voltage beyond the optimum value produces a wide bead shape that is susceptible to cracking, increase undercut and difficulty of slag removal. Lowering the arc voltage results in stiffer arc that improves penetration. Excessively lowering of the arc voltage results in a narrow bead and difficulty of slag removal along the bead edges. A decrease in the welding voltage will decrease the diffusible hydrogen content during underwater welding. In many of the MILLER electric power sources, the constant current output are equipped with a feature called Arc Force, Dig or Arc Control, and Hot Start. In electric arc welding process, as the arc length increases, the voltage increases. The load voltage of a constant current welding machine is controlled by controlling the arc length. However these power sources does not work well for TIG welding process because it is better if the current does not change as the arc length changes in TIG welding. Power sources that have Arc Force (fig. 5B) allow the operator to change the shape of the volt/amp curve to meet the requirement of the operation being performed. Power sources with no Arc Force (fig. 5C) gives a more vertical shape of the volt/amp curve meaning that the current will not change much as the arc length is changed [10, 12-15].

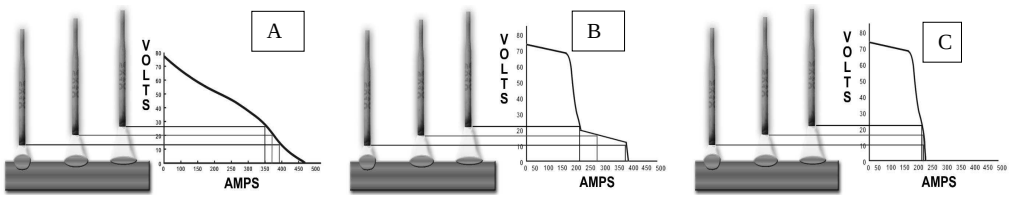

Fig. 5. *Electric arc welding power sources [14].*

3.3. Welding Speed

The linear rate at which the arc is moved along the weld joint influences the heat input per unit length of the weld. An increase in the welding speed will decrease the heat input and less filler metal is applied per unit length of the weld, which will result in less weld reinforcement and a smaller weld bead. The welding speed is the most influencing factor on weld penetration than other parameters except welding current. Excessive welding speed may result in porosity, undercutting, arc blow, uneven bead shape, cracking and increased slag inclusion in the weld metal. Higher welding speed results in less HAZ and finer grains. A relatively slow welding speed gives room for gases to escape from the molten metal, thereby reducing porosity. The bead width at any current is inversely proportional to the welding speed. A fast welding speed with low DCEN or high DCEP can minimize the level of porosity in wet welding [10, 11, 16].

3.4. Contact tube-to-Work Distance

Experimental evidence indicate that weld bead geometry is influenced by the change of the contact tube-to-work distance (CTWD) (Fig. 6) during welding. The CTWD influences the formation of the weld pool and the resulting weld shape by changing the arc length and welding current. the arc length which is related to the welding voltage and CTWD are closely related to the weld bead geometry. The convection in the weld pool affects the weld pool geometry. An increase in arc length due to an increase in CTWD increases the bead width because of the widened arc area at the surface of the weld. Increase in arc length reduces the reinforcement height because the same volume of filler metal is used [17].

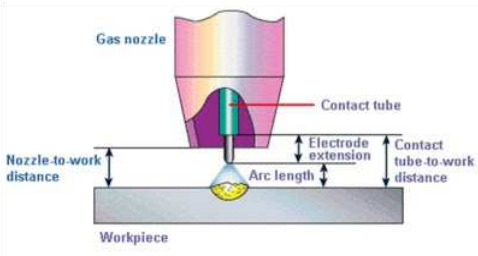

Fig. 6. *Contact tube-to-work distance [18].*

4. Environmental Parameters

4.1. Water Depth

Increased water depth constricts the welding arc resulting in an increased weld penetration on higher rate of filler metal transfer. The arc constriction results in an increased voltage

and current as the water depth increases [19]. Weld metal oxygen, carbon, manganese, and silicon are fairly constant at water depth of 50 m to 100 m. oxygen content controls weld metal manganese and silicon content. At depth greater than 50 m, the diameter of the arc column decreases with increasing pressure (depth). Water reaction becomes increasingly important at depth greater than 50 m. The operating process parameter space decreases with increasing depth because high ionization potential for hydrogen makes it difficult to sustain the welding arc [11].

4.2. Water Temperature

The presence of water and the type of water surrounding the weld metal affects the welding process and the resulting temperatures. This effect is due to the greater convective heat transfer coefficient of water as compared to air which results in the rapid cooling in underwater welding [20]. At higher water temperature, for higher oxygen content, the diffusible hydrogen contents are likely to be less thereby, lowering the tendency of hydrogen assisted cracking. When welding at lower water temperature, there are few inclusions resulting in higher diffusible hydrogen level in the coarsed grain heat affected zone which leads to greater cracking tendency. The weldment sample (fig. 6) at 2.8^0C has cracking over two thirds of the weld height. The macrograph shows that the cracking progressed along the HAZ and a bit into the weld metal. At 10^0C the weldment has two cracks on the left hand edge, and the crack starts from the HAZ and unto the weld metal. The macrograph shows that the cracking is perpendicular to the direction of maximum tensile stress as a result of the cooling. The sample test conducted at the highest water temperature of 31^0C shows the highest volume fraction of inclusions of slag and oxide. This resulted in highest porosity level. Again, because of the higher oxygen content leading to lesser diffusible hydrogen content at higher temperature, thereby, resulting in a lower cracking tendency [19]. Underwater weld pool shape differs from air welds because of the heat transfer conditions caused by the cooling effect of the water and the presence of steam bubble [8].

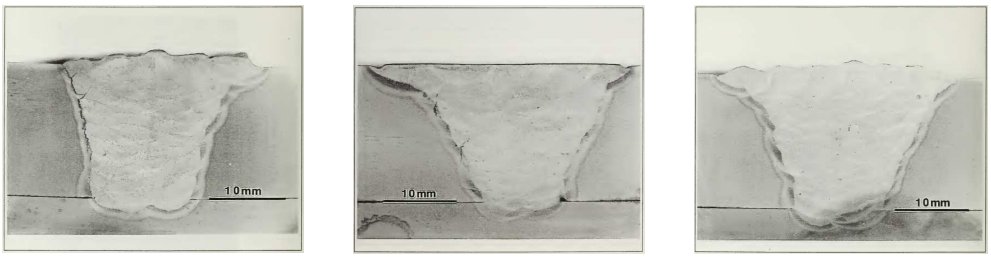

Welded at 2.8^0C water temperature and 6.7 m water depth

Welded at 10^0C water temperature and 5.5 m water depth

Welded at 31^0C water temperature and 7.3 m water depth

Fig. 7. *Macrophotograph of different weld samples [19].*

5. Welding Outputs

5.1. Bead Width

The bead width of a weld is the maximum width of weld metal deposited. This influences the flux consumption rate. The bead width is in direct proportion to the arc current, welding voltage and diameter of the electrode. It is inversely proportional to the welding speed [21, 22].

5.2. Penetration

Penetration is the maximum distance between the top of the base plate and depth of fusion. Penetration is influenced by welding current, welding speed, polarity, electrode stick out, basicity index and physical properties of the flux. Penetration is directly proportional to welding current and inversely proportional to welding speed and diameter of electrode. Increase in thermal conductivity of the weld metal decreases penetration. Deepest penetration is achieved with DCEP polarity than DCEN polarity. A stable arc increases penetration because the arc wander is minimized which allows more efficient heat transfer [19, 20].

5.3. Reinforcement

The reinforcement influences the strength of the weld and wire feed rate. Increasing the wire rate increases the reinforcement irrespective of welding current and polarity. Reinforcement is inversely proportional to welding voltage, welding speed and diameter of electrode. A bigger reinforcement is achieved with DCEN polarity than with DCEP polarity [21, 22].

6. Discussion

Weld joint is considered to be sound and economical if it has a maximum penetration, minimum bead width, reinforcement and dilution [23]. The relationship between speed, voltage, current, bead width, WRFF, and WPSF (Fig. 8) is explained for air welding in the figure below.

Howerever, underwater wet welding show some differences as compared to air welding. Water depth has a great influence on bead geometry when compared to other welding parameters when welding at a water depth less than 10 m. Welding carried out at a water depth greater than 10 m and changing the welding speed highly influence the bead geometry than other welding parameters [2].

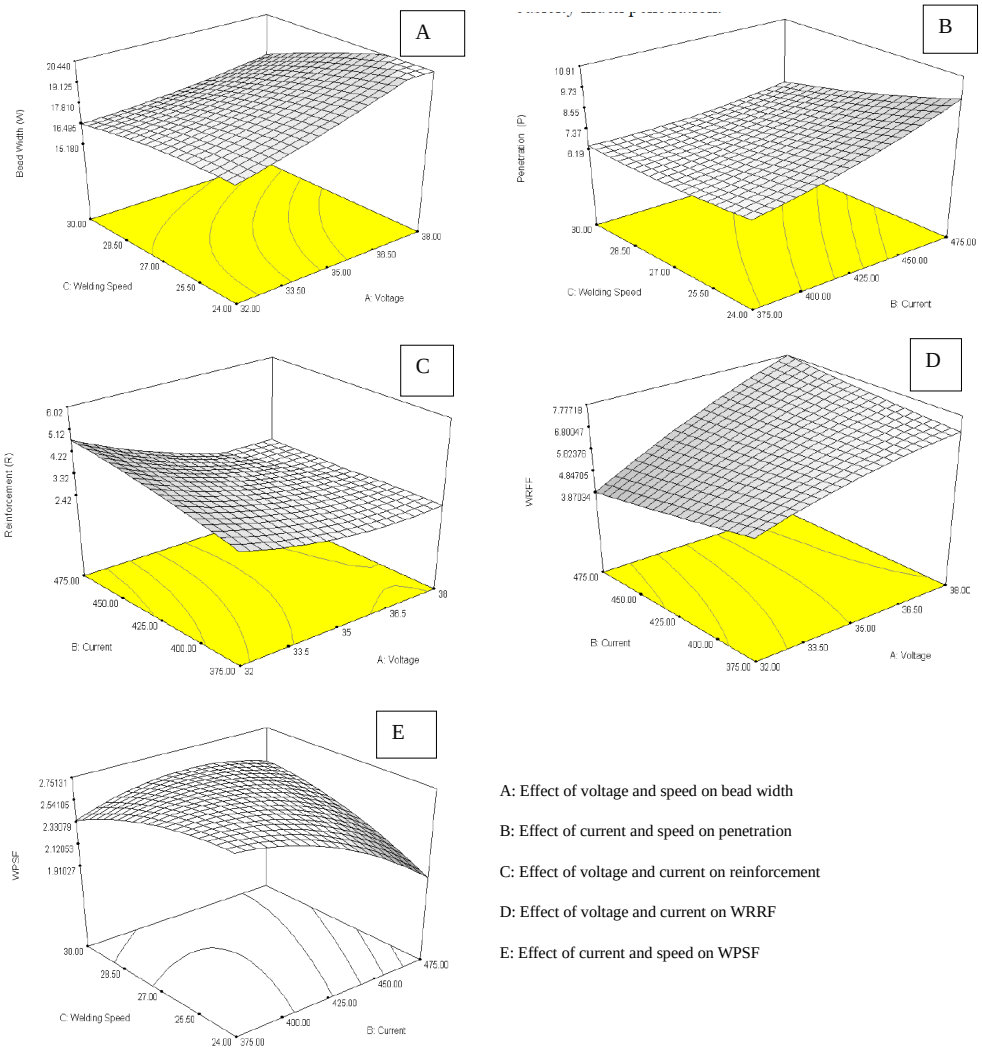

A: Effect of voltage and speed on bead width

B: Effect of current and speed on penetration

C: Effect of voltage and current on reinforcement

D: Effect of voltage and current on WRRF

E: Effect of current and speed on WPSF

Fig. 8. *Effect of various welding parameters on weld bead geometry for air welding [4].*

For all (Fig. 8A) values of speed an increase in voltage increases W. The bead width increases from 17.40 to 21.07 mm and from 16.49 to 17.75 mm with an increase in welding voltage from 32 to 38 volts, at welding speed of 24 and 30 m/hr respectively. This implies that voltage has a positive effect while welding speed has a negative effect on weld bead width [4].

The metal penetration (Fig.8B) increases with an increase in welding current for all values of welding speed. The metal penetration increases from 6.63 to 9.67 mm, and from 6.38 to 7.12 mm when welding current increased at welding speed of 24 and 30 m/hr respectively. Current has a positive effect on penetration while speed has a negative effect on penetration [4].

From (Fig. 8C), reinforcement decreases with increase in voltage with an increase in current from 375 to 475 amperes [4].

WRFF (Fig.8D) increases for all values of current when the voltage is increased from 32 to 38 volts. Voltage has a positive effect on WRFF while current has a negative effect. Weld bead width increases with an increase in voltage but almost remain constant with change of current, while reinforcement decreases with increasing voltage and increase with increase in current [4]. The effect of current and speed on WPSF is shown in Fig. 8E.

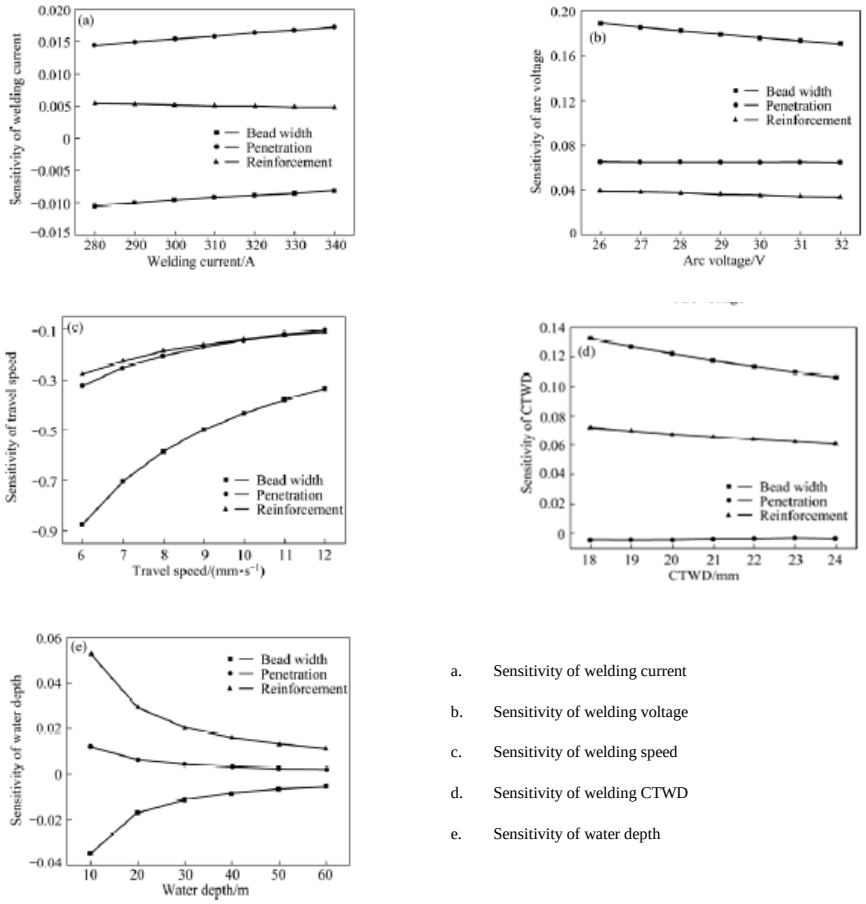

a. Sensitivity of welding current

b. Sensitivity of welding voltage

c. Sensitivity of welding speed

d. Sensitivity of welding CTWD

e. Sensitivity of water depth

Fig. 9. *Sensitivity of various welding parameters (welding current, speed, voltage) and water depth on weld bead geometry in underwater wet welding [2].*

7. Conclusions

The major challenge facing underwater welding is the fast cooling rate of the base metal by the surrounding water. This leads to the formation of microstructures that are susceptible to cracking. The effect of water depth and the cooling rate of the weld metal from the water temperature influence the effect of welding current, welding speed, and voltage on the weld bead geometry during underwater welding. It is evident that a proper adjustment of welding process parameter to minimize hydrogen pick up and alter the influence of the water environment can yield a sound weld in underwater welding as compared to air welding. The weld bead shape of a welded joint determines the mechanical properties of the joint. DCEN polarity is the most suitable power source for underwater wet welding. Arc stability increases penetration because of the reduction of arc wander and efficient heat transfer. Increase in water depth or pressure decreases bead width, but increases penetration, and reinforcement. Increase in voltage will increase bead width, penetration, and reinforcement. Welding current has greater influence on

penetration than on bead width and reinforcement. Porosity in underwater welding can be minimized by the use of low current DCEP or high current DCEN. Voltage increase beyond the optimal value will result in the loss of alloying elements.

References

[1] R. T. Brown & K. Masubuchi, "Fundamental Research on Underwater Welding," *Welding research supplement*, pp. 178-188, 1975.

[2] Yong-hua SHI, Ze-pei ZHENG & Jin HUANG, "Sensitivity model for prediction of bead geometry in underwater wet flux cored arc welding," *Transaction of nonferrous metals society of China*, pp. 1977-1984, 2013.

[3] B. K. Srivastava, S. P. Tewari & J. Prakash, "A review on effect of arc welding parameters on mechanical behaviour of ferrous metals/alloys," *International Journal of Engineering Science and Technology*, vol. 2, no. 5, pp. 1425-1432, 2010.

[4] V. Kumar, "Modeling of weld bead geometry and shape relationships in submerged arc welding using developed fluxes," *Jordan journal of mechanical and industrial engineering*, vol. 5, no. 5, pp. 461-470, 2011.

[5] U. NAVY, "Underwater Cutting and Welding Manual," Naval Sea Systems Command, USA, 2002.

[6] J. D. Majumdar, "Underwater Welding - Present Status and Future Scope," *Journal of Naval Architecture and Marine Engineering*, vol. 3, pp. 39-47, 2006.

[7] WeiMin Zhang , GuoRong Wang, YongHua Shi & BiLiang Zhong, "LSSVM Model for Penetration Depth Detection in Underwater Arc Welding Process," *Journal of Information and Computing Science*, vol. 5, no. 4, pp. 271-278, 2010.

[8] M. Rowe & S. Liu, "Recent Development in Underwater Wet Welding," *Science and Technology of Welding and Joining*, vol. 6, no. 6, pp. 387-396, 2001.

[9] "https://www.hera.org.nz/Category?Action=View&Category_id=522," Hera Innovation in Metals, 2014. [Online]. Available: https://www.hera.org.nz. [Accessed 16 June 2014].

[10] V. Kumar, "Use of Response Surface Modeling in Prediction and control of flux consumption in submerged arc weld deposits," *Use of Response Surface Modeling in Prediction and*, vol. 2, pp. 1-5, 2011.

[11] S. Liu, D. L. Olson & S. Ibarra, "Underwater Welding," *ASM Handbook*, vol. 6, pp. 1010-1015, 1993.

[12] S. P. Tewari, A. Gupta & J. Prakash, "Effect of welding parameters on the weldability of material," *International Journal of Engineering Science and Technology*, vol. 2, no. 4, pp. 512-516, 2010.

[13] J. Singh, C. D. Singh, J. S. Khamba & F. P. Singh, "Influence of Welding Parameters on Flux Consumption in Submerged Arc Welding," *International Journal for Multi Disciplinary Engineering and Business Management*, vol. 2, no. 1, pp. 1-3, 2013.

[14] "http://www.techtrain123.com/publicdownloadsallfiles/Stick%20Welding.pdf," [Online]. Available: http://www.techtrain123.com. [Accessed 15 June 2014].

[15] Miller, "http://www.millerwelds.com/pdf/guidelines_smaw.pdf," July 2013. [Online]. Available: http://www.millerwelds.com. [Accessed 15 June 2014].

[16] L. J. YANG, R. S. Chandel & M. J. Bibby, "The Effects of Process Variables on the Weld Deposit Area of Submerged Arc Welds," *WELDING RESEARCH SUPPLEMENT*, pp. 11-18, 1993.

[17] J. Kim & S. Na, "A Study on the Effect of Contact Tube-to-Workpiece Distance on Weld Pool Shape in Gas Metal Arc Welding," *Welding Research*, pp. 141-152, 1995.

[18] "http://2dayforme.blogspot.fi/2012/11/wps-variables.html," [Online]. Available: http://2dayforme.blogspot.fi. [Accessed 29 June 2014].

[19] R. L. Johnson, "The effect of water temperature on underbead cracking of underwater wet weldments," Naval Postgraduate School, California, 1997.

[20] P. Ghadimi, H. Ghassemi, M. Ghassabzadeh & Z. Kiaei, "Three dimensional simulation of underwater welding and investigation of effective parameters," *Welding Journal* , pp. 239-249, 2013.

[21] B. Singh, Z. A. Khan & A. N. Siddiquee, "Review on effect of flux composition on its behaviour and bead geometry in submerged arc welding," *Journal of mechanical engineering research*, vol. 5, no. 7, pp. 123-127, 2013.

[22] V. K. Panwar & D. K. Choudhary, "Application of Two-Level Half Factorial Design Technique for Developing Mathematical Models of Bead Penetration and Bead Reinforcement in SAW Process.," *International Journal of Innovative Research in Science, Engineering and Technology*, vol. 2, no. 6, pp. 2011-2023, 2013.

[23] J. E. R. Dhas & M. Satheesh, "Sensitivity analysis of submerged arc welding parameters for low alloy steel weldment," *Indian Journal of Engineering and Materials Sciences*, vol. 20, pp. 425-434, 2013.

Publication III

Omajene J. E., Martikainen J., Huapeng W., Kah P., (2014)

Optimization of Underwater Wet Welding Process Parameters Using Neural Network

The paper has been published in the journal "International Journal of Mechanical and Materials Engineering", 9(26), pp. 1-8.

Omajene et al. International Journal of Mechanical and Materials Engineering 2014, 9:26
http://www.springer.com/40712/content/9/1/26

International Journal of Mechanical and Materials Engineering
a SpringerOpen Journal

ORIGINAL ARTICLE Open Access

Optimization of underwater wet welding process parameters using neural network

Joshua Emuejevoke Omajene*, Jukka Martikainen, Huapeng Wu and Paul Kah

Abstract

Background: The structural integrity of welds carried out in underwater wet environment is very key to the reliability of welded structures in the offshore environment. The soundness of a weld can be predicted from the weld bead geometry.

Methods: This paper illustrates the application of artificial neural network approach in the optimization of the welding process parameter and the influence of the water environment. Neural network learning algorithm is the method used to control the welding current, voltage, contact tube-to-work distance, and speed so as to alter the influence of the water depth and water environment.

Results: The result of this work gives a clear insight of achieving proper weld bead width (*W*), penetration (*P*), and reinforcement (*R*).

Conclusions: An interesting implication of this work is that it will lead to a robust welding activity so as to achieve sound welds for offshore construction industries.

Keywords: Backpropagation; Bead geometry; Neural network; Process parameter; Underwater welding

Background

The differences in the weld quality for underwater welding as compared to air welding have made it very necessary to model an artificial neural network (ANN) which is capable of solving difficult and complex problems. The weld bead geometry of an underwater wet welding can be predicted by the neural network control of the input parameters as shown in Figure 1. The water surrounding the weld metal results in a fast cooling of the weld, thereby reducing the ductility and tensile strength of the weld metal by 50% and 20%, respectively (Brown and Masubuchi 1975). The effect of the water environment and the water depth on the welding process parameters significantly affects the quality of welds achieved underwater. The diffusible hydrogen contents are increased at lower water temperature for lower oxygen content. The increase in the diffusible hydrogen content leads to increase in the susceptibility of steels to hydrogen-assisted cracking (Johnson 1997). The water depth plays a role in the stability of the welding arc. Increased water depth constricts the arc, thereby resulting in an increased current and voltage as the water depth increases. An increasing water depth decreases the operating process parameter space (Liu et al. 1993). This paper proposes suitable means of optimizing the welding process parameter using a neural network so as to minimize the effect of the cooling rate and water depth in underwater welding. The main goal is to achieve a weld bead geometry which will give the weld metal the recommended structural integrity as prescribed by the underwater welding specification code AWS D3.6M:2010 (AWS 2010).

Methods

Underwater welding

Underwater welding is used for the repair welding of ships and offshore engineering structures like oil drilling rigs, pipelines, and platforms. The commonly used underwater welding processes nowadays are shielded metal arc welding (SMAW) and flux cored arc welding (FCAW). The water surrounding the weld metal reduces the mechanical properties of weld done underwater due to the effect of the fast cooling rate of the weld. Heat loss by conduction from the

* Correspondence: Joshua.omajene@yahoo.com
LUT Mechanical Engineering, Lappeenranta University of Technology, P.O. Box 20, FI-53851 Lappeenranta, Finland

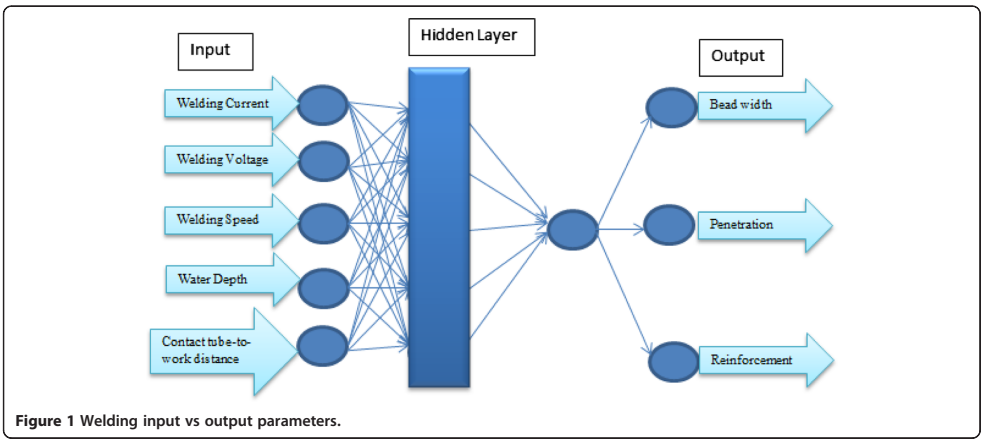

Figure 1 Welding input vs output parameters.

plate surface into the moving water environment and heat loss by radiation are the major heat losses in underwater welding. Underwater welding requires a higher current for the same arc voltage to achieve a higher heat input as compared to air welding. The fast cooling rate of underwater welding results in the formation of constituents such as martensite and bainite for conventional welding of steels. These constituents lead to a high-strength, brittle material and susceptibility to hydrogen-induced cracking. The weld bead shape for underwater wet welding are more spread out and less penetrating than air welds. Underwater welding arc is constricted at increased depth or pressure. However, welding in shallow depth is more critical than that in higher depth. The unstable arc results in porosity which affects the soundness of the weld. Weld metal carbon content increases with increase in water depth. Also, manganese and silicon which are deoxidizers are increasingly lost at increased water depth (Omajene et al. 2014).

Artificial neural network

A neural network is a data modeling tool that captures and represents complex input/output relationships. A neuron gets signals from its input links, computes a new activation level, and sends an output signal through the output link(s). The learning algorithm is the procedure to modify the synaptic weights of the network to achieve the desired objective of the design. Weights are the basic means of long-term memory in artificial neural networks. The multilayer perceptron neural network (NN) is the most applicable network architecture in use today.

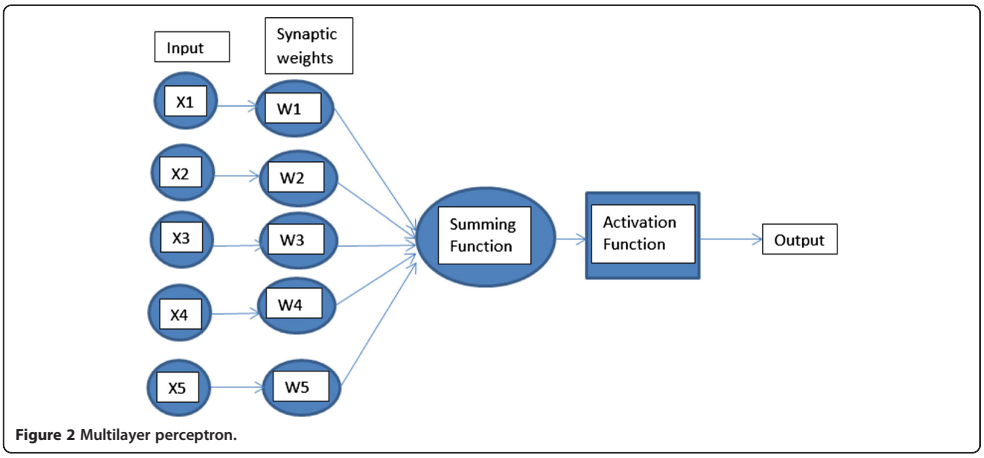

Figure 2 Multilayer perceptron.

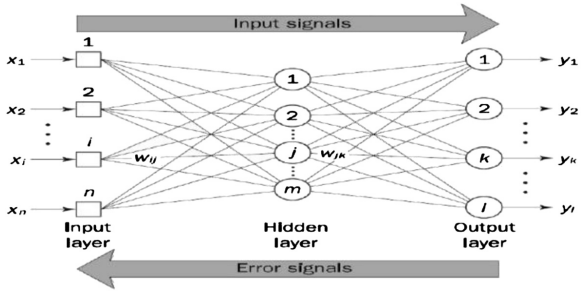

Figure 3 Three-layer backpropagation neural network (Negnevetsky 2005).

Each unit as shown in Figure 2 undergoes a biased weighted sum of its inputs and passes it through an activation function to produce its output. These units are arranged in a layered feed forward topology. The multilayer perceptron neural network learns using backpropagation algorithm as shown in Figure 3. In backpropagation algorithm, the input data is repeatedly presented to the neural network. In each presentation, the output of the neural network is compared to the desired output, thereby computing an error signal. The error is presented back to the neural network to adjust the weights in a manner that the error decreases with each iteration and the neural network model gets closer to the desired target. Figure 3 illustrates a neural network using the backpropagation algorithm whereby the weight is changed as the iteration increases, thereby reducing the error and getting closer to the desired target (Al-Faruk et al. 2010; Juang et al. 1998).

Summary of the backpropagation training algorithm

The summary of the backpropagation training algorithm is illustrated as follows (Negnevetsky 2005).

Step 1: Initialization

$$\left(-\frac{2.4}{F_i}, +\frac{2.4}{F_i}\right)$$

Set the weights and threshold levels of the network to uniformly random numbers distributed in small range. F_i is the total number of inputs of neuron i in the network.

Table 1 Experimental data adapted from (Shi et al. 2013)

Serial number	Process parameters				Water depth	Bead geometry			Error = Output (*W*, *P*, *R*) − Target		
									Target = 0		
	I (A)	*U* (V)	*v* (m/s)	*D* (m)	*H* (m)	*W* (m)	*P* (m)	*R* (m)	Δ*W* (m)	Δ*P* (m)	Δ*R* (m)
1	280	28	10	20	40	10.4	2.5	4.3	0.0061	0.0091	0.0016
2	320	32	6	20	20	12.5	3.8	8	0.0022	−0.0394	0.0998
3	300	32	10	22	60	10.4	3	4	−0.3280	*−1.1397*	*−0.5471*
4	340	28	6	22	0.1	13.9	3.5	3	*1.6136*	−0.1071	*−0.7470*
5	280	30	6	24	60	12.9	3.7	6.1	0.0223	−0.0104	0.0083
6	320	26	10	24	0.1	11.6	1.8	2	0.0093	0.0650	0.0269
7	300	26	6	18	40	12	2.9	5	−0.0177	−0.0126	0.0080
8	340	30	10	18	20	9.4	4.2	4.3	−0.0193	0.1365	0.0038
9	280	26	12	22	20	8.9	1.7	4.5	−0.3662	*−1.0633*	−0.2616
10	320	30	8	22	40	11.8	3.3	4.8	−0.0323	0.0312	0.0007
11	300	30	12	20	0.1	12.8	1.7	1.9	−0.0363	−0.1342	−0.0876
12	340	26	8	20	60	9.5	3.4	4.8	0.0169	−0.0132	0.0008
13	280	32	8	18	0.1	12.5	2	2	0.0089	0.0151	0.0553
14	320	28	12	18	60	7.9	2.7	4.9	*−0.8149*	*−0.9025*	*1.8429*
15	300	28	8	24	20	10.1	3.1	4.9	−0.0211	0.0055	−0.0067
16	340	32	12	24	40	10	3	4	0.0011	−0.0140	0.0213

Step 2: Activation

Activate the backpropagation neural network by applying inputs $x_1(p), x_2(p), \ldots, x_n(p)$ and desired output $y_{d,1}(p)$, $y_{d,2}(p), \ldots, y_{d,n}(p)$.

(a) Calculate the actual outputs of the neurons in the hidden layer:

$$y_j(p) = \text{sigmoid}\left[\sum_{i=0}^{n} x_i(p) * w_{ij}(p) - \theta_j\right]$$

where n is the number of inputs of neuron j in the hidden layer and sigmoid is the sigmoid activation function.

(b) Calculate the actual outputs of the neurons in the output layer.

(c) $$y_k(p) = \text{sigmoid}\left[\sum_{j=0}^{m} y_j(p) * w_{jk}(p) - \theta_k\right]$$

where m is the number of inputs of neuron k in the output layer.

Step 3: Weight training

Update the weights in the backpropagation network propagating backward the errors associated with output neurons.

(a) Calculate the error gradient for the neurons in the output layer:

$$\delta_k(p) = y_k(p) * \left[1 - y_k(p)\right] * e_k(p)$$

where

$$e_k(p) = y_{d,k}(p) - y_k(p)$$

Calculate the weight corrections

$$\Delta w_{jk}(p) = \alpha * y_j(p) * \delta_k(p)$$

Update the weights at the output neurons:

$$w_{jk}(p+1) = w_{jk}(p) + \Delta w_{jk}(p)$$

(b) Calculate the error gradient for the neurons in the hidden layer:

$$\delta_j(p) = y_j(p) * \left[1 - y_j(p)\right] * \sum_{k=0}^{\ell} \delta_k(p) * w_{jk}(p)$$

Calculate the weight corrections

$$\Delta w_{ij}(p) = \alpha * x_i(p) * \delta_j(p)$$

Update the weights at the output neurons:

$$w_{ij}(p+1) = w_{ij}(p) + \Delta w_{ij}(p)$$

Step 4: Increase iteration p by 1, go back to step 2, and repeat the process until the selected error criterion is satisfied.

Results and discussion

The ANN scheme to predict the weld bead geometry in underwater wet welding is shown in Figure 1. The aim is to map a set of input patterns to a corresponding set of output patterns by learning from past examples how the input parameters and output parameters relate. A feed-forward backpropagation network trained with scaled conjugate gradient (SCG) backpropagation algorithm is used. The quality of the weld can be verified when the training pattern fulfills the requirement for the accepted ranges of WPSF (penetration shape factor) = W/P and WRFF (reinforcement form factor) = W/R. The accepted ranges for a weld with good quality are a maximized penetration to width ratio and minimized undercut and reinforcement.

Table 2 Program algorithm

Program algorithm	
load matlab.mat	
% inputs	
I=DataProject(:,1);	D=DataProject(:,4);
U=DataProject(:,2);	H=DataProject(:,5);
v=DataProject(:,3);	F=[I U v D H];
%outputs	
W=DataProject(:,6);	
P=DataProject(:,7);	G=[W P R];
R=DataProject(:,8);	
% training	
p=F(1:12,:);	t=G(1:12,:);
% testing	
x=F(13:16,:);	Z=[x y];
y=G(13:16,:);	
% form the network	
net=feedforwardnet([40],'trainscg');	net.trainParam.max_fail=2000;
net.trainParam.goal=0; % error goal	net.trainParam.lr=0.001;
net.trainParam.epochs=3000; % maximum iterations	net.trainParam.mc=0.9;
net.trainParam.show=25; % showing intervals	
% Network initialization	
net.initFcn='initlay';	[net,tr]=train(net,p',t'); % training the net
net.layers{1}.initFcn='initnw';	view(net)
net=init(net);% initialize the net (weights and biases initialized)	
% simulating the network with training inputs for testing	
f=net(x');	f'
% compare results/target	
Error=f'-y	

Design parameters

The experimental data values in Table 1 for process parameters, water depth and bead geometry are the values used for the training of) the neural network. These values are from an experimental data adapted from the work of Shi et al. (2013). The error results for each testing are included in the modified table (Table 1). The errors in italics are the errors from the training which are big and not desirable. A smaller error tending to zero is desired or an actual zero which is however not so easy to achieve.

Program algorithm

There are five input parameters and three output parameters in this model (Table 2). The training (Figure 4) was done for all the sets of data, so also is the testing. The target is to achieve an error value of 0. The size of the hidden layer was obtained by iterative adjustment while measuring the error during the neural network testing (Nagendra & Khare 2006). The network for this study has two layers; there are 40 neurons in the hidden layer. In this study, the neural network should ideally be able to learn and understand the interaction between the welding process parameters. There are different training algorithms for different processes. The SCG backpropagation algorithm was used for the training of the network because it is suitable for the training of larger networks. Other training algorithms had the problem of overfitting caused by overtraining, resulting in memorization of input/output instead of analyzing them on the internal factors determined by the updated weights. The learning rate used is 0.001 and it gave satisfactory results. In artificial neural networks, a high learning rate may lead to overshooting, while a slow learning rate takes more time for the network to converge.

Validation performance

Epoch is a single presentation of each input/output data on the training set. It indicates the iteration at which the validation performance reached a minimum (Fahlman

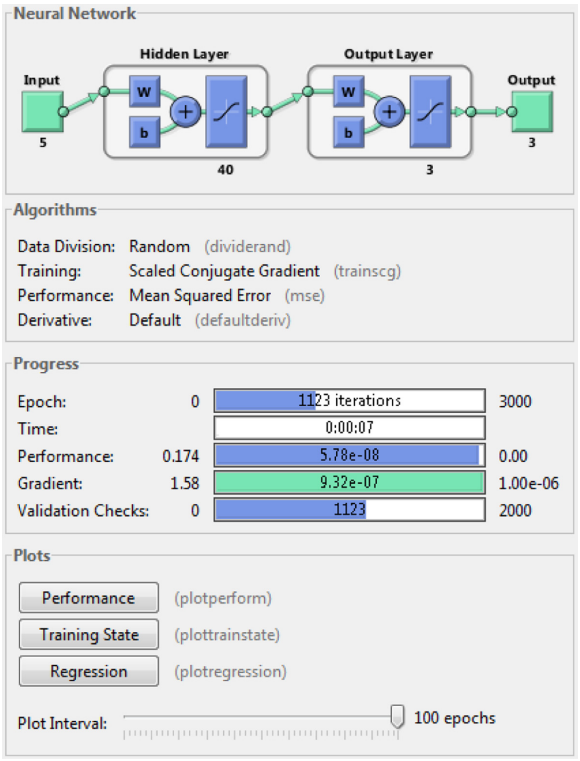

Figure 4 Neural network training tool.

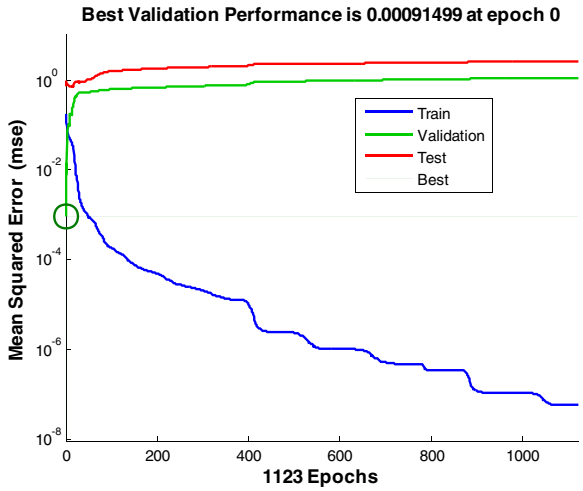

Figure 5 Validation performance curve.

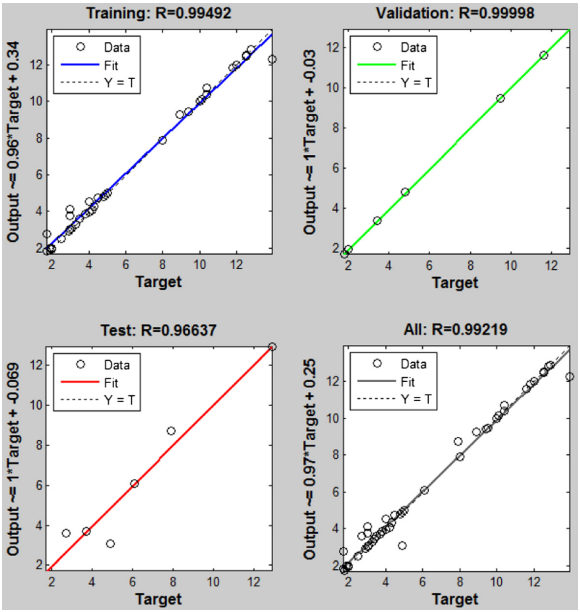

Figure 6 Regression plot.

1988). The training continued for 1,123 more iteration before the training stopped. Figure 5 does not indicate any major problems with the training. The validation and test curve are very similar. If the curve had increased significantly before the validation curve increases, then it is possible that some overfitting might have occurred. The final mean squared error (MSE) is small, which is 9.1499e−4 at zero epoch. The MSE is used to gauge the performance of the network. The MSE is an average of the squares of all the individual errors between the model and the real measurements. The MSE is useful for comparing different models with the same sets of data.

Regression analysis

This plot is used to validate the network performance. The regression plots in Figure 6 display the network outputs with respect to targets for training, validation, and test sets. For a perfect fit, the network outputs are equal to the targets. The fit for this problem is reasonably good for all data sets with *R* values in each case at least 0.96637. These results are achieved by retraining which changes the initial weights of the network. In this problem, 100% of the data sets were used for training, validation, and testing of the network generalization.

Controller for underwater wet welding process

Figure 7 is a proposed schematic diagram for a possible control of underwater wet welding in which the NN optimization of the welding process parameter can be applicable. The NN model in this paper will be an essential part in the control architecture of the proposed controller with the aim of designing a robust controller for underwater wet welding process, and further research work is necessary in this regard. The preliminary explanation of this possible controller is highlighted in this section. The control system is aimed at controlling the welding process parameters for different measured water depth *H*; the water depth is not a control parameter but a measured parameter as welding is being carried out at different water depth. The water depth for the welding process is measured as the depth changes. This change in the measured water depth consequently changes the welding process parameters which in turn alters the

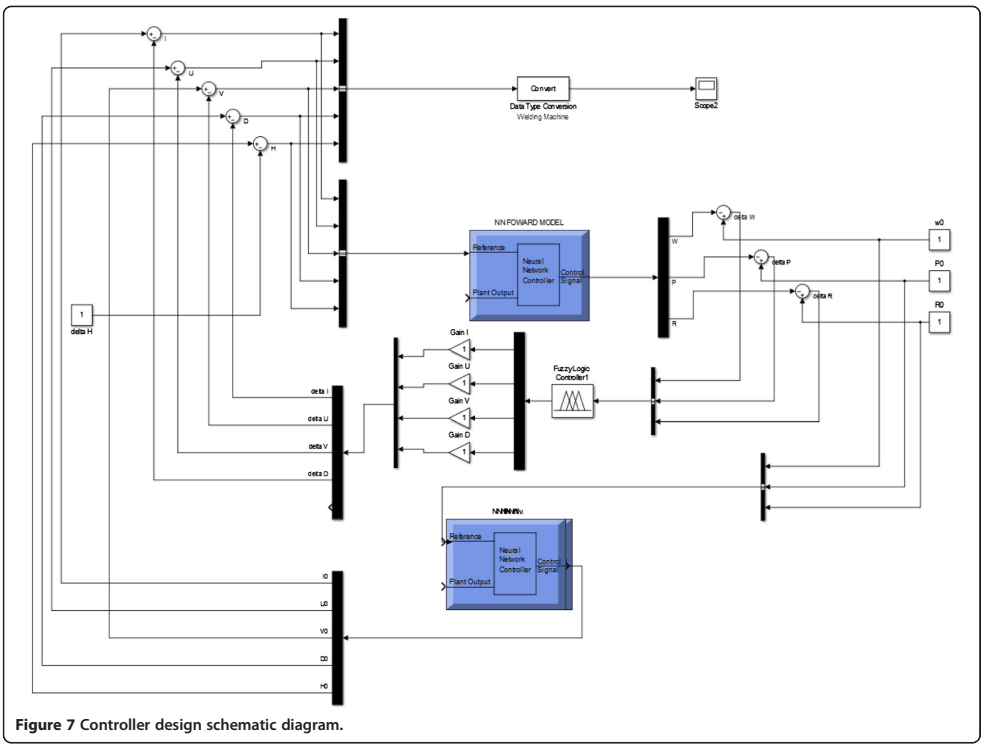

Figure 7 Controller design schematic diagram.

bead geometry W, R, and P. The fuzzy controller compensates for this change and modifies the welding process parameters I, u, V, and D. The inverse NN has a constant parameter value which is the desired bead geometry parameter as inputs to the inverse NN and best parameter of the welding process as the output from the inverse NN. The error values for the training in experiment 1 from Table 1 are the best set of parameters because the errors for W, R, and P are closer to zero compared to the values for the other experiments. The constant output parameters I_0, U_0, v_0, D_0, and H_0 which is the water depth at zero position from the inverse NN are summed up with the difference from the change in the output parameters ΔI, ΔU, Δv, ΔD, respectively, of the fuzzy controller, and this compensates for the change in the welding process parameters and inputs the adjusted welding process parameter to the welding machine. For every measured change in the water depth H, a change in the bead geometry ΔW, ΔP, and ΔR which is the input to the fuzzy controller is modified and gives an output of ΔI, ΔU, Δv, and ΔD. The welding process parameter from the welding machine is equal to the NN forward model, and as such, any change in the NN forward model is a subsequent change in the welding process itself. This control mechanism is a possible robust control process of the welding process and eliminates the need for online measurement of the weld bead geometry.

Conclusions

The optimization of the parameters that affect weld bead geometry during underwater welding can be done by artificial neural network training algorithm. In this study, the regression analysis show that the target follows closely the output as R is at least 96% for training, testing, and validation. The trained neural network with satisfactory results can be used as a black box in the control system of the welding process. The effective optimization of the welding process parameter in underwater wet welding has the ability of welding with an optimized heat input and optimized arc length which will guarantee arc stability. The use of optimized process parameters enables the achievement of an optimized weld bead geometry which is a key factor in the soundness of welds. The control process for underwater welding as suggested in this paper requires further research so as to fully apply the NN optimization process.

Competing interests

The authors declare that they have no competing interests.

Authors' contributions

The main author JEO carried out the research and designed the neural network model and analyzed the training results and prepared the paper. HW was responsible for key technical supervision. PK and JM checked the paper and provided suggestions to improve the paper. All authors read and approved the final manuscript.

Received: 8 September 2014 Accepted: 5 November 2014
Published online: 21 November 2014

References

Al-Faruk, A, Hasib, A, Ahmed, N, Kumar Das, U. (2010). Prediction of weld bead geometry and penetration in electric arc welding using artificial neural networks. *International Journal of Mechanical & Mechatronics Engineering, 10* (4), 19–24.

AWS. (2010). *"Underwater welding code"*. USA: AWS.

Brown, RT, & Masubuchi, K. (1975). "Fundamental Research on Underwater Welding". In *Welding research supplement* (pp. 178–188).

Fahlman, SE. (1988). *An empirical study of learning speed in backpropagation*. USA: Carnegie Mellon University.

Johnson, RL. (1997). *The Effect of Water Temperature on Underbead Cracking of Underwater Wet Weldments*. California: Naval Postgraduate School.

Juang, SC, Tarng, YS, & Lii, HR. (1998). A comparison between the backpropagation and counterpropagation networks in the modeling of TIG welding process. *Journal of Material ocessing Technology, 75*, 54–62.

Liu, S, Olson, DL, & Ibarra, S. (1993). Underwater Welding. *ASM Handbook, 6*, 1010–1015.

Nagendra, SM, & Khare, M. (2006). Artificial neural network approach for modelling nitrogen dioxide dispersion from vehicular exhaust emissions. *Ecological Modelling, 190*(1–2), 99–115.

Negnevetsky, M. (2005). *Artificial Intelligence*. UK: Addison Wesley.

Omajene, JE, Martikainen, J, Kah, P, & Pirinen, M. (2014). Fundamental difficulties associated with underwater wet welding. *International Journal of Engineering Research and Applications, 4*(6), 26–31.

Shi, Y, Zheng, Z, & Huang, J. (2013). "Sensitivity model for prediction of bead geometry in underwater wet flux cored arc welding". In *Transaction of nonferrous metals society of China* (pp. 1977–1984).

doi:10.1186/s40712-014-0026-3
Cite this article as: Omajene *et al.*: **Optimization of underwater wet welding process parameters using neural network.** *International Journal of Mechanical and Materials Engineering* 2014 **9**:26.

Publication IV

Omajene J. E., Martikainen J., Huapeng W., Kah P., Izelu C. O., (2015)

Intelligent Control Mechanism for Underwater Wet Welding

The paper has been published in the journal "International Journal of Mechanical Engineering and Applications", 3(4), pp. 50-56.

Link:(http://article.sciencepublishinggroup.com/pdf/10.11648.j.ijmea.20150304.11.pdf)

International Journal of Mechanical Engineering and Applications
2015; 3(4): 50-56
Published online July 20, 2015 (http://www.sciencepublishinggroup.com/j/ijmea)
doi: 10.11648/j.ijmea.20150304.11
ISSN: 2330-023X (Print); ISSN: 2330-0248 (Online)

Intelligent Control Mechanism for Underwater Wet Welding

Joshua Emuejevoke Omajene[1], Paul Kah[1], Huapeng Wu[1], Jukka Martikainen[1], Christopher Okechukwu Izelu[2]

[1]LUT Mechanical Engineering, Lappeenranta University of Technology, Lappeenranta, Finland
[2]Department of Mechanical Engineering, College of Technology, Federal University of Petroleum Resources, Effurun, Delta State, Nigeria

Email address:
Joshua.omajene@yahoo.com (J. E. Omajene)

To cite this article:
Joshua Emuejevoke Omajene, Paul Kah, Huapeng Wu, Jukka Martikainen, Christopher Okechukwu Izelu. Intelligent Control Mechanism for Underwater Wet Welding. *International Journal of Mechanical Engineering and Applications*. Vol. 3, No. 4, 2015, pp. 50-56.
doi: 10.11648/j.ijmea.20150304.11

Abstract: It is important to achieve high quality weld in underwater welding as it is vital to the integrity of the structures used in the offshore environment. Due to the difficulty in ensuring sound welds as it relates to the weld bead geometry, it is important to have a robust control mechanism that can meet this need. This work is aimed at designing a control mechanism for underwater wet welding which can control the welding process to ensure the desired weld bead geometry is achieved. Obtaining optimal bead width, penetration and reinforcement are essential parameters for the desired bead geometry. The method used in this study is the use of a control system that utilizes a combination of fuzzy and PID controller in controlling flux cored arc welding process. The outcome will ensure that optimal weld bead geometry is achieved as welding is being carried out at different water depth in the offshore environment. The result for the hybrid fuzzy-PID gives a satisfactory outcome of overshoot, rise time and steady error. This will lead to a robust welding system for oil and gas companies and other companies that carry out repair welding or construction welding in the offshore.

Keyword: Control System, Bead Geometry, Fuzzy Logic, Process Parameter, Underwater Welding

1. Background

Owing to the environmental conditions in which structures operate in the offshore, it is important that a high structural integrity is guaranteed. It is evident that structural failures can arise as a result of poor weld quality and other mechanical properties of the loaded structures operating in the offshore. The quality of welds achieved underwater experience a major setback because of the unique feature of the weld metal fast cooling rate and other factors such as the stability of the welding arc, loss of alloying elements and difficulty of a good visibility to weld underwater. This research paper addresses the issue of controlling the welding parameters at different water depth in achieving a desired weld bead geometry that is reasonably satisfactory of the weld quality that can operate in the offshore. A control mechanism which incorporates the design advantages of fuzzy logic control and PID control is implemented in this study. Experimental data to be analyzed in this paper is adopted from the work of Chon L. Tsai et. al. It is a well-known fact that high cooling rate and hydrogen embrittlement are characteristics of underwater wet welding (UWW). Rapid cooling mechanism and their effects have been studied by Chon L. Tsai and Koichi Masubuchi [1]. The final microstructure of the heat affected zone (HAZ) for a given material is determined by the composition, peak temperature and cooling rate. It is possible to control the weld metal composition, the peak temperature and the cooling rate to yield favorable microstructure. However, it is not possible to control the composition of the HAZ of the parent material. Fast cooling effect of the water environment in UWW results in a martensitic heat affected zone having high hardness and poor notch toughness. In UWW, the dissociation of water is a source of hydrogen and this subjects the microstructure of the HAZ to hydrogen cracking. This makes it important to control the weld metal's cooling rate [2]. The ability to reduce cooling rate during underwater welding will ensure a decrease in the content of martensite and upper bainite, increase in proeutectoid ferrite and acicular ferrite [3].

2. Underwater Welding

The application of underwater welding for the repair of

ships and offshore structures like oil drilling rigs, pipelines, and platforms is of high importance in today's welding activities. The demand for quality wet weld at a greater depth and variety of materials is continually on the increase [4]. Nowadays, shielded metal arc welding (SMAW) and flux cored arc welding (FCAW), are the most widely used underwater welding process. FCAW has a high prospect in the future because of its high production efficiency and ease to be automated [5 - 8]. The water surrounding the weld metal reduces the mechanical properties of weld done underwater due to the effect of rapid cooling of the weld. Heat loss by conduction from the surface of the base metal directly into the moving water surrounding and heat loss by radiation are the major channels in which heat is lost during underwater welding. In order to achieve higher heat input in underwater welding, it is important to apply higher current to a comparable arc voltage for welds done in the air. Underwater welding high rate of cooling of the base metal results in the creation of unfavorable microstructure such as martensite and bainite for conventional welding of steels. Martensitic and bainitic constituents are high strength and brittle which are prone to cracking in the presence of high hydrogen content [3]. Underwater wet welding bead geometry have weld bead shape that are wider and lower penetration which is the opposite situation in air welding. The welding arc in underwater welding is constricted at a higher water depth. However, shallow water depth welding is more demanding than higher depth. The welding arc instability results in porosity which affects the soundness of the weld. Weld metal carbon content increases with increase in water depth. Also, deoxidizers such as manganese and silicon are lost in higher amounts at increased water depth [9] [10].

3. Flux Cored Arc Welding Process

FCAW is a semiautomatic welding process and the operation continues until completing the weld pass, whereas SMAW process requires changing of the electrodes from time to time. The weld crack sensitivity for FCAW is reduced compared to SMAW because of the interruption of the welding pass in SMAW, especially for steels with CE less than 0.4 %. However, one major disadvantages of FCAW is the difficulty in tracking the joint precisely under the condition of poor visibility underwater. Another challenge is that the diver/welder has difficulty in hearing the arc sound or viewing the plasma during underwater welding and this poses the challenge of him having information regarding the frequent changes in the welding current and voltage. For this reason, it is very important to design a robust control system to control the welding process in the underwater environment [11].

4. Mathematical Model of FCAW

In FCAW, a constant voltage power source and constant wire feeding rate are usually used [11]. The output characteristics of the power supply at the working point is described in the equations below. The mathematical model for the design of the controller in this paper is adopted from the work of Chon L. Tsai et. al [11].

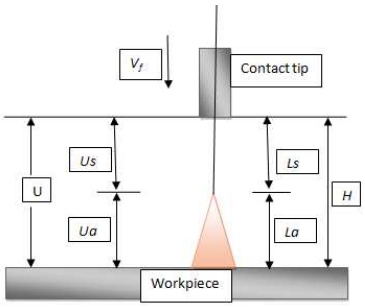

Fig. 1. *Illustration of arc parameters adapted Chon L. Tsai et. al [11].*

$$U = U_{ol} - R_s I \quad (1)$$

Where U_{ol} is the equivalent open loop voltage, and R_s is the equivalent source resistance including the cables.

The output voltage is distributed in two parts which are the arc voltage and U_{ol} and the wire stickout voltage U_s.

$$U = U_\alpha + U_s \quad (2)$$

FCAW arc voltage-current characteristics can be described as in equation 3:

$$U_\alpha = K_a L_a + R_a I + U_c \quad (3)$$

Where K_a is electrical field intensity which is the voltage drop per unit length of arc column. R_a is the arc resistance. U_c is a constant that is related to the anode and cathode voltage.

The voltage drop on the wire stickout is described as equation 4:

$$U_s = \rho\frac{L_s}{A} = K_s L_s I \quad (4)$$

Where ρ is the electric resistivity of the wire over the temperature ranges. A is electrode or wire cross-section area. K_s is average resistance per unit length of wire stickout.

The melting rate can be described as:

$$V_m = K_m I + K_e L_s I^2 \quad (5)$$

Where V_m is the melting rate, $K_m I$ is the melting rate from the arc heat, K_m is the constant related to the anode voltage drop $K_e L_s I^2$ is the stickout wire resistance heat contribution to the melting rate, K_e is also another constant.

$V_m = V_f$ (when in steady state, the melting rate, if represented in wire length per unit time, equals the wire feed rate).

The contact-tip-to-workpiece distance comprises of the arc length and stickout length.

$$H = L_s + L_a \quad (6)$$

In the welding process, the power source voltage, CTWD, wire feed rate, arc length and current are controllable parameters. In welding practice, it is observed that an increase in the length of CTWD will at the same time increase the arc length and will later shorten when a steady state is reached, that is at the state of fixed CTWD, wire feed rate, power source setting, and the arc is stable. The dynamic model of a welding arc power describes the transient characteristics in the change of one or more parameters. The dynamic model is based on the equation in the static model deviation [11].

The dynamic equation of power source

$$U = U_{ol} - R_s I - M_s \frac{di}{dt} \quad 7$$

Where M_s is power source inductance.

Its frequency domain expression (Fourier Transform) is:

$$\Delta U(s) = - R_s(T_p S + 1)\Delta I(s) \quad 8$$

The final dynamic model after setting a reasonable range of GMAW is given by the transfer function as represented in equation 9.

$$\frac{I(S)}{H(S)} = -3.46 \frac{0.0168s^2+0.457s+1}{1.28e{-}005\, s^3+0.01576\, s^2+0.1776s+1} \quad 9$$

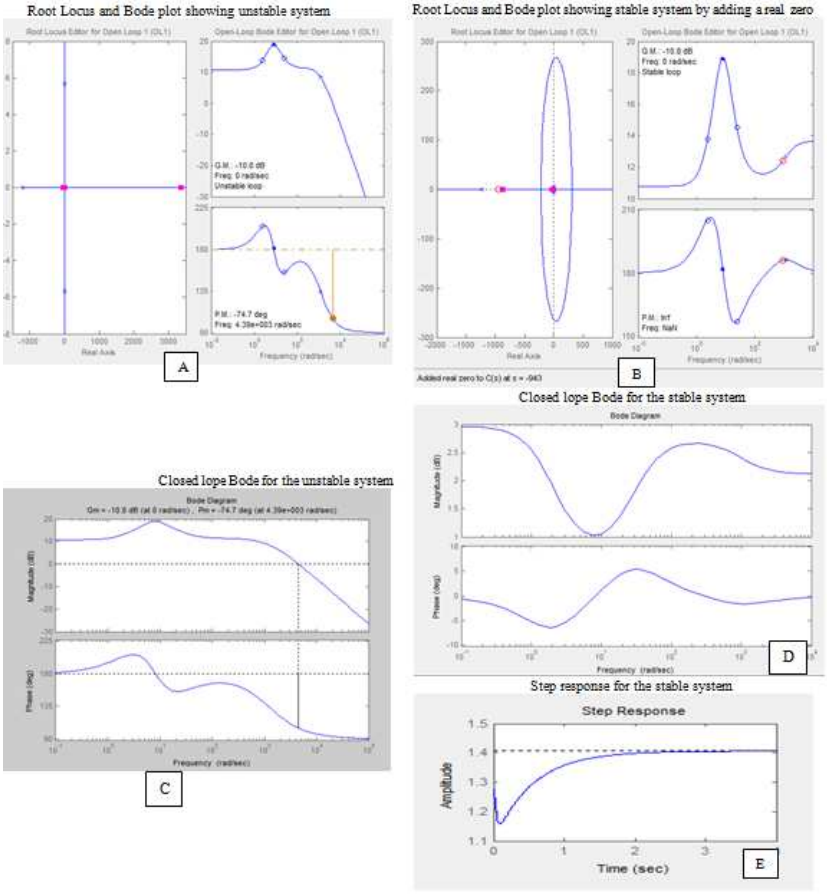

Fig. 2. *Stability analysis using Bode plot, Root Locus and step response.*

This transfer function is used as the plant model in the control system. The transfer function is the relationship between the arc current and CTWD. The transfer function of the system is unstable but can be adjusted by adjusting the position of the poles by adding a real zero. This is done by the implementation Table. 1 of the following algorithm below. The SISOTOOL in MATLAB helps us to adjust the position of the poles or zeros in the Root Locus. The Bode plot Fig. 2 shows the relationship between the output signal $I(S)$ and the input signal $H(S)$ that describes the linear system. The Bode

plot for the transfer function of the plant shows that the system is unstable. The closed loop Bode plot in Fig. 2A has a gain margin of -10.8 dB at 0 rad/sec and phase margin of 74.7 degrees at 4390 rad/sec shown in Fig. 2C. This means that for the system to be stable, we need to decrease the gain by 10.8 dB. However adding a real zero at s= -943 shown in Fig. 2B will make the transfer function of the system stable. The closed loop Bode Fig. 2D of this system has a peak response of 2.96 dB at a frequency of 3.71e-008 rad/sec. The step response Fig. 2E of the stable system has input amplitude of 1.4. The output response follows closely the input response without an overshoot.

Table 1. *MATLAB implementation*

```
NUM=-3.46*[0.01685 0.4575 1]
DEN=[1.28e-5 1.576e-2 1.776e-1 1]
sys=tf(NUM,DEN)
sisotool(sys)
```

5. Controller for Underwater Wet Welding Process

Fuzzy controller: This control system is a fuzzy logic controller that controls the plant which is the welding machine. The SMAW and FCAW mostly used in underwater welding are dependent on several process parameters that usually vary over a wide domain. Fuzzy logic technique is able to learn the relationship between the welding process input variable and output variable. Fuzzy set theory application is valuable in experimental data modeling which involves unpredictability between the relationships of the welding process input variables and the subsequent bead geometry output. The fuzzy model is used to analyze the appropriateness of the fuzzy relations in predicting the characteristics of the weld bead geometry profile. Fuzzy control is effective for systems which have dissimilarities of system dynamics. The model of the system can perform well for processes that are not precisely defined unlike PID controller. Fuzzy controllers are suitable in achieving a decreased rise time and slight overshoot [12].The structure of the two inputs (error e and error change Δe) and three output (proportional gain K_p, integral gain K_i and derivative gain K_d) are designed for the fuzzy rules used in the hybrid fuzzy controller. The structure for the fuzzy logic controller designed for this research paper is two inputs (error e and error change Δe) and single output of the error and error change. The linguistic variables defined are sentences in normal English language such as negative big (NB), negative small (NS), zero (Z), positive big (PB), postive small (NS), which are expressed by fuzzy sets. The fuzzy sets are characterized by fuzzification (assigning input variables), membership functions (mapping of the input space to a membership value), fuzzy rule (IF-THEN conditional statements), inference system (mapping inputs to outputs) and defuzzification (quantification of expressions). The outputs of the fuzzy sets are obtained in crisp form. The Fig.3 summarizes the operations that are carried out in a fuzzy logic controller. In this research, the output from the defuzzifier which is a proportional, integral and derivative gain is fed into the input signal of the transfer function of the welding machine. The aim of the fuzzy logic in the controller design is to tune the parameters of the PID controller. This will significantly improve the performance of the system as compared to the conventional PID controller.

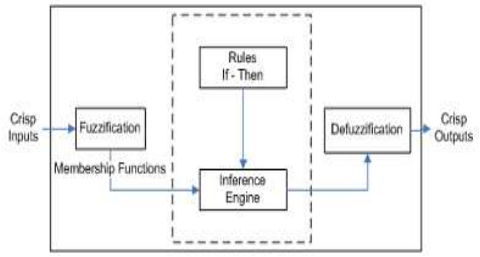

Fig. 3. *Fuzzy logic controller block diagram [13].*

5.1. Rules

The fuzzy control rule is a collection of fuzzy IF-THEN rules in which the preconditions are the error and error change variable and consequents are the output from the fuzzy logic variables which involves linguistic variables. The fuzzy control rule for the hybrid fuzzy PID controller have preconditions as the error and error change variable and consequence as gain parameters

5.2. Defuzzification Process

The defuzzification process converts the fuzzy output into a crisp using a defuzzification approach that relates the membership functions in Fig. 4 with the fuzzy rules [14]. In this paper, the centroid defuzzification technique is used. The defuzzification process is shown in the Fig. 5 is as a result of the assumptions reached for membership function and fuzzy rules. From the figure, it can be found that as each individual set of input parameters are changed, a subsequent change in the output parameter is effected.

PID controller: PID controller is widely utilized industrially for control applications. This controller is suitable in improving a systems transient response and steady state error simultaneously [15]. The control logic of the PID controller is implemented by finding suitable gain parameters K_p, K_i, and K_d. The transfer function of the PID controller is obtained by adding the terms of the proportional, integral and derivative controller (Equation 10). One major setback of a PID controller is that it does not effectively control a system having big lag, uncertainties and parameter variations. This makes it necessary for a fuzzy-PID hybrid control system [16].

$$PID(s) = K_p + K_i/s + sK_d \qquad 10$$

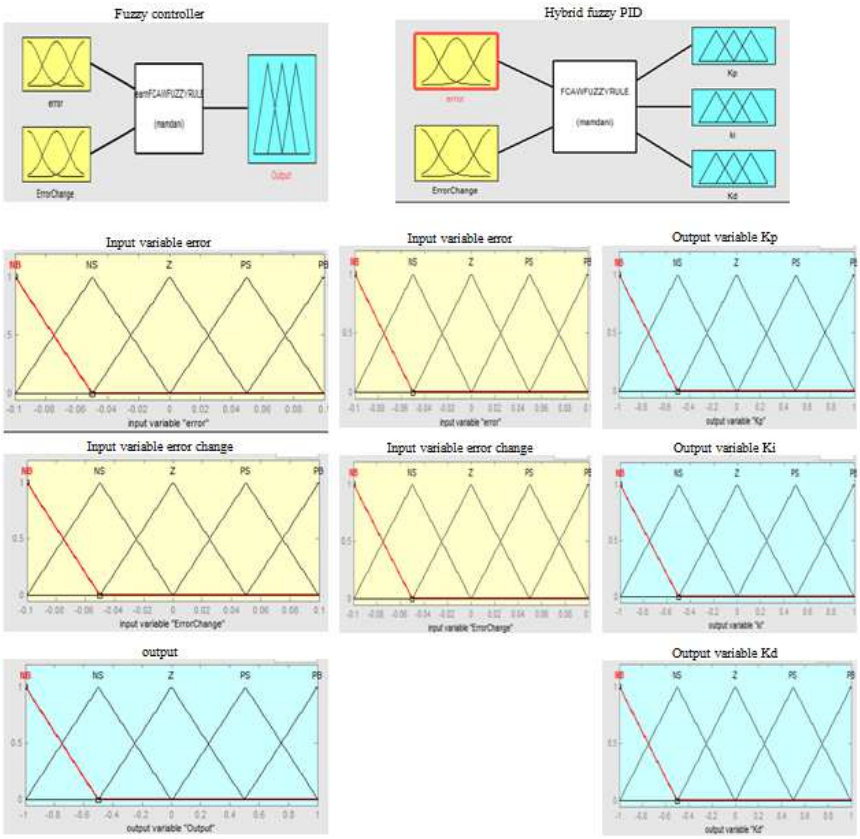

Fig. 4. *Membership function diagram*

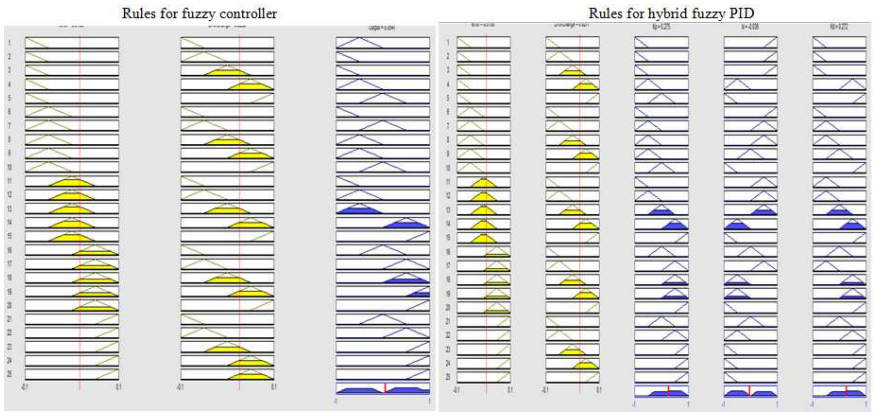

Fig. 5. *Centroid defuzzification using max-min inferencing.*

Hybrid fuzzy PID controller: The control system is a typical fuzzy-PID hybrid control system. It utilizes the advantages of a fuzzy controller and a PID controller. This controller is capable of overcoming the presence of nonlinearities and uncertainties in a system. Tuning of the different parameters of the PID controller is executed with the fuzzy logic controller. Fuzzy rules are designed for effective tuning of the parameter K_p, K_i, and K_d according to functions of the actuating error signal. The proportional term is responsible for the entire control process that is proportional to the error. The aim of the integral term is to help in reducing the steady-state error through low frequency compensation with the aid of an integrator. While the derivative term helps in improving the transient response through high frequency compensation [16].The design and implementation of the control system uses efficient technique that can achieve performance requirement in the presence of disturbances and uncertainty [17]

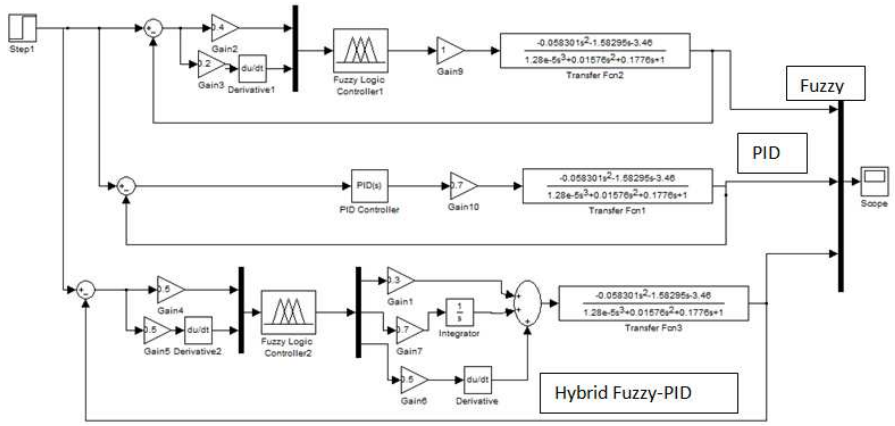

Fig. 6. *Control system for underwater FCAW.*

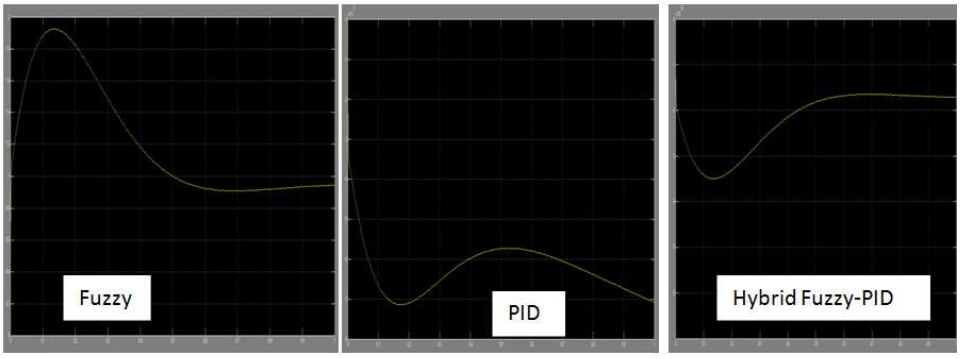

Fig. 7. *Matlab simulation results of PID, Fuzzy and hybrid fuzzy PID controller.*

6. Results and Discussion

The plant model executed in this paper (Figure 6) made use of the application of the control dynamics of PID, fuzzy and hybrid fuzzy PID. The performances for the different control systems were compared as can been seen in the simulation results in Fig. 7. The system response was tested using a step input signal. From the analysis of the dynamic response of the various control system indicate that fuzzy controller produces a more suitable result compared to the PID controller. From the results, it is evident that the fuzzy controller exhibits a faster response than the PID controller. Results from the PID controller gave rise to overshoot. However, results from the hybrid fuzzy PID controller gave a more satisfactory result of overshoot, rise time and steady state error. The proposed hybrid fuzzy PID controller demonstrates the advantages of fuzzy and PID controller. Application of the hybrid fuzzy PID controller is suitable for FCAW process used in underwater welding since the input current and output CTWD can be predicted and controlled.

7. Conclusion

The control of welding arc current in relationship to CTWD of FCAW for underwater welding application is effective way of ensuring the desired heat input and arc length during welding. The application of a hybrid fuzzy PID controller has the potentials of eliminating the effect of uncertainties and disturbance during underwater welding. A properly control underwater welding process will result bead geometry that is favorable for a sound and reliable weld for welding of offshore structures underwater.

References

[1] Chong-Liang Tsai, Kiochi Masubuchi, "Mechanism of rapid cooling in underwater welding," Applied ocean research, vol. 1, no. 2, pp. 99-110, 1979.

[2] Yong-hua SHI, Zei-pei ZHENG & Jin HUANG, "Sensitivity model for prediction of bead geometry in underwater wet flux cored arc welding," Transaction of nonferrous metals society of China, pp. 1977-1984, 2013.

[3] H. T. Zhang, X. Y. DAI, J. C. FENG & L. L. HU, "Preliminary investigation on real time induction heating assisted underwater wet welding," Welding research , vol. 94, pp. 8-15, 2015.

[4] J. Labanowski, "Development of Underwater Welding Techniques," Welding International, vol. 25, pp. 933-937, 2011.

[5] Yara H., Makishi Y., Kikuta Y., & Matsuda F., "Mechanical and metallurgical properties of an experimental covered electrode for wet underwater welding," Welding International, vol. 1, pp. 835-839, 1987.

[6] Liu S., Olsen D. L., & Ibarra S. J., "Designing shielded metal arc consumables for underwater wet welding in offshore applications," Journal of Offshore Mechanica and Arctic Engineering, vol. 117, pp. 212-220, 1995.

[7] Kononenko V. Y., "Mechanised welding with self-shielding flux-cored wires for repairing hydraulic installations and vessels in underwater," Welding International , vol. 10, pp. 994-997, 1996.

[8] Jia C. B. , Zhang T., Maksimov S. Y., & Yuan X., "Spectroscopic analysis of the arc plasma of underwater wet flux-cored arc welding," Journal of Materials Processing Technology, vol. 213, pp. 1370-1377, 2013.

[9] Brown R. T. &. Masubuchi K., "Effects of water environment on metallurgical structures of welds," Welding Research Supplement, pp. 178-188, 1975.

[10] Liu S. & Olsen D., "Underwater welding," ASM International, vol. 6, pp. 1010-1015, 1993.

[11] Chon L. Tsai, Baojian Liao, David A. Clukey & Josept. S. Breeding., "Development of a Microprocessor based Tracking and Operation Guidance System for Underwater Welding," Ohio State University, Ohio, 2000.

[12] Sinthipsomboon K. et al., "http://cdn.intechopen.com/pdfs/39444/A hybrid of fuzzy and fuzzy self tuning pid controller for servo electro hydraulic system," INTECH, pp. 1-16, 2012.

[13] "Tribal Engineering," [Online]. Available: http://www.tribalengineering.com/technology/fuzzy-ictl.aspx. [Accessed 9 February 2015].

[14] Ion Iancu & Mihai Gabroveanu, "Fuzzy logic controller based on association rules," Annals of the University of Craiova, Mathematics and Computer Science Series, vol. 37, no. 3, pp. 12-21, 2010.

[15] Parnichkun M. & Ngaecharoenkul C., "Hybrid of fuzzy and PID in kinematics control of a pneumatic system," in Industrial Electronics Society 26th Annual Confjerence of the IEEE, Thailand, 2000.

[16] Pornjit Pratumsuwan, Siripun Thongchai & Surapun Tansriwong "A Hybrid of Fuzzy and Proportional-Integral-Derivative Controller for Electro-Hydraulic Position Servo System," Energy Research Journal, vol. 1, no. 2, pp. 62-67, 2010.

[17] Majid Ali, Majid Ali, Saifullah Khan, Muhammad Waleed & Islamuddin,"Application of an Intelligent Self-Tuning Fuzzy PID Controller on DC-DC Buck Converter," International Journal of Advanced Science and Technology, vol. 48, pp. 139-148, 2012.

ACTA UNIVERSITATIS LAPPEENRANTAENSIS

639. ZHANG, YUNFAN. Modification of photocatalyst with enhanced photocalytic activity for water treatment. 2015. Diss.

640. RATAVA, JUHO. Modelling cutting states in rough turning of 34CrNiMo6 steel. 2015. Diss.

641. MAYDANNIK, PHILIPP. Roll-to-roll atomic layer deposition process for flexible electronics applications. 2015. Diss.

642. SETH, FRANK. Empirical studies on software quality construction: Exploring human factors and organizational influences. 2015. Diss.

643. SMITH, AARON. New methods for controlling twin configurations and characterizing twin boundaries in 5M Ni-Mn-Ga for the development of applications. 2015. Diss.

644. NIKKU, MARKKU. Three-dimensional modeling of biomass fuel flow in a circulating fluidized bed furnace. 2015. Diss.

645. HENTTU, VILLE. Improving cost-efficiency and reducing environmental impacts of intermodal transportation with dry port concept – major rail transport corridor in Baltic Sea region. 2015. Diss.

646. HAN, BING. Influence of multi-phase phenomena on semibatch crystallization processes of aqueous solutions. 2015. Diss.

647. PTAK, PIOTR. Aircraft tracking and classification with VHF passive bistatic radar. 2015. Diss.

648. MAKKONEN, MARI. Cross-border transmission capacity development – Experiences from the Nordic electricity markets. 2015. Diss.

649. UUSITALO, ULLA-MAIJA. Show me your brain! Stories of interdisciplinary knowledge creation in practice. Experiences and observations from Aalto Design Factory, Finland. 2015. Diss.

650. ROOZBAHANI, HAMID. Novel control, haptic and calibration methods for teleoperated electrohydraulic servo systems. 2015. Diss.

651. SMIRNOVA, LIUDMILA. Electromagnetic and thermal design of a multilevel converter with high power density and reliability. 2015. Diss.

652. TALVITIE, JOONAS. Development of measurement systems in scientific research: Case study. 2015. Diss.

653. ZUBEDA, MUSSA. Variational ensemble kalman filtering in hydrology. 2015. Diss.

654. STEPANOV, ALEXANDER. Feasibility of industrial implementation of laser cutting into paper making machines. 2015. Diss.

655. SOKOLOV, MIKHAIL. Thick section laser beam welding of structural steels: methods for improving welding efficiency. 2015. Diss.

656. GORE, OLGA. Impacts of capacity remunerative mechanisms on cross-border trade. 2015. Diss.

657. AURINKO, HANNU. Risk assessment of modern landfill structures in Finland. 2015. Diss.

658. KAIJANEN, LAURA. Capillary electrophoresis: Applicability and method validation for biorefinery analytics. 2015. Diss.

659. KOLHINEN, JOHANNA. Yliopiston yrittäjämäisyyden sosiaalinen rakentuminen. Case: Aalto-yliopisto. 2015. Diss.

660. ANNALA, SALLA. Households' willingness to engage in demand response in the Finnish retail electricity market: an empirical study. 2015. Diss.

661. RIABCHENKO, EKATERINA. Generative part-based Gabor object detector. 2015. Diss.

662. ALKKIOMÄKI, VILLE. Role of service and data reuse in enterprises. 2015. Diss.

663. VÄNTSI, OLLI. Utilization of recycled mineral wool as filler in wood plastic composites. 2015. Diss.

664. KLEMOLA, KATJA. Tuottavuuden, vaikuttavuuden ja kustannusvaikuttavuuden arviointi alueellisesti integroiduissa sosiaali- ja terveyspalveluissa – palvelujen käyttöön perustuva malli ja esimerkkejä. 2015. Diss.

665. HEROLD, KRISTIINA. Impact of Word-of-Mouth on consumer decision-making: An information processing perspective in the context of a high-involvement service. 2015. Diss.

666. OLABODE, MUYIWA. Weldability of high strength aluminium alloys. 2015. Diss.

667. VANHALA, ERNO. The role of business model in computer game development organizations. 2015. Diss.

668. SALAMPASIS, DIMITRIOS. Trust-embedded open innovation: Towards a human-centric approach in the financial industry. 2015. Diss.

669. DE SMET, DIETER. Innovation ecosystem perspectives on financial services innovation. 2015. Diss.

670. PORRAS, PÄIVI. Utilising student profiles in mathematics course arrangements. 2015. Diss.

671. SALMINEN, JUHO. The role of collective intelligence in crowdsourcing innovations. 2015. Diss.

672. ROSAS, SAILA. Co-operative acquisitions – the contextual factors and challenges for co-operatives when acquiring an investor-owned firm. 2015. Diss.

673. SINKKONEN, TIINA. Item-level life-cycle model for maintenance networks – from cost to additional value. 2015. Diss.

674. TUUNANEN, JUSSI. Modelling of changes in electricity end-use and their impacts on electricity distribution. 2015. Diss.

675. MIELONEN, KATRIINA. The effect of cationic-anionic polyelectrolyte multilayer surface treatment on inkjet ink spreading and print quality. 2015. Diss.